

Lassoed Boosting and Linear Prediction in the Equities Market

Xiao Huang*

May 21, 2024

Abstract

We consider a two-stage estimation method for linear regression. First, it uses the lasso in [Tibshirani \(1996\)](#) to screen variables and, second, re-estimates the coefficients using the least-squares boosting method in [Friedman \(2001\)](#) on every set of selected variables. Based on the large-scale simulation experiment in [Hastie *et al.* \(2020\)](#), lassoed boosting performs as well as the relaxed lasso in [Meinshausen \(2007\)](#) and, under certain scenarios, can yield a sparser model. Applied to predicting equity returns, lassoed boosting gives the smallest mean-squared prediction error compared to several other methods.

JEL Classification: C18, C21

Keywords: Lassoed boosting, linear regression, variable selection, return prediction, parameter attribution

*Department of Economics, Finance, and Quantitative Analysis, Coles College of Business, Kennesaw State University, GA 30144, USA. Email: xhuang3@kennesaw.edu.

1 Introduction

To analyze consumer behavior, predict sales, and track price movement, business and economic researchers must routinely sift through massive amount of data to select relevant variables. In an influential paper, [Tibshirani \(1996\)](#) proposed a shrinkage method called lasso to simplify estimation, and it has become a critical tool in high-dimensional analysis. Extensions include the elastic net in [Zou and Hastie \(2005\)](#) and the group lasso in [Yuan and Lin \(2006\)](#). [Fan and Li \(2001\)](#); [Zhang \(2010\)](#); [Mazumder *et al.* \(2011\)](#) also discuss nonconvex penalty function approaches. [Bühlmann and van de Geer \(2011\)](#); [Hastie *et al.* \(2015\)](#) provide thorough expositions of the lasso and related methods.

With so many variable-selection methods available, data analysts will profit from some general advice on their use. [Hastie *et al.* \(2020\)](#) recently conducted a large-scale simulation to compare the performance of (a) the lasso; (b) forward stepwise selection, which generates models by sequentially adding the regressor that most improves the fit; (c) best subset selection of regressors for each model size; (d) the relaxed lasso in [Meinshausen \(2007\)](#), which emerged as the overall winner with good accuracy and sparsity recovery. The paper also commented on many other competitors of the lasso, such as the Dantzig selector and square-root lasso, and concluded that their performance is either close to the lasso or somewhere between the lasso and the best subset.

This paper investigates whether we can design a new estimator that is as simple as the relaxed lasso but even more effective under certain scenarios. We propose one example: *lassoed boosting*. The relaxed lasso uses linear interpolation between every lasso solution and the corresponding least-squares (LS) solution to create additional coefficient paths; the linear interpolation forces coefficients to grow proportionally toward an LS solution. In lassoed boosting, we use the lasso in the first stage to screen variables and, for each subset of variables, we use LS-boost ([Friedman \(2001\)](#)) to grow coefficients in the second stage. We hypothesize that, for some data, a good solution may appear outside the grid of (proportional) solutions generated by the relaxed lasso; using boosting to rebuild coefficients allows

us to explore possibly better solutions. Our method complements the use of the relaxed lasso in practice.

Both lassoed boosting and the relaxed lasso can be connected to a strand of literature on refitting strategies (see, e.g., [Chzhen *et al.* \(2019\)](#) and references therein). The simple idea of combining the lasso with LS-boost comes with some obvious benefits. Using a large iteration number in the second stage, LS-boost should (a) mitigate the overshrinkage problem of the lasso; (b) remove the proportional constraints when spawning solutions so that coefficient paths can grow freely; and (c) give the estimation procedure a second chance, increasing the likelihood of finding a sparser model. Moreover, tuning both the lasso and LS-boost procedures should lead to better solutions.

This paper discusses the method of lassoed boosting and its good performance in the simulation experiment in [Hastie *et al.* \(2020\)](#) and an application. Based on the results in [Freund *et al.* \(2017\)](#) (hereafter FGM), we also discuss the convergence rate of lassoed boosting estimator. We apply lassoed boosting to predict equity returns and compare the results to several other methods. An R package `lboost` that implements our method can be found at <https://github.com/xhuang20/lboost>.

The rest of the paper is organized as follows. Section 2 discusses the convergence property of LS-boost and lassoed boosting. Section 3 introduces several other two-stage methods. Section 4 discusses the simulation experiment, and Section 5, the application to equity-returns prediction. Section 6 concludes. The online supplement contains all proofs, additional discussions, and figures.

2 Lassoed boosting

We begin by defining the lasso and LS-boost procedures. Consider n observations $\{(x_i, y_i)\}_1^n$, where $x_i = (x_{i1}, \dots, x_{ip})$ is the $1 \times p$ row vector of variables and y_i is the i th response variable. In matrix notation, define the $n \times 1$ vector \mathbf{y} and the $n \times p$ matrix \mathbf{X} with the j th column

\mathbf{x}_j and the i th row x_i . Let β^* be the true coefficient vector and $u_i \sim (0, \sigma^2)$. Let $\|\cdot\|_1$ and $\|\cdot\|_2$ be the ℓ_1 and ℓ_2 norms, respectively. Consider the linear regression model

$$\mathbf{y} = \mathbf{X}\beta^* + \mathbf{u}. \quad (1)$$

The LS solution $\hat{\beta}_{\text{LS}}$ is obtained by minimizing the following loss function:

$$L_n(\beta) = \frac{1}{2n} \|\mathbf{y} - \mathbf{X}\beta\|_2^2. \quad (2)$$

The lasso estimate, $\hat{\beta}^\lambda$, results from minimizing

$$\frac{1}{2n} \|\mathbf{y} - \mathbf{X}\beta\|_2^2 + \lambda \|\beta\|_1 \quad (3)$$

for some tuning parameter $\lambda > 0$. A sequence of λ s, $\{\lambda_q\}_0^Q$, is used to tune the coefficient solutions with $\lambda_0 = \max_j |\frac{1}{n} \langle \mathbf{x}_j, \mathbf{y} \rangle| > \lambda_1 > \dots > \lambda_Q$. Let \mathcal{A}_q be the active set of selected variables at step q and $\hat{\beta}^{\lambda_q}$ be the coefficient estimate. When $\lambda = \lambda_0$, no variable is selected and \mathcal{A}_0 is empty; the size of the active set increases as more variables are included in \mathcal{A}_q when λ decreases. When $\lambda = 0$, \mathcal{A}_q includes all variables and eq. (3) reduces to eq. (1).

The LS-boost algorithm works by choosing the variable x_{j_k} that best fits the current residual $\hat{\mathbf{u}}^{k-1}$ at each iteration step k and then updating the j_k th regression coefficient. Choose a learning rate $0 < \varepsilon < 1$. Initialize $\hat{\beta}^0 = 0$ and $\hat{\mathbf{u}}^0 = \mathbf{y}$. For each iteration $k \geq 1$,

Step 1. Select the variable \mathbf{x}_{j_k} with

$$j_k \in \underset{1 \leq j \leq p}{\operatorname{argmin}} \sum_{i=1}^n (\hat{u}_i^{k-1} - \hat{\beta}_j x_{ij})^2 \text{ with } \hat{\beta}_j = \frac{\sum_{i=1}^n \hat{u}_i^{k-1} x_{ij}}{\sum_{i=1}^n x_{ij}^2}.$$

Step 2. Update $\hat{\beta}^k$ and $\hat{\mathbf{u}}^k$ by

$$\hat{\beta}_{j_k}^k = \hat{\beta}_{j_k}^{k-1} + \varepsilon \hat{\beta}_{j_k}, \quad \hat{\beta}_j^k = \hat{\beta}_j^{k-1} \text{ for } j \neq j_k, \quad \text{and } \hat{\mathbf{u}}^k = \hat{\mathbf{u}}^{k-1} - \varepsilon \cdot \mathbf{x}_{j_k} \hat{\beta}_{j_k}.$$

Iterating between Step 1 and Step 2 until we reach a prespecified stopping criterion gives the solution paths. LS-boost can sometimes generate coefficient paths similar to those of the lasso, but they are two different methods in general.

2.1 The algorithm and its implementation

Lassoed boosting works by rebuilding coefficient paths for variables in each \mathcal{A}_q using LS-boost.

Algorithm 1: Lassoed boosting

- 1 **Assume** a sequence of Q tuning parameters $\{\lambda_q\}_1^Q$ for the lasso problem.
 - 2 **for** $q = 1$ to Q **do**
 - 3 Use the lasso to obtain an active set of variables, \mathcal{A}_q , for each λ_q .
 - 4 Use LS-boost to compute the coefficient path for each variable in \mathcal{A}_q .
 - 5 **end for**
 - 6 **return** Q sets of coefficient paths for validation or cross-validation.
-

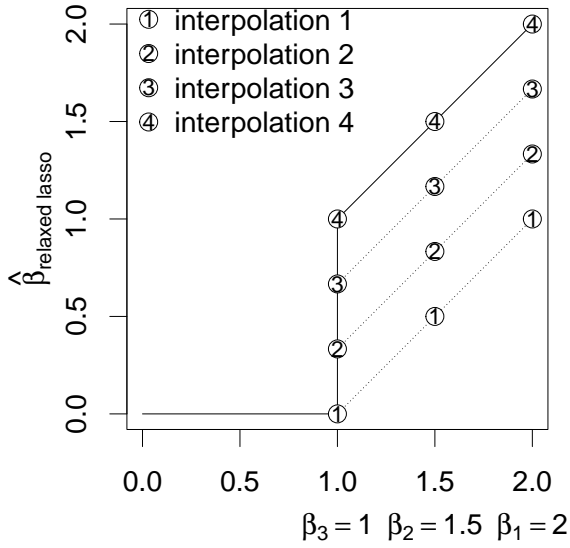
A few remarks are in order.

Remark 1. Both the relaxed lasso and lassoed boosting use the lasso in the first stage. Afterward, the relaxed lasso takes the lasso solution $\hat{\beta}^{\lambda_q}$, along with the full LS solution $\hat{\beta}_{\text{LS}}^{\lambda_q}$ for variables in \mathcal{A}_q and a sequence of weights such as $\{0, 0.33, 0.66, 1.0\}$, to generate the interpolated coefficient path

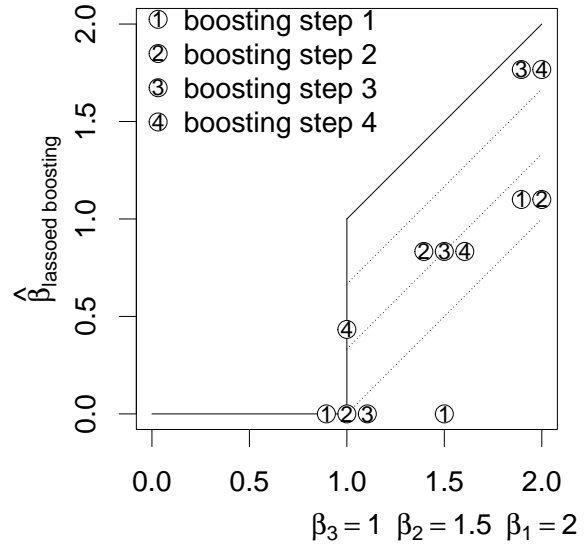
$$\hat{\beta}_{\text{relax}}^{\lambda_q} = \text{weight} \times \hat{\beta}_{\text{lasso}}^{\lambda_q} + (1 - \text{weight}) \times \hat{\beta}_{\text{LS}}^{\lambda_q}. \quad (4)$$

As long as the lasso solution paths are monotonic, eq. (4) creates a sequence of solution paths that grows proportionately toward the LS solution $\hat{\beta}_{\text{LS}}^{\lambda_q}$, and the computation cost is close to zero. Lassoed boosting does not use the lasso solution $\hat{\beta}_{\text{lasso}}^{\lambda_q}$ but only the variables in \mathcal{A}_q to start LS-boost, so the generated solution paths will differ from those of the relaxed lasso. Figure 1 illustrates this difference in the estimates for β_1, β_2 , and β_3 . Figures 1(c) and 1(d) compare interpolation step 2 and boosting step 2 for the two methods. The boosting estimates exhibit no proportional increase.

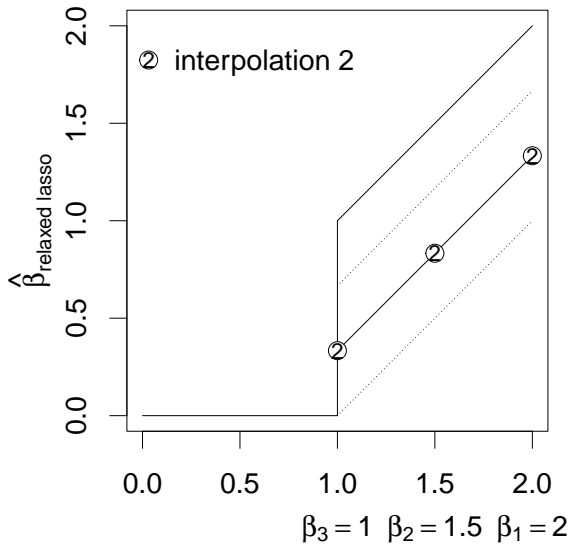
Remark 2. Our simulation and application indicate that lassoed boosting sometimes yields a sparser model (see Figures 1(c) and 1(d)). Starting with an active set $\mathcal{A}_q = (\mathbf{x}_1, \mathbf{x}_2, \mathbf{x}_3)$,



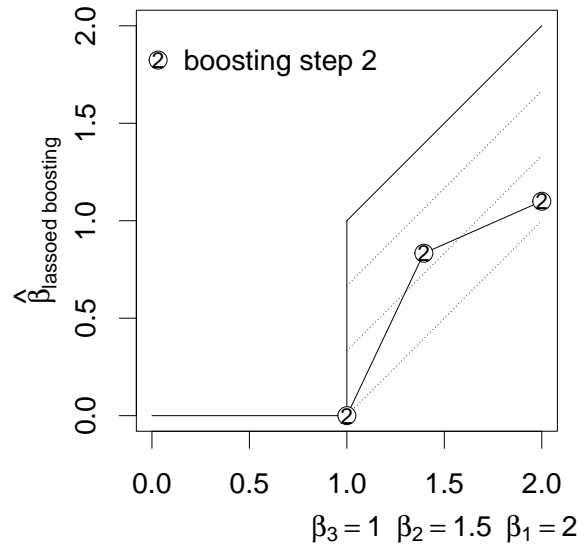
(a) Relaxed lasso solution paths



(b) Lassoed boosting solution paths



(c) Step 2 in relaxed lasso



(d) Step 2 in lassoed boosting

Figure 1: Figure 1(a) gives an example of the relaxed lasso solution paths for three parameters with linear interpolation weights (0, 0.33, 0.66, 1). Figure 1(b) shows a boosting solution path for the same three parameters with four steps. Figures 1(c) and 1(d) select the coefficient solutions of the second interpolation and the second boosting step, respectively.

the relaxed lasso pulls the lasso solution, marked ①, proportionately toward the LS solution, marked ④ in Figure 1(a), and all three β s increase in the second interpolation in Figure 1(c). With boosting, coefficients are updated one at a time and β_3 is not updated in step 2 in Figure 1(d) despite the fact that \mathbf{x}_3 is already included in the active set. Hence, given the same set of variables in \mathcal{A}_q , LS-boost might generate sparser solution paths than the relaxed lasso does.

Remark 3. The solution path of the relaxed lasso always includes the LS solution for a given active set, which is not the case for LS-boost. After four steps, the relaxed lasso reaches the LS solution in Figure 1(a), while the solution of LS-boost, marked ④ in Figure 1(b), does not. Using an information criterion such as the corrected AIC in Hurvich *et al.* (1998) for early stopping is a common practice in boosting to avoid overfitting. It is easy to verify that, for many data, a typical boosting solution stops short of the LS solution. One can increase the iteration number, but in practice there is no guarantee that the solution will be close to the LS solution even when $n > p$.

2.2 Convergence Results

In this section, we discuss the asymptotic convergence result for lassoed boosting. Let $\hat{\beta}^{\lambda_q, k}$ be the boosting solution at step k for the variables in the active set \mathcal{A}_q associated with λ_q . Let $K_{\mathcal{A}_q} = |\mathcal{A}_q|$ be the number of elements in \mathcal{A}_q . The active set for the true model is $\mathcal{A} = \{1, \dots, s\}$ and $K_{\mathcal{A}} = s$. We make the following assumptions for Propositions 1 and 2.

Assumption 1. The data are generated according to eq. (1) with $u_i \sim (0, \sigma^2)$. \mathbf{X} is deterministic.

Assumption 2. The parameter vector is s -sparse so $\beta^* = (\beta_1, \dots, \beta_s, 0, \dots, 0)^T$ and $s < p$.

We also implicitly assume $\log(p)/n \rightarrow 0$ in the proof of Propositions 1 and 2 in the supplement (Section S.1), but this assumption is not needed for Theorem 1.

2.2.1 The asymptotic rate

The following proposition shows that lassoed boosting shares the same loss-function convergence rate with the relaxed lasso in Theorem 6 in [Meinshausen \(2007\)](#).

Proposition 1. Under Assumptions 1 and 2, as $n \rightarrow \infty$, we have

$$\inf_{\lambda_q, k \in [1, \infty]} L_n(\hat{\beta}^{\lambda_q, k}) = O_p(n^{-1}).$$

The proof is given in Section S.1. The convergence rate for lassoed boosting is faster than the lasso's in Theorem 5 in [Meinshausen \(2007\)](#).

The relaxed lasso and lassoed boosting share the same fast convergence rate because both of their solution paths include the LS solution when the lasso correctly identifies the variables. This observation suggests that any lasso-based two-stage method that includes the LS solution in the second step will also enjoy the rate in Proposition 1. Proposition 2 summarizes this result. Let $\hat{\beta}_{\text{two-stage}}^{\lambda_q, \mathcal{K}}$ be a two-stage estimator that uses either the lasso solution or the active set \mathcal{A}_q to generate solution paths that include the full LS solution for each \mathcal{A}_q , and \mathcal{K} is the vector of all tuning parameters in the second stage.

Proposition 2. Under Assumptions 1 and 2, as $n \rightarrow \infty$,

$$\inf_{\lambda_q, \mathcal{K}} L_n(\hat{\beta}_{\text{two-stage}}^{\lambda_q, \mathcal{K}}) = O_p(n^{-1}).$$

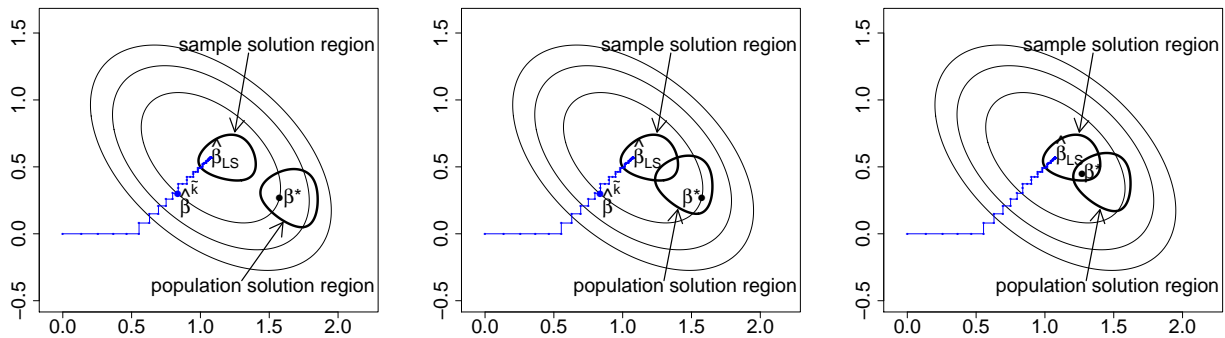
See Section S.1 for the proof. Proposition 2 indicates that the relaxed lasso and lassoed boosting are two examples of a large class of two-stage estimators.

2.2.2 Linear convergence of predictions

We begin our discussion of some linear convergence results for LS-boost and extend it to lassoed boosting on an active set \mathcal{A}_q . Let $\hat{\beta}^k$ be the LS-boost solution at step k ; $\hat{\beta}_{\text{LS}}^k$ a possibly non-unique least squares solution at step k ; and $\hat{\beta}_{\text{LS}}$ the full LS solution. Note that $\hat{\beta}_{\text{LS}}$ is non-unique when $p > n$. Theorem 2.1 in FGM gives the linear convergence result for

$\|\mathbf{X}\hat{\beta}^k - \mathbf{X}\hat{\beta}_{LS}\|_2$. First, we investigate the convergence result for $\|\mathbf{X}\hat{\beta}^k - \mathbf{X}\beta^*\|_2$.

Without any identification assumption, both $\hat{\beta}_{LS}$ and β^* are underidentified, as shown in Figure 2(a). The boosting solution converges to $\hat{\beta}_{LS}$, which is one of many solutions in the flat sample solution region, or the irregular shape at the center of the contour plot. The linear model in eq. (1) is also underidentified at the population level, leading to a flat population solution region in Figure 2(a). In general, the two regions do not completely overlap. Figures 2(b) and 2(c) show where they might intersect, and in Figure 2(c), $L_n(\hat{\beta}_{LS}) = L_n(\beta^*)$.



(a) Distinct solution regions

(b) Overlapping solution regions

(c) $\hat{\beta}_{LS}$ and β^* have the same LS loss

Figure 2: Assume there are two unidentified elements in β^* . The blue line is an LS-boost solution path starting from a zero vector and $\hat{\beta}^k$ is the boosting solution at step \tilde{k} . Figures 2(a) and 2(b) show $L_n(\hat{\beta}_{LS}) < L_n(\beta^*)$, and in Figure 1(c), $L_n(\hat{\beta}_{LS}) = L_n(\beta^*)$.

Let $\lambda_{\min}(\mathbf{X}^T\mathbf{X})$ be the smallest nonzero eigenvalue of $\mathbf{X}^T\mathbf{X}$ and define

$$\gamma := \left(1 - \frac{\varepsilon(2 - \varepsilon)\lambda_{\min}(\mathbf{X}^T\mathbf{X})}{4p}\right). \quad (5)$$

FGM show that $0.75 \leq \gamma < 1$. Let $\nabla L_n(\beta)$ be the gradient vector at β .

Theorem 1. Under Assumption 1, for $k \geq 0$, LS-boost has the following prediction bound:

$$\|\mathbf{X}\hat{\beta}^k - \mathbf{X}\beta^*\|_2 \leq \|\mathbf{X}\hat{\beta}_{LS}^k\|_2 \gamma^{k/2} + \sqrt{2n\|\nabla L_n(\beta^*)\|_2 \cdot \|\hat{\beta}_{LS} - \beta^*\|_2}. \quad (6)$$

A proof is given in the online supplement. Compared to Theorem 2.1 in FGM, eq. (6) has an extra term that relates to the gradient vector and the ℓ_2 error of $\hat{\beta}_{LS}$. Without additional

assumptions, this extra term will not disappear as $k \rightarrow \infty$.

Remark 4. In the special case when β^* is located inside the sample solution region (see Figure 2(c)), $\|\nabla L_n(\beta^*)\|_2 = 0$ and eq. (6) reduces to the result in Theorem 2.1 in FGM. This result holds even when $\|\hat{\beta}_{\text{LS}} - \beta^*\|_2 > 0$.

Clearly, eq. (6) indicates that, in a finite sample case when $n \not\rightarrow \infty$, LS-boost prediction will not recover the true sparse regression function, $\mathbf{X}\beta^*$. Theorem 12.2 in Bühlmann and van de Geer (2011) and Theorem 1 in Bühlmann (2006) show that, as both $n \rightarrow \infty$ and $k \rightarrow \infty$, $\|\mathbf{X}\hat{\beta}^k - \mathbf{X}^T\beta^*\|_2^2/n = o_p(1)$. This result does not contradict the nonasymptotic result in eq. (6). A heuristic argument follows.

Remark 5. As $n \rightarrow \infty$ and sample data get closer to population, the sample solution region will converge to the population solution region at the center. We expect $\nabla L_n(\beta^*) \rightarrow 0$ in eq. (6), so the second term in eq. (6) will disappear asymptotically, and we will have $\|\mathbf{X}\hat{\beta}^k - \mathbf{X}\beta^*\|_2^2/n \rightarrow o_p(1)$ when $k \rightarrow \infty$. Section S.2 provides a more detailed explanation.

Remark 6. Both Theorem 12.2 of Bühlmann and van de Geer (2011) and Theorem 1 present a prediction convergence result. How do they compare? Theorem 1 uses an exponential function to the base of γ to characterize the convergence of $\|\mathbf{X}\hat{\beta}^k - \mathbf{X}\beta^*\|_2^2/n$ as $k \rightarrow \infty$, while Theorem 12.2 in Bühlmann and van de Geer (2011) relies on a power function of k to achieve the same goal. See Section S.2 for a more detailed discussion.

Next, we discuss the faster convergence rate of lassoed boosting. Let $|\mathcal{A}_q| = p_q$. Consider two active sets \mathcal{A}_{q_1} and \mathcal{A}_{q_2} that are generated on the lasso solution path. We focus on the specific case when $p_{q_1} < p_{q_2} < n$ with either $n < p$ or $n \geq p$ and discuss why it is worth considering.

The linear convergence rate γ plays a critical role in determining the speed of convergence in Theorem 1 and Theorem 2.1 in FGM. Figure 4 in FGM shows a general pattern: γ decreases, and $\lambda_{\text{pmin}}(\mathbf{X}^T\mathbf{X})$ increases as p increases. However, the two relationships are not

strictly monotonic, suggesting that the convergence will be faster as p increases, in agreement with result (ii) in Theorem 2.1 of FGM

$$\|\hat{\beta}^k - \hat{\beta}_{\text{LS}}^k\|_2 \leq \frac{\|\mathbf{X}\hat{\beta}_{\text{LS}}\|_2}{\sqrt{\lambda_{\text{pmin}}(\mathbf{X}^T\mathbf{X})}}\gamma^{k/2}. \quad (7)$$

A similar conclusion can be drawn for the convergence result in Theorem 1. We would expect the opposite: the convergence for the estimator and the prediction will slow down when p increases and more variables add “noise” and competition to the variable selection process.

We provide an alternative explanation to complement the results in Figure 4 in FGM. Notice it represents cases when $p > n$ with $n = 50$ and $p \geq 73$. The same figures will give a different pattern when $p < n$. In lassoed boosting, we apply LS-boost sequentially to variables in $\{\mathcal{A}_q\}_{q=1}^Q$. If the lasso does a good job, and the model really is sparse, we expect that in the early stage of variable selection, some of the \mathcal{A}_q will include the correct variables and $|\mathcal{A}_q|$ will be much smaller than n ($\ll n$). For a sparse model, those active sets with $|\mathcal{A}_q| \ll n$ are arguably the most interesting since the boosting solutions spawned on these sets will be more likely to mimic the true and sparse elements in β^* . LS-boost on each \mathcal{A}_q can be viewed as separate exercises. We can add the subscript \mathcal{A}_q to results in Theorem 1 and eq. (7). Consider eq. (7) for the active set \mathcal{A}_q with $|\mathcal{A}_q| \ll n$.

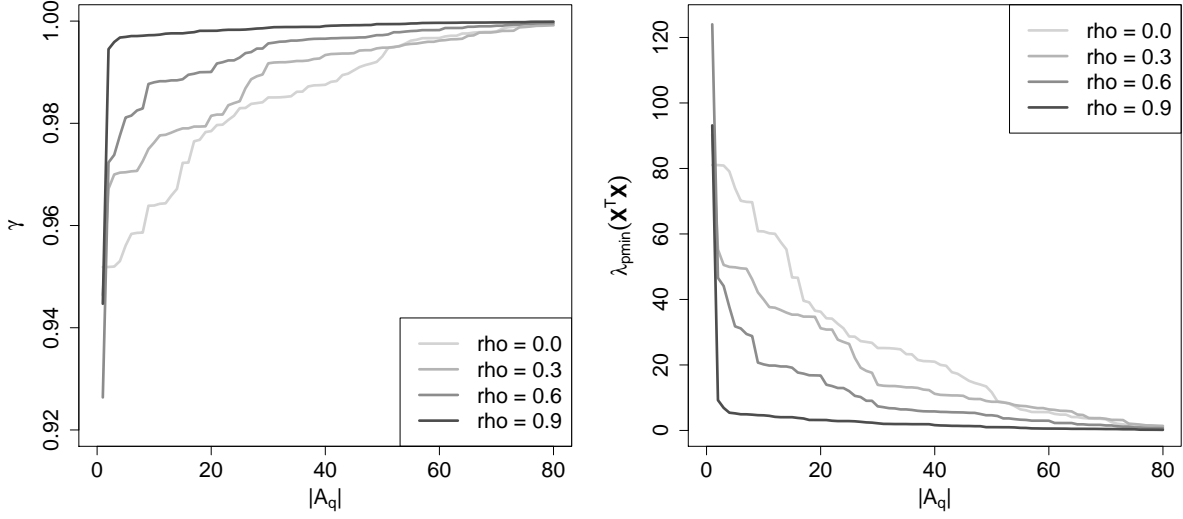
$$\|\hat{\beta}_{\mathcal{A}_q}^k - \hat{\beta}_{\text{LS},\mathcal{A}_q}^k\|_2 \leq \frac{\|\mathbf{X}_{\mathcal{A}_q}\hat{\beta}_{\text{LS},\mathcal{A}_q}\|_2}{\sqrt{\lambda_{\text{pmin}}(\mathbf{X}_{\mathcal{A}_q}^T\mathbf{X}_{\mathcal{A}_q})}}\gamma_{\mathcal{A}_q}^{k/2}, \quad (8)$$

where all quantities are restricted to the active set \mathcal{A}_q and

$$\gamma_{\mathcal{A}_q} := \left(1 - \frac{\varepsilon(2 - \varepsilon)\lambda_{\text{pmin}}(\mathbf{X}_{\mathcal{A}_q}^T\mathbf{X}_{\mathcal{A}_q})}{4p_q}\right). \quad (9)$$

Since $|\mathcal{A}_q| < n$, all parameters can be identified.

Next, we show a simulation result that describes $\gamma_{\mathcal{A}_q}$ and $\lambda_{\text{pmin}}(\mathbf{X}_{\mathcal{A}_q}^T\mathbf{X}_{\mathcal{A}_q})$ as a function of $|\mathcal{A}_q|$. Figure 3 describes the relationship of the linear convergence rate and minimum eigenvalue with $p_q(= |\mathcal{A}_q|)$ when $p_q < n$. It reverses the patterns in Figure 4 in FGM.



(a) plot of γ as $|\mathcal{A}_q|$ increases

(b) plot of $\lambda_{\text{pmin}}(\mathbf{X}_{\mathcal{A}_q}^T \mathbf{X}_{\mathcal{A}_q})$ as $|\mathcal{A}_q|$ increases

Figure 3: Simulation results for $\gamma_{\mathcal{A}_q}$ and $\lambda_{\text{pmin}}(\mathbf{X}_{\mathcal{A}_q}^T \mathbf{X}_{\mathcal{A}_q})$ with $n = 100$ and $|\mathcal{A}_q| \leq 80$. The symbol ρ refers to correlation among variables. Figure 3(a) shows $\gamma_{\mathcal{A}_q}$ is an increasing function of $|\mathcal{A}_q|$. Figure 3(b) shows $\lambda_{\text{pmin}}(\mathbf{X}_{\mathcal{A}_q}^T \mathbf{X}_{\mathcal{A}_q})$ is a decreasing function of $|\mathcal{A}_q|$.

We stress that both figures are correct, but Figure 3 helps to explain the convergence rate when $p_q < n$. As the lasso penalty parameter λ_q decreases, and p_q increases, the minimum eigenvalue of $\mathbf{X}_{\mathcal{A}_q}^T \mathbf{X}_{\mathcal{A}_q}$ will decrease monotonically and remain positive. Such decrease in minimum eigenvalue as matrix dimension increases is a standard result in matrix theory (see, e.g., Theorem 4.3.8 in Horn and Johnson (1985)). Figure 3(b) and eq. (9) imply Figure 3(a). Hence, for two active sets \mathcal{A}_{q_1} and \mathcal{A}_{q_2} with $p_{q_1} < p_{q_2} < n$, we have $\gamma_{\mathcal{A}_{q_1}} < \gamma_{\mathcal{A}_{q_2}}$ and the convergence rate for $\hat{\beta}_{\mathcal{A}_q}^k$ in eq. (8) is faster when boosting on \mathcal{A}_{q_1} than on \mathcal{A}_{q_2} . This result applies to both eq. (8) and Theorem 1 after we replace $\mathbf{X}^T \mathbf{X}$ with $\mathbf{X}_{\mathcal{A}_q}^T \mathbf{X}_{\mathcal{A}_q}$ in lassoed boosting. It is beneficial, particularly in the early stages of the lasso; when \mathcal{A}_q includes correct variables and $p_q < n$, the parameters are identified; convergence is faster; and the convergence rate for prediction in Theorem 1 is also faster. When $|\mathcal{A}_q| > n$, parameters are underidentified and $\hat{\beta}_{\text{LS}, \mathcal{A}_q}^k$ in eq. (8) may differ for each k and \mathcal{A}_q .

3 Additional examples of two-stage procedure

In this section, we give several additional examples of two-stage estimators.

3.1 Lassoed forward stagewise regression

The forward stagewise regression algorithm in [Hastie *et al.* \(2009\)](#) is a popular method for building coefficients and the regression function in small steps. In the k th step, it identifies the predictor \mathbf{x}_{j_k} that best correlates with the current residual \mathbf{r}_k and makes the following update:

$$\hat{\beta}_{j_k}^{k+1} = \hat{\beta}_{j_k}^k + \varepsilon \cdot \text{sign}(\mathbf{r}_k^T \mathbf{x}_{j_k}), \hat{\beta}_j^{k+1} = \hat{\beta}_j^k \text{ for } j \neq j_k, \text{ and } \mathbf{r}_{k+1} = \mathbf{r}_k - \varepsilon \cdot \text{sign}(\mathbf{r}_k^T \mathbf{x}_{j_k}) \mathbf{x}_{j_k}. \quad (10)$$

This algorithm can also be implemented on lasso-generated active sets. We call it lassoed forward stagewise regression.

Like [Theorem 1](#), [Theorem 2](#) in the online supplement gives a convergence result for the prediction function of the estimator in [Algorithm 2](#). In the case of $p_q < n$, applying [Theorem 2](#) to the active set \mathcal{A}_q and using the same argument as for lassoed boosting, we conclude that the convergence rate for lassoed forward stagewise regression is faster.

Algorithm 2: Lassoed forward stagewise regression

- 1 **Assume** a sequence of Q tuning parameters $\{\lambda_q\}_1^Q$ for the lasso problem.
 - 2 **for** $q = 1$ to Q **do**
 - 3 Use the lasso to obtain an active set of predictors, \mathcal{A}_q , for each λ_q .
 - 4 Use forward stagewise regression to compute the coefficient path for each predictor in \mathcal{A}_q .
 - 5 **end for**
 - 6 **return** Q sets of coefficient paths for validation (or cross-validation) purposes.
-

3.2 Twiced lasso

[Hastie *et al.* \(2009, p. 91\)](#) write, “one can use the lasso to select the set of non-zero predictors,

and then apply the lasso again, but using only the selected predictors from the first step. This is known as the *relaxed lasso* (Meinshausen, 2007).” The idea of using the lasso twice refers to the “Simple Algorithm” in Meinshausen (2007, p. 377), where after obtaining the active set \mathcal{A}_q , the lasso is applied again on \mathcal{A}_q with the penalty parameter on $[0, \lambda_q]$. Algorithm 3 describes the procedure of lassoing twice, and we call it twiced lasso.

Algorithm 3: Twiced lasso

- 1 **Assume** a sequence of Q tuning parameters $\{\lambda_q\}_1^Q$ for the lasso problem
 - 2 **for** $q = 1$ to Q **do**
 - 3 Use the lasso to obtain an active set of variables, \mathcal{A}_q , for each λ_q .
 - 4 Apply the lasso again on \mathcal{A}_q to compute the coefficient path for each predictor in \mathcal{A}_q with $\{\lambda_1, \dots, \lambda_Q\}$.
 - 5 **end for**
 - 6 **return** Q sets of coefficient paths for validation (or cross-validation) purposes.
-

The key difference between twiced lasso and the relaxed lasso is, in step 4 of Algorithm 3, the former always starts at λ_1 while the latter starts at λ_{q+1} . Obviously, starting from λ_1 for every \mathcal{A}_q creates computational redundancy. However, the formulation in Algorithm 3 allows direct comparison with lassoed boosting in Algorithm 1 and helps to explain the change in the convergence rate.

Adapt the restricted eigenvalues condition in equation (11.10) in Hastie *et al.* (2015) to the active set \mathcal{A}_q and we have, as a constant $\tilde{\lambda} > 0$,

$$\frac{\nu^T \left(\mathbf{X}_{\mathcal{A}_q}^T \mathbf{X}_{\mathcal{A}_q} / n \right) \nu}{\|\nu\|_2^2} \geq \tilde{\lambda} \text{ for all nonzero } \nu \text{ in a constrained set } \mathcal{C}. \quad (11)$$

The constrained set \mathcal{C} defines directions along which parameters can be identified. The discussion on lassoed boosting also applies here. When the lasso does a good job selecting variables in step 3 of Algorithm 3, \mathcal{A}_q contains the correct variables, and $p_q < n$. In this case, the least-squares loss is strictly convex ($\nabla^2 L_n(\beta) = \mathbf{X}_{\mathcal{A}_q}^T \mathbf{X}_{\mathcal{A}_q} / n$ is positive definite) and eq. (11) holds for all $\nu \in \mathbb{R}^{p_q}$. Hence, $\tilde{\lambda} = \lambda_{\text{pmin}}(\mathbf{X}_{\mathcal{A}_q}^T \mathbf{X}_{\mathcal{A}_q} / n)$, and as Figure 3(b) suggests, $\tilde{\lambda}$

decreases as p_q increases. Theorem 11.1 in [Hastie *et al.* \(2015\)](#) implies

$$\|\hat{\beta}_{\mathcal{A}_q} - \beta_{\mathcal{A}_q}^*\|_2 \leq \frac{3}{\lambda_{\text{pmin}}(\mathbf{X}_{\mathcal{A}_q}^T \mathbf{X}_{\mathcal{A}_q}/n)} \sqrt{\frac{p_q}{n}} \sqrt{n} \lambda_n, \quad (12)$$

where λ_n is the tuning parameter such that $\lambda_n \geq 2\|\mathbf{X}_{\mathcal{A}_q}^T \mathbf{u}\|_\infty/n > 0$. A smaller p_q will tighten the bound in eq. (12), implying a faster convergence rate.

Remark 7. In sum, in the twiced lasso, the first-stage screening can pare down the number of variables so that the convergence rate for the second-stage lasso estimator will be faster when $p_q < n$.

When $s \leq p_q < n$, and \mathcal{A}_q correctly includes the nonzero variables, the non-zero elements of $\beta_{\mathcal{A}_q}^*$ are equal to those in β^* .

3.3 Twiced boosting

Another extension uses boosting twice. Step 1 in Algorithm 4 uses LS-boost to screen variables and organizes them into sequentially increasing sets. Step 2 uses LS-boost again to grow the coefficient paths on each active set. The iteration stopping criterion in step 1 is when the active set includes all variables, and we can use the standard AIC-type criterion to stop boosting in the second stage.

Algorithm 4: Twiced boosting

- 1 **Run** a first round of LS-boost to obtain a sequence of Q different active sets of variables, \mathcal{A}_q with $q = 1, \dots, Q$ — not the same \mathcal{A}_q from the lasso procedure.
 - 2 **for** $q = 1$ to Q **do**
 - 3 Run LS-boost on each active set of variables, \mathcal{A}_q , and obtain coefficient paths for all predictors in \mathcal{A}_q .
 - 4 **end for**
 - 5 **return** Q sets of coefficient paths for validation (or cross-validation) purposes
-

Algorithm 4 differs from the twin boosting algorithm in [Bühlmann and Hothorn \(2010\)](#). Twin boosting uses the estimate in the first stage to guide variable selection in the second stage, similar to the idea of the adaptive lasso in [Zou \(2006\)](#).

4 Monte Carlo simulation

Our Monte Carlo simulations study the performance of five estimators: forward stepwise, lasso, lassoed boosting, relaxed lasso, and twiced lasso (see online supplement). We do not consider the best subset selection method in [Bertsimas *et al.* \(2016\)](#) due to its computation cost. Our simulation design is the same as that in [Hastie *et al.* \(2020\)](#) except that we use 50, rather than 10, equally spaced values between 0 and 1 as weights for the relaxed lasso.

4.1 Simulation setup

The data-generating process (DGP) is determined by a combination of 4 beta types, 4 sample-size and sparsity patterns, 3 error correlation values, and 10 signal-to-noise (SNR) levels, for a total of $480 (= 4 \times 4 \times 3 \times 10)$ DGPs.

Beta types. We consider four coefficient settings for the sparse coefficient β^* .

beta-type 1: β^* has s elements equal to 1, equally spaced between 1 and p , and the rest equal to 0;

beta-type 2: The first s elements of β^* equal 1, and the rest equal 0;

beta-type 3: The first s elements of β^* equal s interpolated values between 10 and 0.5, and the rest equal 0;

beta-type 5: The first s elements of β^* equal 1. The rest decay to 0, $\beta_i^* = 0.5^{i-s}$ for $i = s + 1, \dots, p$.

The first three beta-types are considered in [Bertsimas *et al.* \(2016\)](#); beta-type 5 is added in [Hastie *et al.* \(2020\)](#). We do not consider beta-type 4 in [Bertsimas *et al.* \(2016\)](#) due to its similar result to beta-type 3.

Size and sparsity. We consider the following data size and sparsity combinations:

- low: $n = 100, p = 10, s = 5$
- medium: $n = 500, p = 100, s = 5$
- high-5: $n = 50, p = 1000, s = 5$
- high-10: $n = 100, p = 1000, s = 10$

Error correlation. We try $\rho = 0, 0.3$ and 0.7 in the DGP.

SNR levels. The SNR level takes 10 values: $v = (0.05, 0.09, 0.14, 0.25, 0.42, 0.71, 1.22, 2.07, 3.52, 6.00)$.

Let $\hat{\beta}$ be the estimated coefficient from one of the five methods.

Evaluation metrics. We apply the following four evaluation metrics on the test data:

- Relative risk:

$$\text{RR}(\hat{\beta}) = \frac{E(x_0^T \hat{\beta} - x_0^T \beta^*)^2}{E(x_0^T \beta^*)^2} = \frac{(\hat{\beta} - \beta^*)^T \Sigma (\hat{\beta} - \beta^*)}{\beta^{*T} \Sigma \beta^*}.$$

$\text{RR}(\hat{\beta}) = 0$ if $\hat{\beta} = \beta^*$; $\text{RR}(\hat{\beta}) = 1$ if $\hat{\beta} = 0$ (the null model.)

- Relative test error:

$$\text{RTE}(\hat{\beta}) = \frac{E(y_0 - x_0^T \hat{\beta})^2}{\sigma^2} = \frac{(\hat{\beta} - \beta^*)^T \Sigma (\hat{\beta} - \beta^*) + \sigma^2}{\sigma^2}.$$

$\text{RTE}(\hat{\beta}) = 1$ if $\hat{\beta} = \beta^*$; $\text{RTE}(\hat{\beta}) = \text{SNR} + 1$ if $\hat{\beta} = 0$.

- Proportion of variance explained:

$$\text{PVE}(\hat{\beta}) = 1 - \frac{E(y_0 - x_0^T \hat{\beta})^2}{\text{Var}(y_0)} = 1 - \frac{(\hat{\beta} - \beta^*)^T \Sigma (\hat{\beta} - \beta^*) + \sigma^2}{\beta^{*T} \Sigma \beta^* + \sigma^2}.$$

$\text{PVE}(\hat{\beta}) = \text{SNR}/(1 + \text{SNR})$ if $\hat{\beta} = \beta^*$; $\text{PVE}(\hat{\beta}) = 0$ if $\hat{\beta} = 0$.

- Number of nonzeros: $\text{NNZ}(\hat{\beta}) = \|\hat{\beta}\|_0 = \sum_{j=1}^p 1\{\hat{\beta}_j \neq 0\}$. In figures that plot $\|\hat{\beta}\|_0$, we also print the number (averaged over 10 replications) of correctly identified coefficients for each method at each SNR level, which allows us to infer the true- and false- positive rates in variable recovery.

The simulation study has the following steps:

Step 1 Data simulation Choose a beta-type for β^* . Draw rows of \mathbf{X} i.i.d. from $N(0, \Sigma_{p \times p})$, where the ij th element of Σ is $\rho^{|i-j|}$ with $\rho = 0, 0.35$ or 0.7 . Draw \mathbf{y} from $N(\mathbf{X}\beta^*, \sigma^2 \mathbf{I}_n)$ and $\sigma^2 = \beta^{*T} \Sigma \beta^* / v$.

Step 2 Model selection Run each method on (\mathbf{X}, \mathbf{y}) with a sequence of tuning parameters; select a tuning parameter by minimizing prediction error on a validation set the same size as (\mathbf{X}, \mathbf{y}) and generated independently.

Step 3 Model evaluation Record four metrics.

Step 4 Average Repeat steps 1 to 3 ten times and compute the average of all metrics.

Parameter tuning again follows that in [Hastie *et al.* \(2020\)](#). We use the R package `glmnet` to generate the lasso solutions and to select variables for lassoed boosting. We use 50 values of λ for the lasso at the low setting and 100 values of λ in the other three settings. We also use 50 values of equally spaced weights between 0 and 1 for the relaxed lasso. The forward stepwise procedure is tuned up to 50 steps. We use the R package `mboost` to apply LS-boost to each active set of variables. Early stopping in boosting typically prevents an LS solution, while the relaxed lasso can always reach a full LS solution. To reduce the difference between lassoed-boosting and relaxed-lasso solutions, we use the corrected AIC in [Hurvich *et al.* \(1998\)](#) to obtain the iteration number and then double it as the final stopping criterion in LS-boost. In the interval between 1 and the final stopping number, we use 50 equally spaced steps and extract the corresponding LS-boost coefficients on each \mathcal{A}_q . The learning rate is set to 0.01.

Like [Hastie *et al.* \(2020\)](#), for all methods, we use a training set to generate solution paths, a validation set to select the best solution, and a test set to compute the final prediction. Hence, our results require no direct tuning of the lasso penalty parameter λ .

Lassoed boosting is more computationally expensive than the relaxed lasso. By the time the lasso and the relaxed lasso finishes, lassoed boosting just gets started at generating solutions for each of the active set. We can employ parallelization and warm starts to improve the speed and reduce redundancy in computation.

4.2 Simulation results

This discussion focuses on cases for beta-type 2 and $\rho = 0.35$ based on validation tuning. The supplement includes the complete set of results for both validation and oracle tuning, where parameters are chosen to minimize the average risk over 10 replications. We also skip the results for the twiced lasso because they resemble those for the relaxed lasso, but they are reported in all figures in the supplement.

Figures 4 to 7 plot the average of relative risk (RR), relative test error (RTE), proportion of variance explained (PVE), and number of nonzero (NNZ) coefficients for each of the data size-and-sparsity combinations over 10 replications. The dotted line in the RTE plots is the RTE of the null model; the dotted line in the PVE plots is the perfect score $\text{SNR}/(1 + \text{SNR})$; the horizontal dotted line in the number of nonzeros plots is the value of s . On top of each NNZ plot, we print the average number of correctly identified variables over 10 replications for each method at each of the 10 SNR levels, allowing us to infer the true positive rate.

In the RR plots across Figures 4 to 7, the performance of lassoed boosting and the relaxed lasso are much the same, except for a small difference in Figure 6. In Figures 4 and 5 with small and medium settings, lassoed boosting and the relaxed lasso outperform forward stepwise and the lasso when SNR is low; the performance of all four methods starts to converge when SNR increases. In Figures 6 and 7 with large p , forward stepwise and the lasso seem to outperform the other two methods when SNR is small. However, some low SNR results must be interpreted with caution. For example, in the NNZ plot, the lasso, lassoed boosting, and the relaxed lasso can barely identify any correct variable, and the RR score is larger than 1. Forward stepwise sticks to the null model at very low SNR values and obtains a null score of $RR = 1$.

In all RTE plots in Figures 4 to 7, lassoed boosting and the relaxed lasso perform almost identically, and significantly outperform the other two methods when SNR is relatively high. The only exception appears in Figure 5, where the RTE of forward stepwise is the smallest of the four when SNR is relatively large, though the numerical difference is small compared

to that of lassoed boosting and the relaxed lasso.

In the PVE plots in Figures 4 and 5, all four methods give good results that seems to improve as SNR increases. This result is no surprise since all methods better identify the correct variables at higher SNR. In Figures 6 and 7, lassoed boosting and relaxed lasso perform similarly and better than the other options at most of the SNR levels.

In the NNZ plots across all four figures, lassoed boosting and the relaxed lasso show similar capability in sparsity recovery. In Figure 4, when SNR is relatively high, all methods recover the true variables; the relaxed lasso achieves slightly sparser models than lassoed boosting. However, when SNR decreases, lassoed boosting sometimes achieves sparser models while identifying, on average, the same number of nonzero parameters. The NNZ plot in Figure 6 seems to suggest that the relaxed lasso performs better when SNR is low, which is not generally the case (see the third row in Figure 8 for instances when lassoed boosting yields sparser models at low SNR levels). Again, in Figure 6, almost no nonzero parameter is recovered when SNR is low, making any comparison dubious.

The first three metrics seems to suggest that lassoed boosting and the relaxed lasso share similar coefficient paths, but the NNZ plots in Figures 4 to 7 demonstrate that they differ. Several examples of beta-types 1 and 3 in Figure 8 from the supplement show that lassoed boosting produces sparser models in quite a few cases, and while the lasso can recover the true parameters, its false inclusion rate is high. Furthermore, from the NNZ plots, we conclude that all methods may fail to recover variables correctly when SNR is very low.

Overall, we can roughly conclude that the performance of lassoed boosting is comparable to that of the relaxed lasso in the first three metrics, and it can produce a sparser model under certain scenarios, which happens more likely when the SNR is moderately large in validation tuning (see Figure 8 for several examples). We can also easily spot multiple occasions when the relaxed lasso gives sparser models.

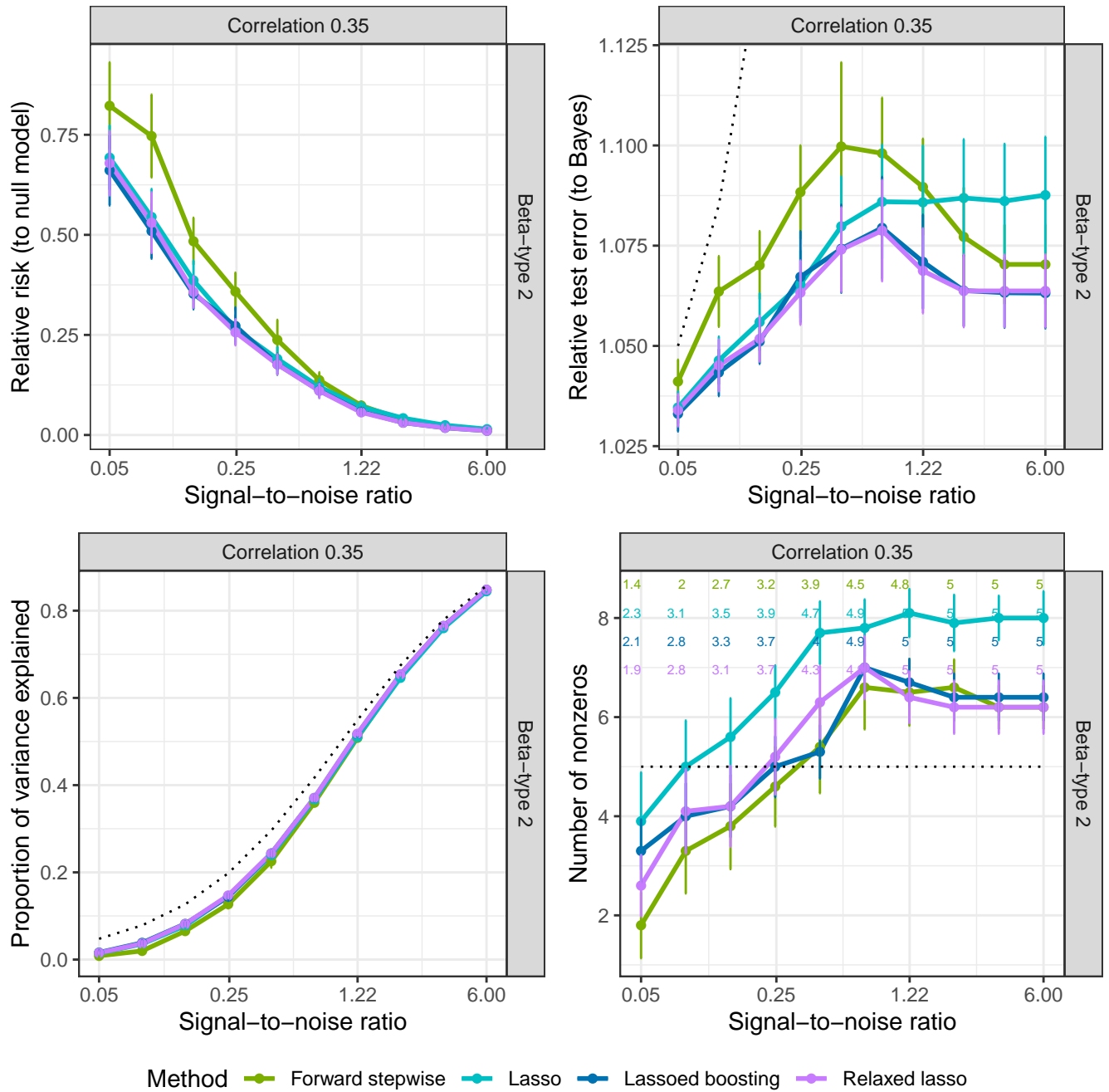


Figure 4: Curves of relative risk, relative test error, proportion of variance explained, and number of nonzeros as a function of SNR in the low setting with $n = 100$, $p = 10$, and $s = 5$. The numbers at the top of the nonzeros figure are the average variables correctly identified by each method at each of the 10 SNR values. The order of the numbers, from row 1 to row 4, matches the order of the four legend labels from left to right.

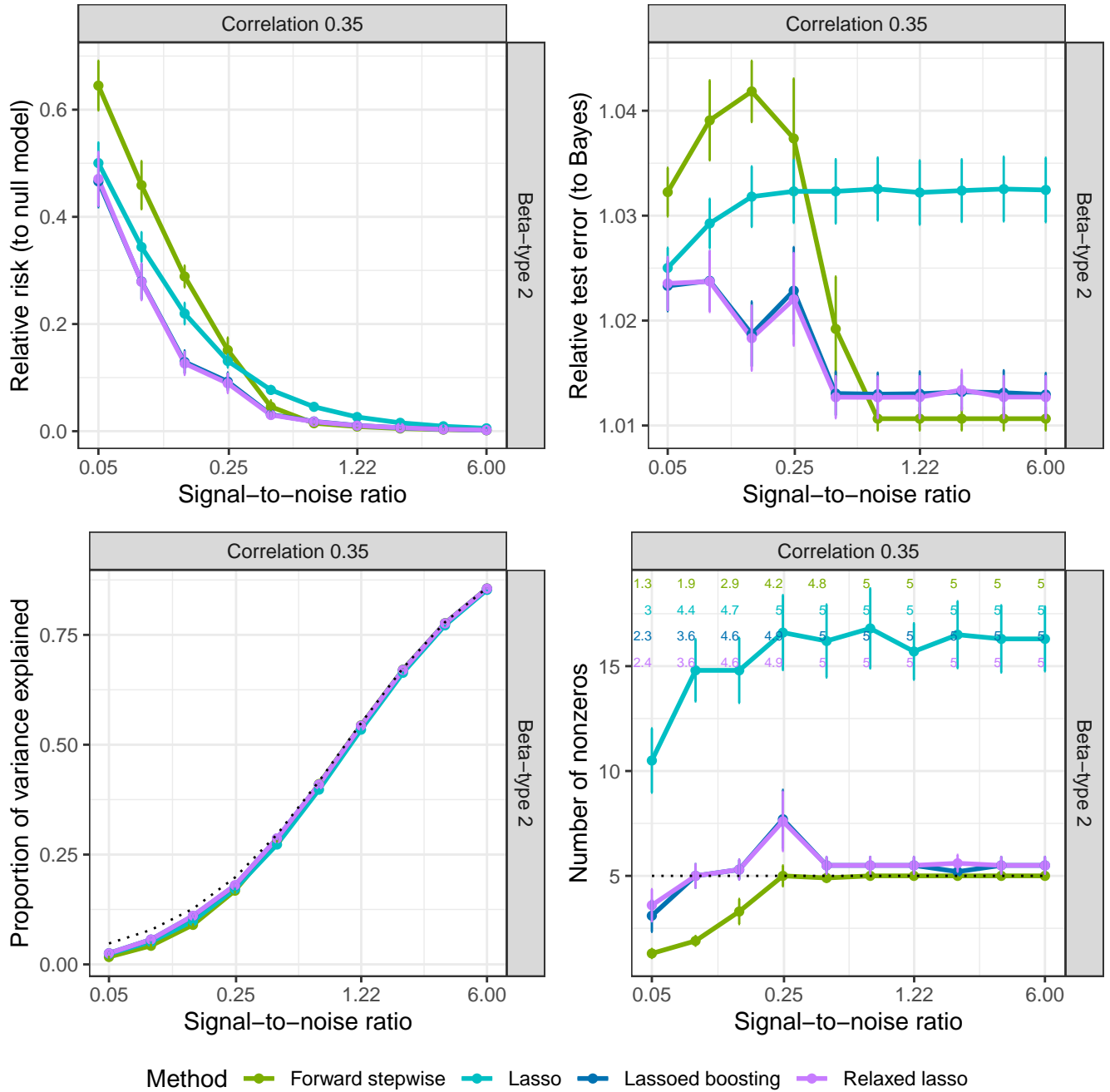


Figure 5: Curves of relative risk, relative test error, proportion of variance explained, and number of nonzeros as a function of SNR in the medium setting with $n = 500$, $p = 100$, and $s = 5$. The numbers at the top of the nonzeros figure are the average variables correctly identified by each method at each of the 10 SNR values. The order of the numbers, from row 1 to row 4, matches the order of the four legend labels from left to right.

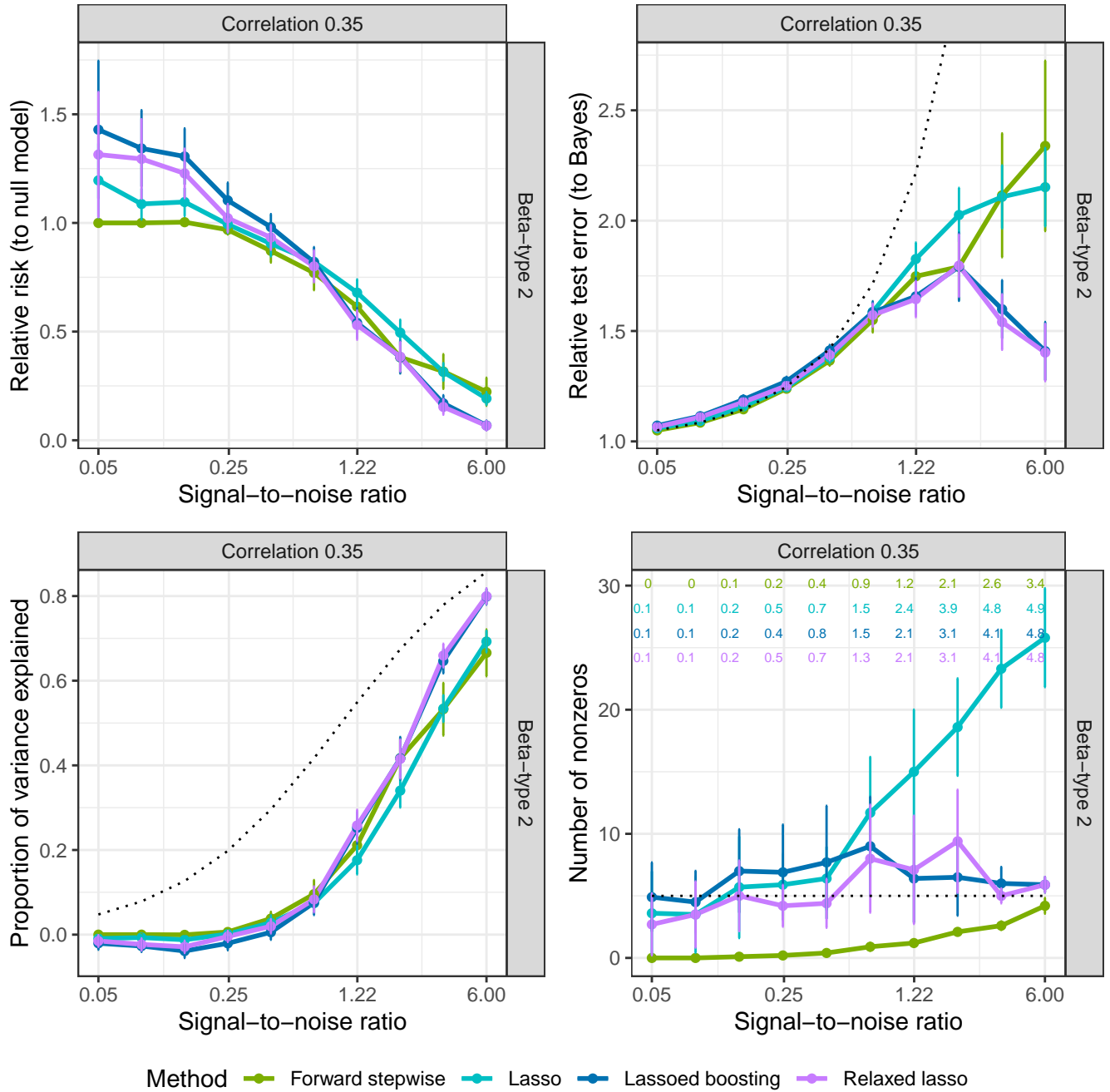


Figure 6: Curves of relative risk, relative test error, proportion of variance explained, and number of nonzeros as a function of SNR in the high-5 setting with $n = 50, p = 1000$, and $s = 5$. The numbers at the top of the nonzeros figure are the average variables correctly identified by each method at each of the 10 SNR values. The order of the numbers, from row 1 to row 4, matches the order of the four legend labels from left to right.

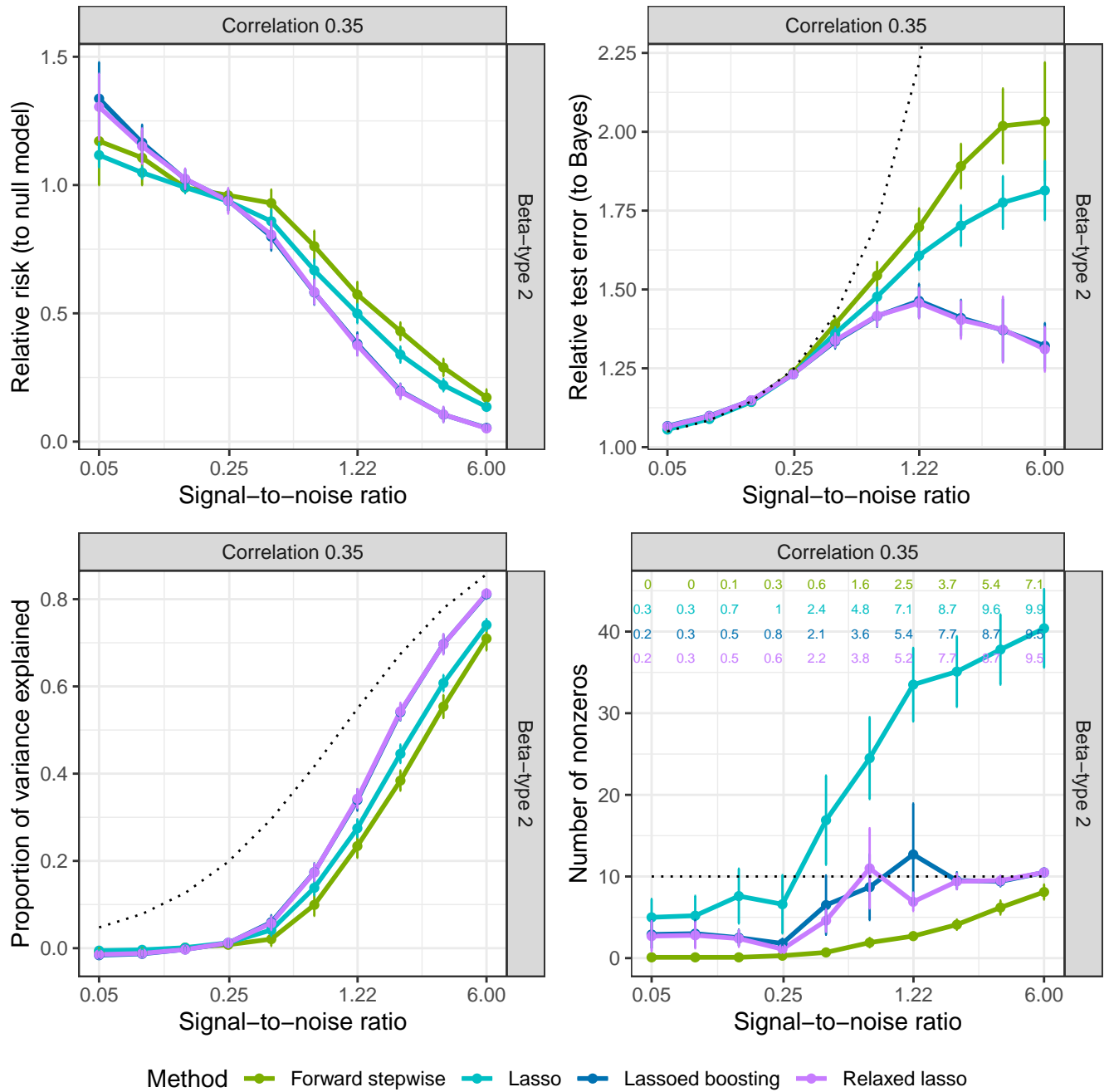


Figure 7: Curves of relative risk, relative test error, proportion of variance explained, and number of nonzeros as a function of SNR in the high-10 setting with $n = 100, p = 1000$, and $s = 10$. The numbers at the top of the nonzeros figure are the average variables correctly identified by each method at each of the 10 SNR values. The order of the numbers, from row 1 to row 4, matches the order of the four legend labels from left to right.

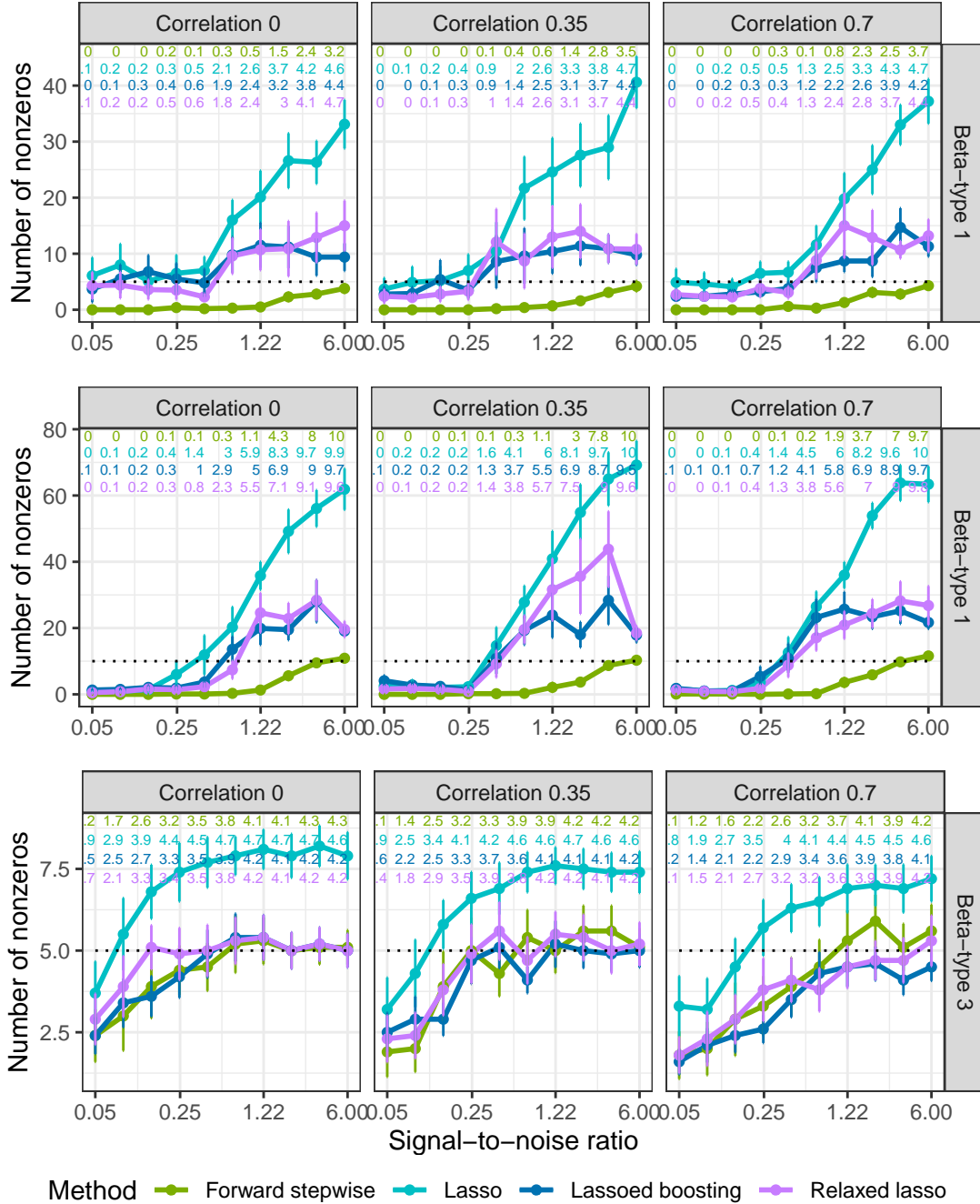


Figure 8: Top row: NNZ plots for beta-type 1 in the high-5 setting with $n = 50, p = 1000, s = 5$. Middle row: NNZ plots for beta-type 1 in the high-10 setting with $n = 100, p = 1000, s = 10$. Bottom row: NNZ plots for beta-type 3 in the low setting with $n = 100, p = 10, s = 5$. The numbers at the top of each figure are the average variables correctly identified by each method at each of the 10 SNR values. The order of the numbers, from row 1 to row 4, matches the order of the four legend labels from left to right.

5 An application in equities return prediction

In this section, we compare the prediction accuracy of various methods to lassoed boosting's. Sections S.6 and S.7 also discuss the use of path integrated gradient to compare the path differences between the LS-boost and the lasso.

[Green *et al.* \(2017\)](#) use 94 variables from the databases CRSP, Compustat and I/B/E/S to study the determinants of average monthly US stock returns in a series of Fama-MacBeth regressions. We update their data to 2018 and use data from 2010 to 2018 for a total of 376544 firm-month observations in 108 months. The number of stocks (firms) in each month varies from 3269 to 3883. We add 8 variables that were removed in [Green *et al.* \(2017\)](#) due to collinearity concerns. The dummy variable *ipo* is removed since it varies little during certain time periods. In total, we have 101 ($94 + 8 - 1$) variables (see Table 2 in Section S.5). For example, we have 3883 observations for January 2010. \mathbf{y} becomes a 3883×1 vector of one-month-ahead, cross-sectional stock returns, and \mathbf{X} includes all variables plus a column of ones for the intercept. Missing values are replaced by the mean of the variable. We use 50%, 25%, and 25% of the 3883 observations for training, validation, and testing, respectively, and record the mean-squared prediction error (MSPE) for the test set of that month. After repeating this exercise for the remaining 107 months, we report the mean and median of the 108 MSPEs.

The goal of our exercise is to find a good linear model to predict stock returns, rather than to identify what determines the cross-section of expected stock returns, which is addressed in the large finance literature on anomalies. Active arbitrage in the market also implies that many analysts may have exploited all the variables under consideration, so we do not expect any linear model to exhibit broad predictive power. The data ignore many macro variables and such popular variables as the Fama-French factors and the q -factors.

Table 1 reports the prediction results from different methods. The tuning procedure in simulation is also used for the lasso, forward stepwise (FS), twiced lasso (TLasso), relaxed lasso (RLasso), and lassoed boosting (LB_1) in Table 1. LB_2 reports lassoed boosting with

a learning rate equal to 0.001 and a stopping criterion equal to the corrected AIC. GHZ represents a linear regression with 12 variables identified in [Green *et al.* \(2017\)](#) as significant in explaining the cross-section of stock returns but only for the non-microcap return data before 2003, and only two are significant for data after 2003. We use the 12-variable regression model for simple benchmarking purposes.

Table 1: Average MSPE and model size of the different methods

	Lasso	FS	TLasso	RLasso	LB ₁	LB ₂	GHZ
Mean	0.020057	0.023027	0.020057	0.020046	0.020027	0.020015	0.020455
Median	0.018206	0.021190	0.018212	0.018188	0.018221	0.018144	0.018484
# of tun. par.	100	50	100 × 50	100 × 50	100 × 50	100 × 50	N/A
avg. model size	22.14	6.15	12.44	12.37	12.47	9.22	12

Notes: FS, TLasso, RLasso, and LB refer to forward stepwise, twiced lasso, relaxed lasso, and lassoed boosting, respectively. GHZ refers to a linear regression model based on the 12 variables identified in [Green *et al.* \(2017\)](#) as significant in explaining the cross-section of expected returns for non-microcap stocks. Rows 1 and 2 report the mean and median of MSPE for the 108 monthly test sets from January, 2010 to December, 2018. Row 3 reports the number of tuning parameters used, where the forward stepwise (FS) method is tuned over 50 steps. Row 4 reports the average number of selected variables over 108 test sets for each method. For the GHZ method, the number of variables (model size) is fixed at 12.

The differences in prediction among the methods are small. The average MSPE of LB₁ is smaller than that of the lasso and the relaxed lasso but its median MSPE is larger. The relaxed lasso outperforms the lasso with a smaller mean MSPE and a smaller median MSPE. The results of the twiced lasso closely follow those of the lasso and the relaxed lasso. When tuned with a learning rate of 0.001, lassoed boosting starts to perform even better. LB₂ has the smallest mean MSPE and median MSPE among all the methods. Note that the lasso and lasso-based methods all outperform the FS method and the 12-variable GHZ model.

The numerical difference between the relaxed lasso and lassoed boosting (LB₂) in Table 1 is also very small. The difference in mean MSPE is 0.000031. Does such a small difference

matter? We note that MSPE is defined as

$$\text{MSPE} = \frac{1}{n_T} \sum_{i=1}^{n_T} (y_i - x_i \hat{\beta})^2, \quad (13)$$

where n_T is the size of the test set. MSPE measures the average squared distance between prediction and the true value. By taking the square root of the MSPE, we obtain the average absolute distance, which is 0.0056 (= 0.56%), which translates to 56 cents of difference when trading 100 dollars. A practitioner can better assess its economic significance. Based on the 108 MSPEs, a paired one-sided t -test for the null hypothesis $\text{MSPE}_{\text{RLasso}} < \text{MSPE}_{\text{LB}_2}$ gives a p -value of 0.007. Hence, we reject the null and conclude that the MSPE of LB_2 is smaller than that of the relaxed lasso.

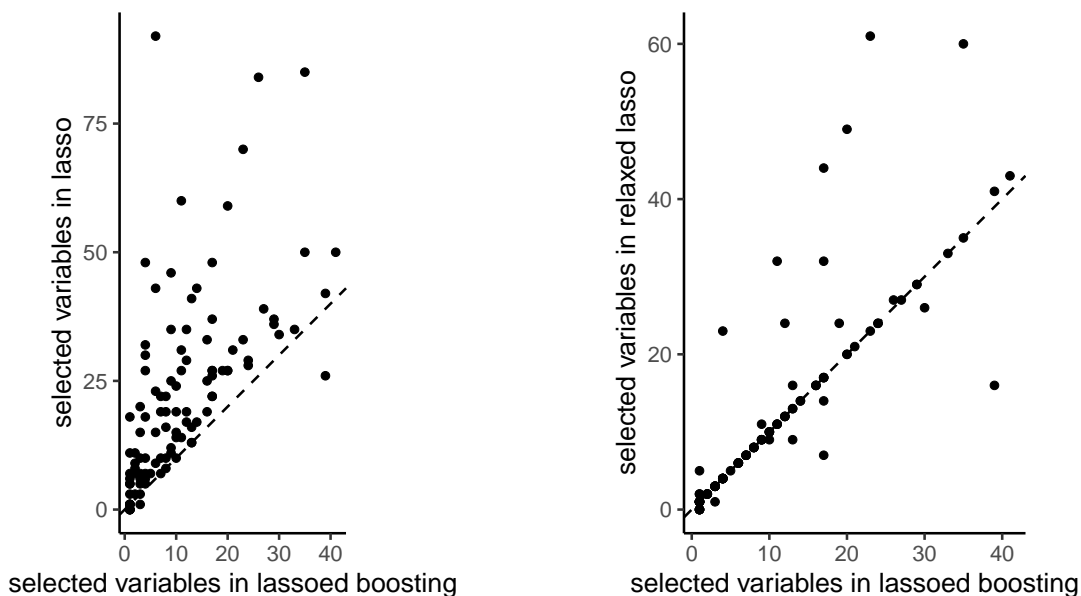


Figure 9: Each dot in the left figure represents the number of selected nonzeros in lassoed boosting and lasso for each of the 108 test sets. The dotted line is 45° line. Out of 108 test sets, compared to the lasso, lassoed boosting has a smaller, bigger, and the equal model size in 91, 6, and 11 cases, respectively. The right figure compares the same differences between lassoed boosting and the relaxed lasso, where the three numbers are 25, 14, and 69.

The last row of Table 1 reports the average number of selected variables across the 108 test sets. On average, the number for LB_2 is less than half that for the lasso. Compared to the relaxed lasso, lassoed boosting also offers a sparser solution on average. Figure 9

plots the number of nonzeros identified in lassoed boosting (LB_2) vs. the lasso (left) and the relaxed lasso (right). The dotted line is 45° line. Out of 108 test sets, lassoed boosting yields a sparser model in 91 cases; the lasso in only 6. Compared to the relaxed lasso, the number of nonzeros identified by lassoed boosting is smaller in 25 cases, larger in 14 cases, and the same in 69 cases. Overall, our empirical results are consistent with simulation: lassoed boosting can yield sparser model in certain cases. The large variation in model size also indicates model instability, though a stable model like GHZ underperforms the unstable models.

Combining the information in Table 1 and Figure 9, we conclude that, based on this application, lassoed boosting can deliver better prediction with a more compact model.

6 Conclusions

This paper finds that lassoed boosting, a refitting strategy based on the lasso, has good finite-sample properties in both our simulation experiment and an application. We also introduce the idea of using path integrated gradient to study the difference between the lasso and LS-boost in parameter attribution.

Our application uses one data set and the simulation compares only five variable-selection methods. It takes one line of R code to connect our method to the `bestsubset` package in [Hastie *et al.* \(2020\)](#) and to reproduce the simulation results (see the github page for instructions.) We invite readers to try lassoed boosting in more simulations and applications to further study its properties.

Our work can be extended in several directions. First, lassoed boosting should be compared to other methods in a classification exercise such as credit rating and default analysis. Second, a valid p -value should be attached to the estimates. Third, Proposition 2 suggests that both the relaxed lasso and lassoed boosting may be examples of many other two-stage approaches. An analyst should explore other possibilities to find a better method.

Acknowledgments

I am grateful to two referees for their insightful comments and suggestions. The computation and research support from the Office of Research and Coles College of Business at Kennesaw State University are greatly acknowledged.

References

- BERTSIMAS, D., KING, A. and MAZUMDER, R. (2016). Best subset selection via a modern optimization lens. *The Annals of Statistics*, **44** (2), 813 – 852.
- BÜHLMANN, P. (2006). Boosting for high-dimensional linear models. *The Annals of Statistics*, **34** (2), 559 – 583.
- BÜHLMANN, P. and HOTHORN, T. (2010). Twin boosting: improved feature selection and prediction. *Statistics and Computing*, **20** (2), 119 – 138.
- and VAN DE GEER, S. (2011). *Statistics for High-Dimensional Data*. Springer series in statistics, Springer, 1st edn.
- CHZHEN, E., HEBIRI, M. and SALMON, J. (2019). On Lasso refitting strategies. *Bernoulli*, **25** (4A), 3175 – 3200.
- FAN, J. and LI, R. (2001). Variable selection via nonconcave penalized likelihood and its oracle properties. *Journal of the American Statistical Association*, **96** (456), 1348–1360.
- FREUND, R. M., GRIGAS, P. and MAZUMDER, R. (2017). A new perspective on boosting in linear regression via subgradient optimization and relatives. *The Annals of Statistics*, **45** (6), 2328–2364.
- FRIEDMAN, J. H. (2001). Greedy function approximation: A gradient boosting machine. *The Annals of Statistics*, **29** (5), 1189–1232.
- GREEN, J., HAND, J. R. M. and ZHANG, X. F. (2017). The Characteristics that Provide Independent Information about Average U.S. Monthly Stock Returns. *The Review of Financial Studies*, **30** (12), 4389–4436.
- HASTIE, T., TIBSHIRANI, R. and FRIEDMAN, J. (2009). *The Elements of Statistical Learning: Data Mining, Inference, and Prediction*. Springer series in statistics, Springer, 2nd edn.
- , — and TIBSHIRANI, R. (2020). Best Subset, Forward Stepwise or Lasso? Analysis and Recommendations Based on Extensive Comparisons. *Statistical Science*, **35** (4), 579 – 592.

- , — and WAINWRIGHT, M. (2015). *Statistical Learning with Sparsity: The Lasso and Generalizations*. Chapman and Hall/CRC.
- HORN, R. A. and JOHNSON, C. R. (1985). *Matrix Analysis*. Cambridge University Press.
- HURVICH, C. M., SIMONOFF, J. S. and TSAI, C.-L. (1998). Smoothing parameter selection in nonparametric regression using an improved akaike information criterion. *Journal of the Royal Statistical Society: Series B (Statistical Methodology)*, **60** (2), 271–293.
- MAZUMDER, R., FRIEDMAN, J. H. and HASTIE, T. (2011). Sparsenet: Coordinate descent with nonconvex penalties. *Journal of the American Statistical Association*, **106** (495), 1125–1138, PMID: 25580042.
- MEINSHAUSEN, N. (2007). Relaxed lasso. *Computational Statistics & Data Analysis*, **52** (1), 374–393.
- TIBSHIRANI, R. (1996). Regression shrinkage and selection via the lasso. *Journal of the Royal Statistical Society. Series B (Statistical Methodology)*, **58** (1), 267–288.
- YUAN, M. and LIN, Y. (2006). Model selection and estimation in regression with grouped variables. *Journal of the Royal Statistical Society: Series B (Statistical Methodology)*, **68** (1), 49–67.
- ZHANG, C.-H. (2010). Nearly unbiased variable selection under minimax concave penalty. *The Annals of Statistics*, **38** (2), 894 – 942.
- ZOU, H. (2006). The adaptive lasso and its oracle properties. *Journal of the American Statistical Association*, **101** (476), 1418–1429.
- and HASTIE, T. (2005). Regularization and variable selection via the elastic net. *Journal of the Royal Statistical Society. Series B (Statistical Methodology)*, **67** (2), 301–320.

SUPPLEMENTARY MATERIAL TO “LASSOED BOOSTING AND LINEAR PREDICTION IN THE EQUITIES MARKET”¹

XIAO HUANG

May 21, 2024

This supplement contains all proofs, additional discussions and figures.

Contents

S.1	Proofs	3
S.2	Comparison of convergence results in Theorem 1 and Theorem 12.2 in Bühlmann and van de Geer (2011)	4
S.3	Validation tuning figures in simulation	6
S.3.1	Low setting: $n = 100, p = 10, s = 5$	6
S.3.1.1	Relative risk (to null model)	6
S.3.1.2	Relative test error (to Bayes)	7
S.3.1.3	Proportion of variance explained	8
S.3.1.4	Number of nonzero coefficients	9
S.3.2	Medium setting: $n = 500, p = 100, s = 5$	10
S.3.2.1	Relative risk (to null model)	10
S.3.2.2	Relative test error (to Bayes)	11
S.3.2.3	Proportion of variance explained	12
S.3.2.4	Number of nonzero coefficients	13
S.3.3	High-5 setting: $n = 50, p = 1000, s = 5$	14
S.3.3.1	Relative risk (to null model)	14
S.3.3.2	Relative test error (to Bayes)	15
S.3.3.3	Proportion of variance explained	16
S.3.3.4	Number of nonzero coefficients	17
S.3.4	High-10 setting: $n = 100, p = 1000, s = 10$	18
S.3.4.1	Relative risk (to null model)	18
S.3.4.2	Relative test error (to Bayes)	19

¹Email: xhuang3@kennesaw.edu

	S.3.4.3	Proportion of variance explained	20
	S.3.4.4	Number of nonzero coefficients	21
S.4		Oracle tuning figures in simulation	22
	S.4.1	Low setting: $n = 100, p = 10, s = 5$	22
	S.4.1.1	Relative risk (to null model)	22
	S.4.1.2	Relative test error (to Bayes)	23
	S.4.1.3	Proportion of variance explained	24
	S.4.1.4	Number of nonzero coefficients	25
	S.4.2	Medium setting: $n = 500, p = 100, s = 5$	26
	S.4.2.1	Relative risk (to null model)	26
	S.4.2.2	Relative test error (to Bayes)	27
	S.4.2.3	Proportion of variance explained	28
	S.4.2.4	Number of nonzero coefficients	29
	S.4.3	High-5 setting: $n = 50, p = 1000, s = 5$	30
	S.4.3.1	Relative risk (to null model)	30
	S.4.3.2	Relative test error (to Bayes)	31
	S.4.3.3	Proportion of variance explained	32
	S.4.3.4	Number of nonzero coefficients	33
	S.4.4	High-10 setting: $n = 100, p = 1000, s = 10$	34
	S.4.4.1	Relative risk (to null model)	34
	S.4.4.2	Relative test error (to Bayes)	35
	S.4.4.3	Proportion of variance explained	36
	S.4.4.4	Number of nonzero coefficients	37
S.5		Variable definitions in the application	38
S.6		Path difference and parameter attribution	40
S.7		Additional figures for parameter attribution in the lasso and LS-boost	43

S.1 Proofs

Proof of Proposition 1. From Theorem 11.3 in [Hastie et al. \(2015\)](#), we know there exists a λ such that the lasso is variable selection consistent as $\log(p)/n \rightarrow 0$ when $n \rightarrow \infty$. Let λ_* be a penalty value so that $\mathcal{A}_{\lambda_*} = \mathcal{A}$. Given the correctly identified active set \mathcal{A}_{λ_*} , the LS-boost solution at step $k = \infty$ is equal to the LS solution on the active set \mathcal{A}_{λ_*} , $\hat{\beta}^{\lambda_*, \infty} = \hat{\beta}_{LS}^{\lambda_*}$. Since $\inf_{\lambda, s \in [1, \infty]} L_n(\hat{\beta}^{\lambda, k}) \leq L_n(\hat{\beta}_{LS}^{\lambda_*})$, we have, for $c > 0$,

$$P\left(\inf_{\lambda, k \in [1, \infty]} L_n(\hat{\beta}^{\lambda, k}) > cn^{-1}\right) \leq P(L_n(\hat{\beta}_{LS}^{\lambda_*}) > cn^{-1}) \rightarrow 0 \text{ as } n \rightarrow \infty,$$

where the last result follows the standard convergence property of the LS estimator. \square

Proof of Proposition 2. The proof is similar to the proof of Proposition 1. Using Theorem 11.3 in [Hastie et al. \(2015\)](#), as $n \rightarrow \infty$, gives a λ_* so that $\mathcal{A}_{\lambda_*} = \mathcal{A}$ with high probability. Since $\inf_{\lambda, \mathcal{K}} L_n(\hat{\beta}^{\lambda, \mathcal{K}}) \leq L_n(\hat{\beta}_{LS}^{\lambda_*})$ as the tuning vector \mathcal{K} can generate the case of a full LS solution, we have, for $c > 0$,

$$P\left(\inf_{\lambda, \mathcal{K}} L_n(\hat{\beta}^{\lambda, \mathcal{K}}) > cn^{-1}\right) \leq P(L_n(\hat{\beta}_{LS}^{\lambda_*}) > cn^{-1}) \rightarrow 0 \text{ as } n \rightarrow \infty,$$

where the last result again follows the standard convergence property of the LS estimator. \square

Proof of Theorem 1. By the triangular inequality, we have

$$\|\mathbf{X}\hat{\beta}^k - \mathbf{X}\beta^*\|_2 \leq \|\mathbf{X}\hat{\beta}^k - \mathbf{X}\hat{\beta}_{LS}\|_2 + \|\mathbf{X}\hat{\beta}_{LS} - \mathbf{X}\beta^*\|_2, \quad (\text{S.1})$$

where the bound for the term $\|\mathbf{X}\hat{\beta}^k - \mathbf{X}\hat{\beta}_{LS}\|_2$ is given in Theorem 2.1 in [Freund et al. \(2017\)](#). Consider the second term $\|\mathbf{X}\hat{\beta}_{LS} - \mathbf{X}\beta^*\|_2$. Recall $L_n(\beta^*) \geq L_n(\hat{\beta}_{LS})$.

$$\begin{aligned} 2n(L_n(\beta^*) - L_n(\hat{\beta}_{LS})) &= \|\mathbf{y} - \mathbf{X}\beta^*\|_2^2 - \|\mathbf{y} - \mathbf{X}\hat{\beta}_{LS}\|_2^2 \\ &= -2\mathbf{y}^T \mathbf{X}\beta^* + \|\mathbf{X}\beta^*\|_2^2 + 2\mathbf{y}^T \mathbf{X}\hat{\beta}_{LS} - \|\mathbf{X}\hat{\beta}_{LS}\|_2^2 \\ &= -2\hat{\beta}_{LS} \mathbf{X}^T \mathbf{X}\beta^* + \|\mathbf{X}\beta^*\|_2^2 + 2\hat{\beta}_{LS} \mathbf{X}^T \mathbf{X}\hat{\beta}_{LS} - \|\mathbf{X}\hat{\beta}_{LS}\|_2^2 \\ &= \|\mathbf{X}\hat{\beta}_{LS} - \mathbf{X}\beta^*\|_2^2, \end{aligned}$$

where we use the f.o.c. of eq. (2), $\mathbf{y}^T \mathbf{X} = \hat{\beta}_{LS} \mathbf{X}^T \mathbf{X}$, in the third equality. Hence, we have

$$\|\mathbf{X}\hat{\beta}_{LS} - \mathbf{X}\beta^*\|_2 = \sqrt{2n(L_n(\beta^*) - L_n(\hat{\beta}_{LS}))}. \quad (\text{S.2})$$

By the convexity of $L_n(\cdot)$, we have

$$\begin{aligned}
L_n(\hat{\beta}_{\text{LS}}) &\geq L_n(\beta^*) + \nabla L_n(\beta^*)^T(\hat{\beta}_{\text{LS}} - \beta^*) \\
&\geq L_n(\beta^*) - \|\nabla L_n(\beta^*)\|_2 \cdot \|\hat{\beta}_{\text{LS}} - \beta^*\|_2.
\end{aligned}$$

Rearranging the last inequality gives

$$L_n(\beta^*) - L_n(\hat{\beta}_{\text{LS}}) \leq \|\nabla L_n(\beta^*)\|_2 \cdot \|\hat{\beta}_{\text{LS}} - \beta^*\|_2. \quad (\text{S.3})$$

Substituting Theorem 2.1 (iii) in FGM and eqs. (S.2) and (S.3) into eq. (S.1) completes the proof. \square

Next, similar to Theorem 1, we give a prediction convergence result for Algorithm 2.

Theorem 2. Let $k \geq 0$ be the number of iterations. Under Assumption 1, there exists an $i \in \{0, \dots, k\}$ so that the following bound hold:

$$\|\mathbf{X}\hat{\beta}^i - \mathbf{X}\beta^*\|_2 \leq \frac{\sqrt{p}}{\sqrt{\lambda(\mathbf{X}^T\mathbf{X})}} \left[\frac{\|\mathbf{X}\hat{\beta}_{\text{LS}}\|_2^2}{\varepsilon(k+1)} + \epsilon \right] + \sqrt{2n\|\nabla L_n(\beta^*)\|_2 \cdot \|\hat{\beta}_{\text{LS}} - \beta^*\|_2}. \quad (\text{S.4})$$

Proof of Theorem 2. Applying the triangular inequality, we have

$$\|\mathbf{X}\hat{\beta}^i - \mathbf{X}\beta^*\|_2 \leq \|\mathbf{X}\hat{\beta}^i - \mathbf{X}\hat{\beta}_{\text{LS}}\|_2 + \|\mathbf{X}\hat{\beta}_{\text{LS}} - \mathbf{X}\beta^*\|_2. \quad (\text{S.5})$$

Bound for the first term on the r.h.s. follows Theorem 3.1 (iii) in FGM, while bound for the second term on the r.h.s. follows the same result in the proof of Theorem 1. Combining the two results gives the bound in Theorem 2. \square

S.2 Comparison of convergence results in Theorem 1 and Theorem 12.2 in Bühlmann and van de Geer (2011)

The convergence rate in Theorem 12.2 in Bühlmann and van de Geer (2011) is obtained after choosing an iteration number k (“ m ” in the book’s notation) to minimize the upper bound. We can consider the pre-optimized rate result in the first equation on page 426 of Bühlmann and van de Geer (2011) to gain some insight. For ease of reference, we reproduce the equation below.

$$\frac{1}{n} \|\mathbf{X}\hat{\beta}^k - \mathbf{X}\beta^*\|_2^2 = \|\hat{R}^k f^0\|_n^2 \leq \max\{2k^{-\frac{D\kappa}{2+D\kappa}}, \kappa^{-1}(1-\kappa/2)^{-1}2\Delta_n(\|\beta_n^0\|_1 + k\gamma_n) + k\Delta_n\}, \quad (\text{S.6})$$

where we replace “ m ” in the original equation with k to denote the boosting iteration number, and

$$\begin{aligned} f^0 &= \mathbf{X}\beta_n^0 \text{ (and } \beta_n^0 = \beta^* \text{ in this paper),} \\ \hat{R}^k f^0 &= \mathbf{X}\beta_n^0 - \mathbf{X}\hat{\beta}^k, \quad \kappa \in (0, \frac{1}{2}), \quad D_\kappa = (1 - \kappa)(1 - \kappa/2), \\ \Delta_n &= \max_{j=1, \dots, p} \frac{1}{n} \sum_{i=1}^n |u_i x_{ij}| = O_p(\sqrt{\log(p)/n}), \\ \gamma_n &= (1 + \sigma^2) + o_p(1) = O_p(1). \end{aligned}$$

Under the assumption of $\|\beta_n^0\|_1 = o\left(\sqrt{\frac{n}{\log(p)}}\right)$ and $k = o(\sqrt{n/\log(p)})$ in the same theorem, the second term in eq. (S.6) is dominated by $\kappa^{-1}(1 - \kappa/2)^{-1}2\Delta_n\|\beta_n^0\|_1$, which has order $\Delta_n\|\beta_n^0\|_1$. Although it is $o_p(1)$, it is not a function of k and we cannot compare it directly to the result in Theorem 1. For this reason, let us consider the first term in eq. (S.6). Given the value of κ , $\frac{D_\kappa}{2+D_\kappa}$ varies on the interval $(0.158, 0.333)$. Hence $2k^{-\frac{D_\kappa}{2+D_\kappa}}$ is a power function of k with its power on the interval of $(-0.333, -0.158)$.

From Theorem 1 and eq. (S.1), we have

$$\begin{aligned} \frac{1}{n}\|\mathbf{X}\hat{\beta}^k - \mathbf{X}\beta^*\|_2^2 &\leq \frac{1}{n}\|\mathbf{X}\hat{\beta}_{\text{LS}}^k\|_2^2\gamma^k + \frac{1}{n}\|\mathbf{X}\hat{\beta}_{\text{LS}} - \mathbf{X}\beta^*\|_2 \\ &\leq \frac{1}{n}\|\mathbf{y}\|_2^2\gamma^k + \frac{1}{n}\|\mathbf{X}\hat{\beta}_{\text{LS}} - \mathbf{X}\beta^*\|_2, \end{aligned} \tag{S.7}$$

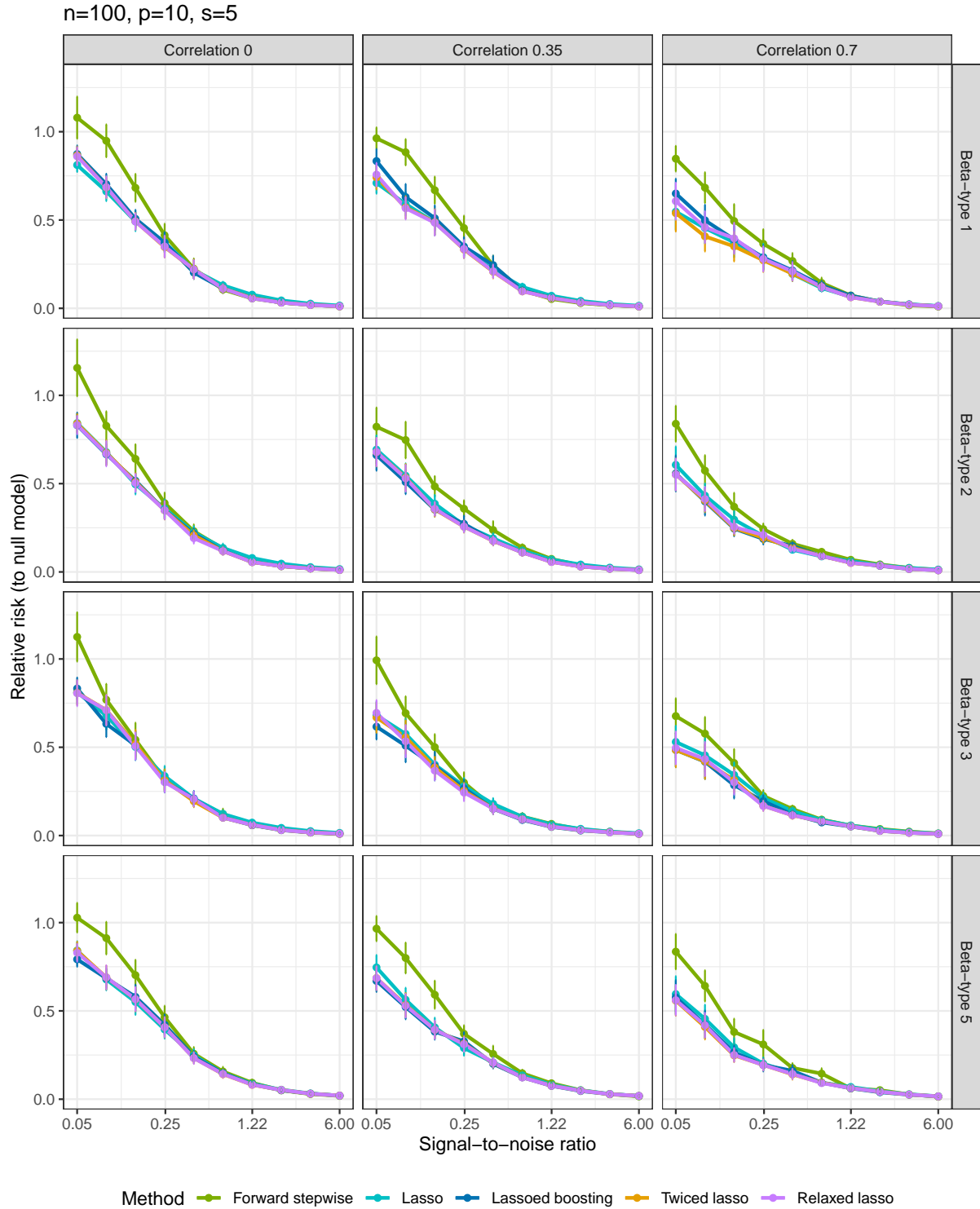
where we can assume $\frac{1}{n}\|\mathbf{y}\|_2^2 = O_p(1)$. Hence the first term on the r.h.s. of eq. (S.7) is an exponential function to the base of γ with $\gamma \in [0.75, 1)$. Thus, we conclude that while Theorem 2.12. in Bühlmann and van de Geer (2011) uses a power function to describe the convergence of the prediction in LS-boost as the procedure iterates, Theorem 1 (and Theorem 2.1 in FGM) uses an exponential function to characterize the convergence.

With additional assumptions, we can further comment on the behavior of the second term on the r.h.s. of eq. (S.7). Assume the error term u_i belongs to the class of sub-Gaussian distribution with variance proxy σ^2 , $u_i \sim \text{subG}(\sigma^2)$. If $p \leq n$, Theorem 2.2 in Rigollet and Hütter (2019) shows the second term is $O_p(1/n)$; if $p > n$ and β^* is s -sparse, Corollary 2.8 in Rigollet and Hütter (2019) indicates that the second term is $O_p(\log(p)/n)$. These results hold with high probability. To summarize, under the additional assumption of $O_p(\log(p)/n) \rightarrow 0$ as $n, p \rightarrow \infty$, the second term in eq. (S.7) disappears asymptotically, which allows us to focus on the exponential function, γ^k , to study the convergence of predictions in LS-boost.

S.3 Validation tuning figures in simulation

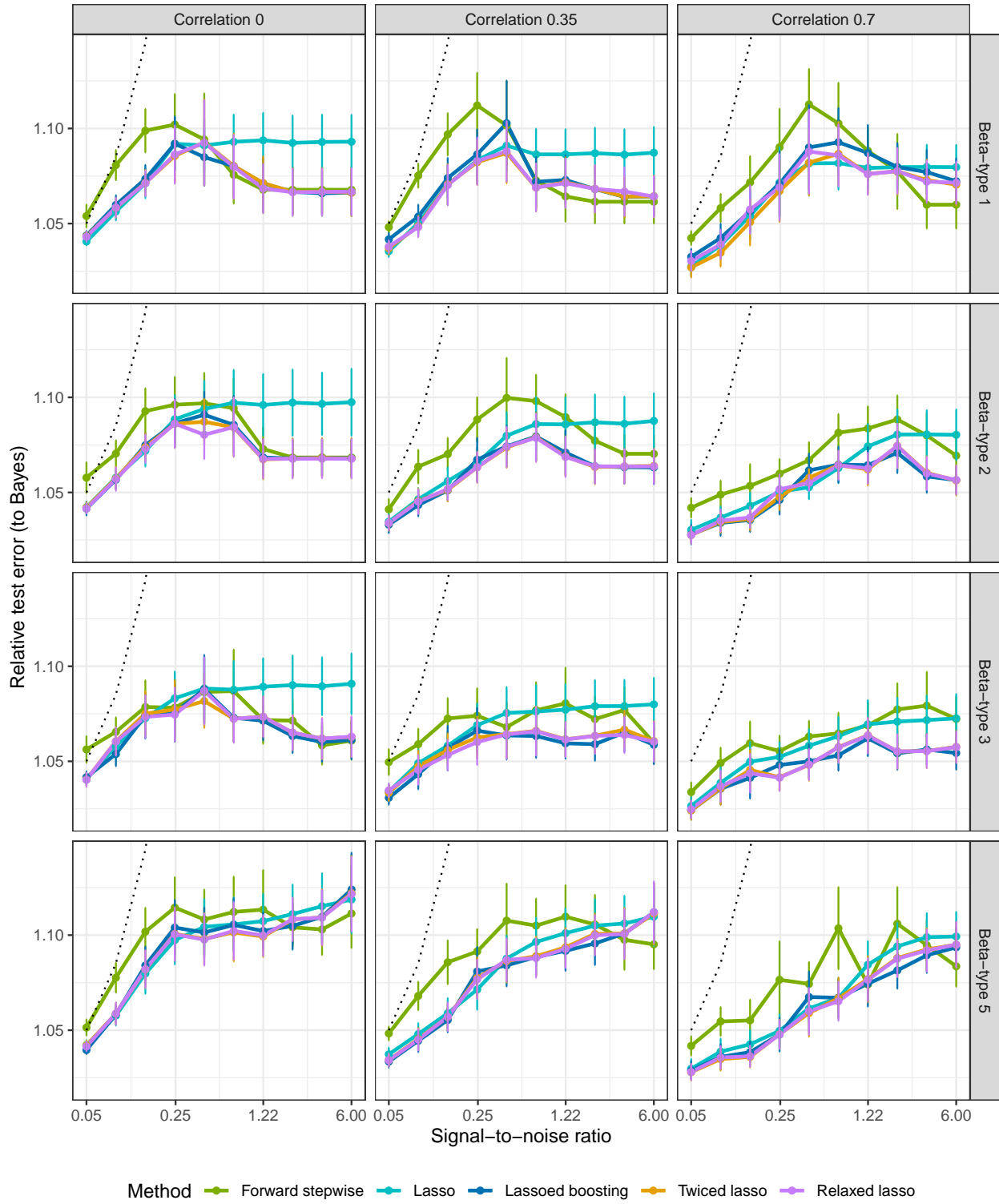
S.3.1 Low setting: $n = 100, p = 10, s = 5$

S.3.1.1 Relative risk (to null model)



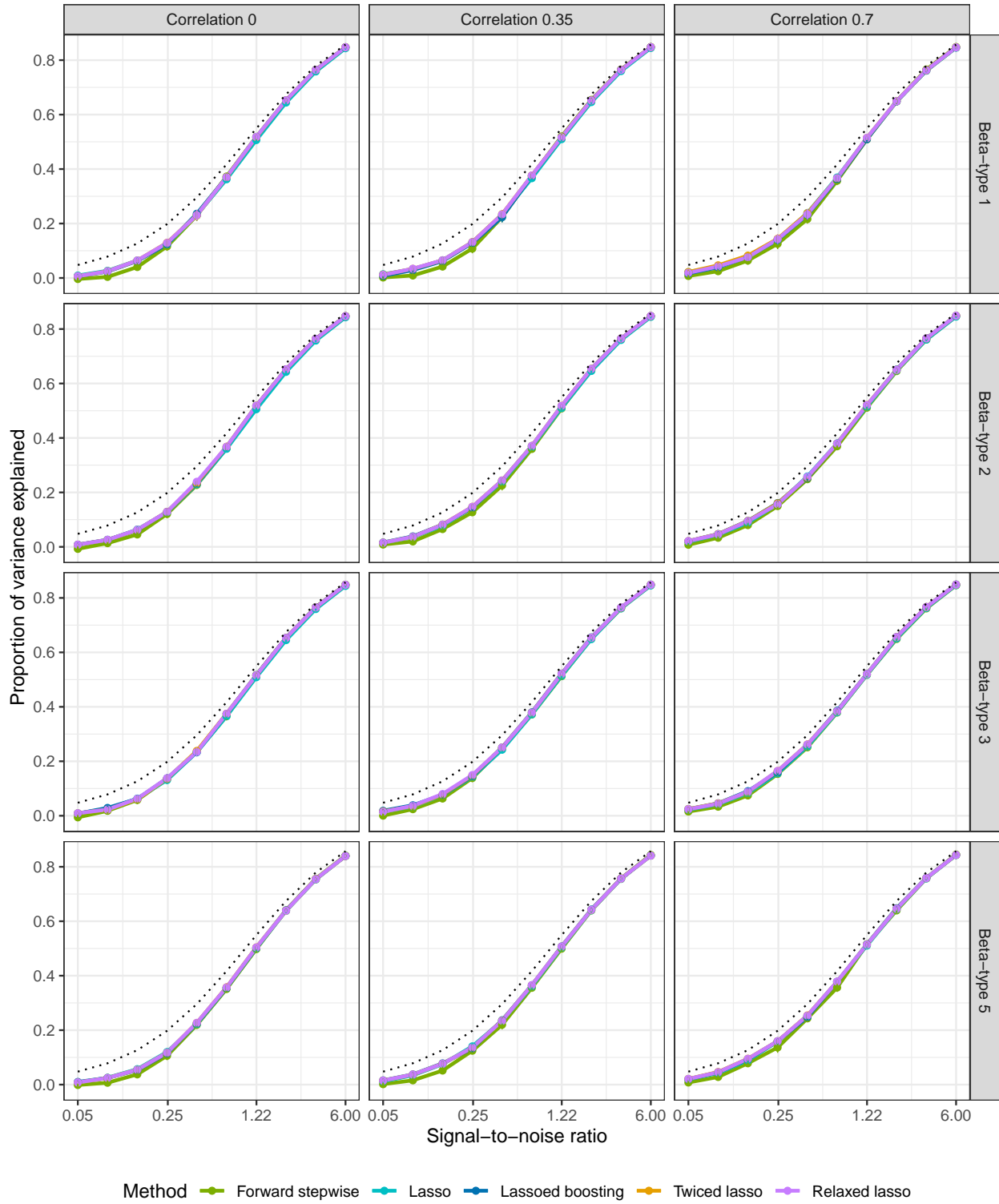
S.3.1.2 Relative test error (to Bayes)

$n=100, p=10, s=5$



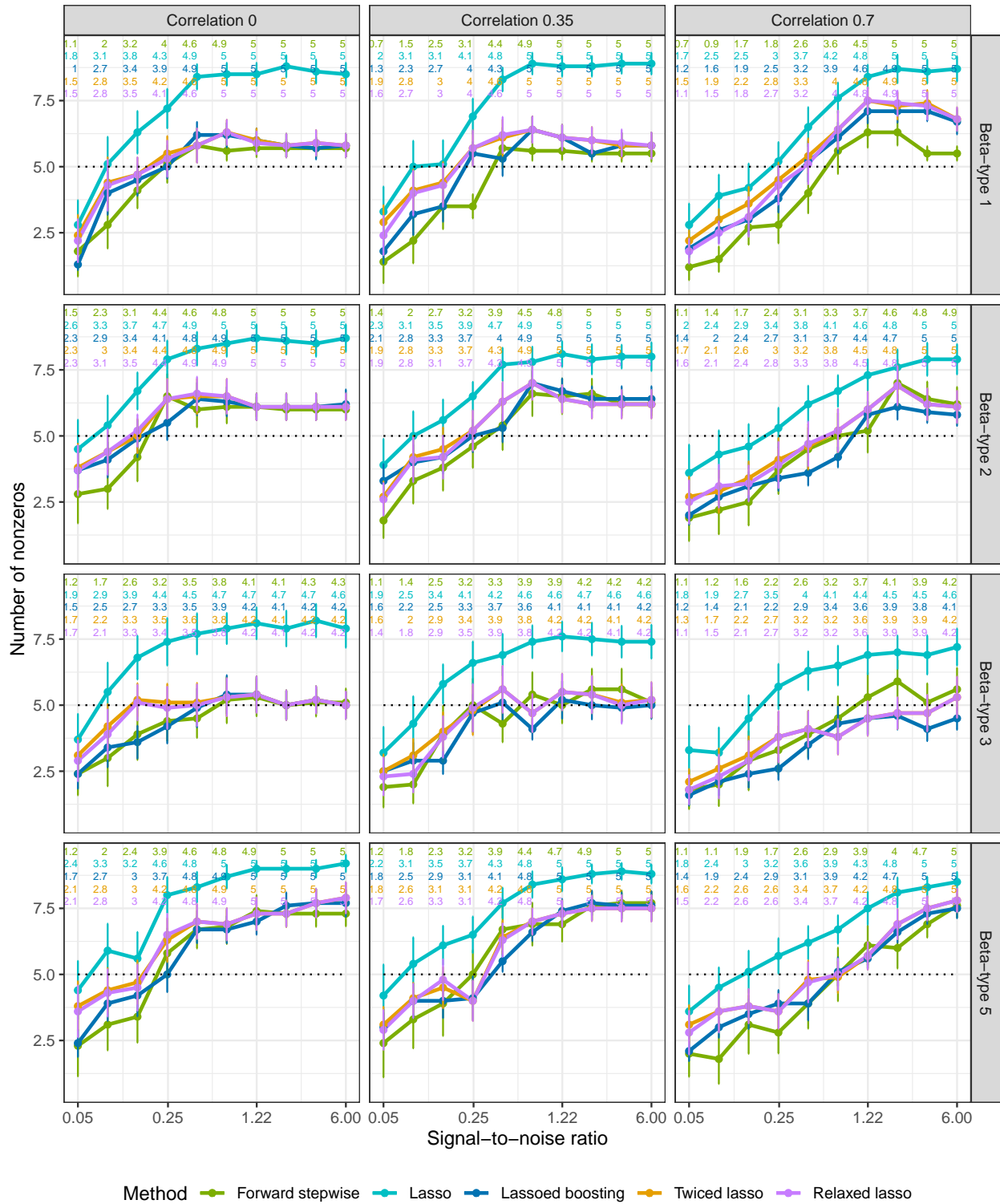
S.3.1.3 Proportion of variance explained

$n=100, p=10, s=5$



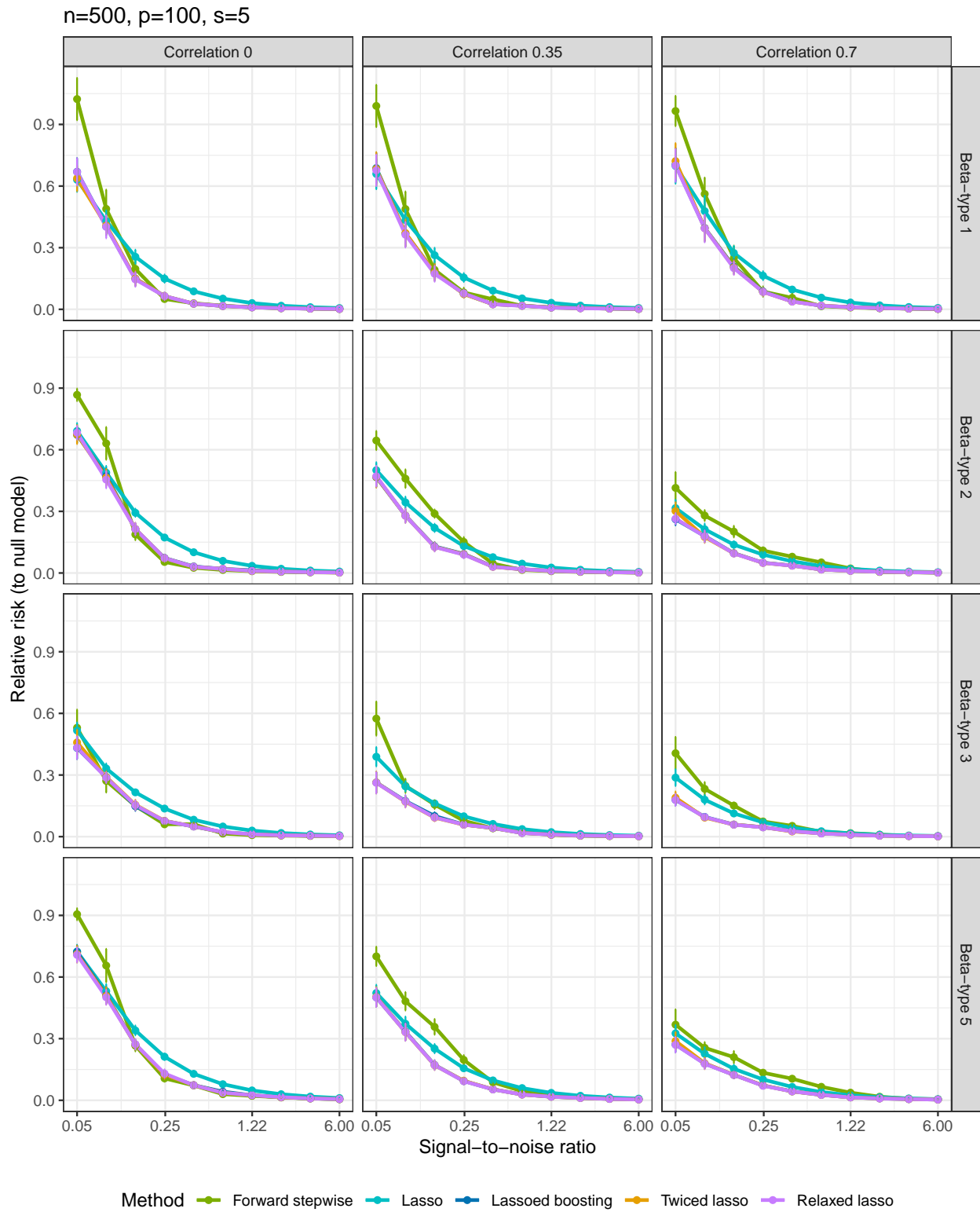
S.3.1.4 Number of nonzero coefficients

n=100, p=10, s=5



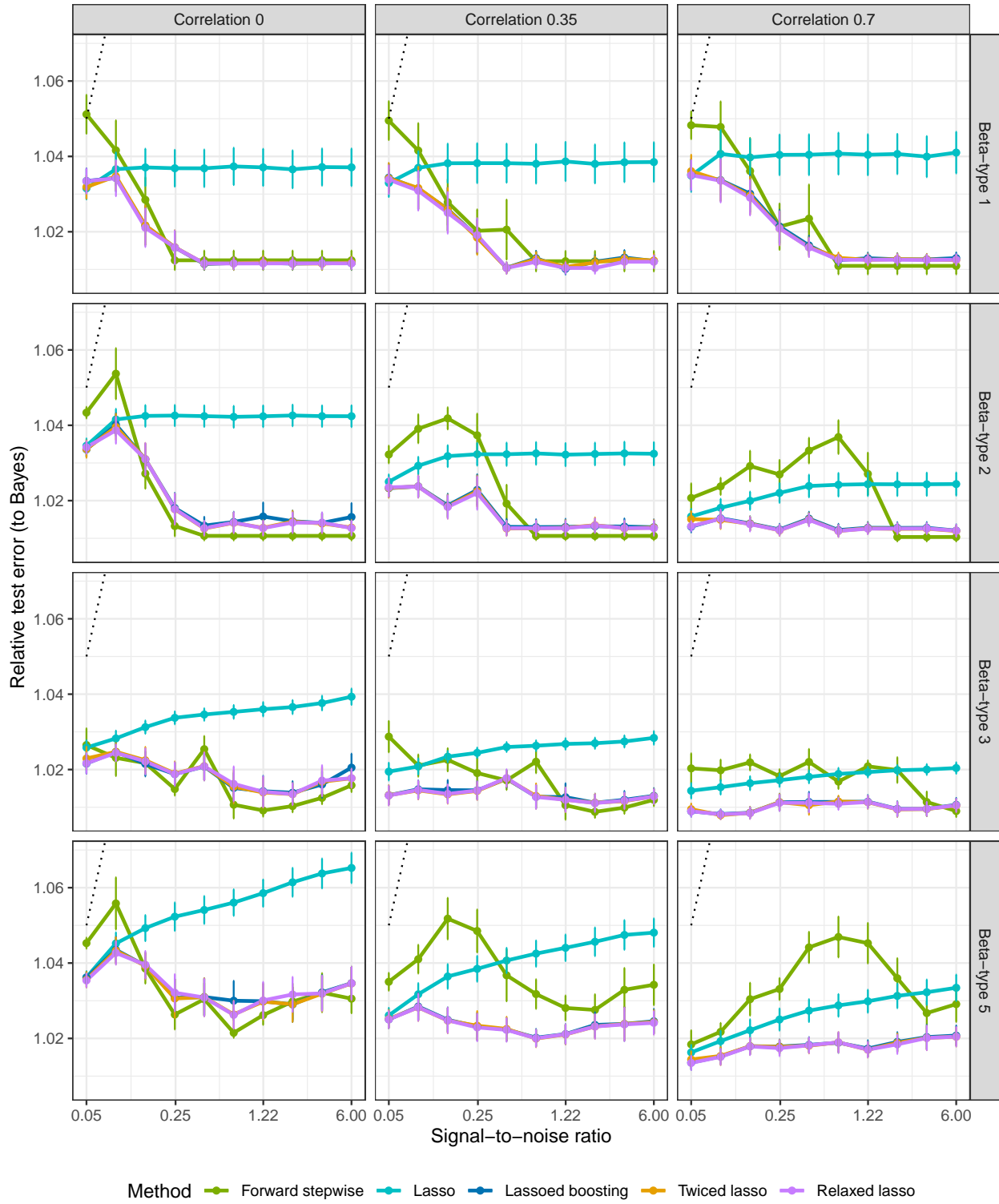
S.3.2 Medium setting: $n = 500, p = 100, s = 5$

S.3.2.1 Relative risk (to null model)



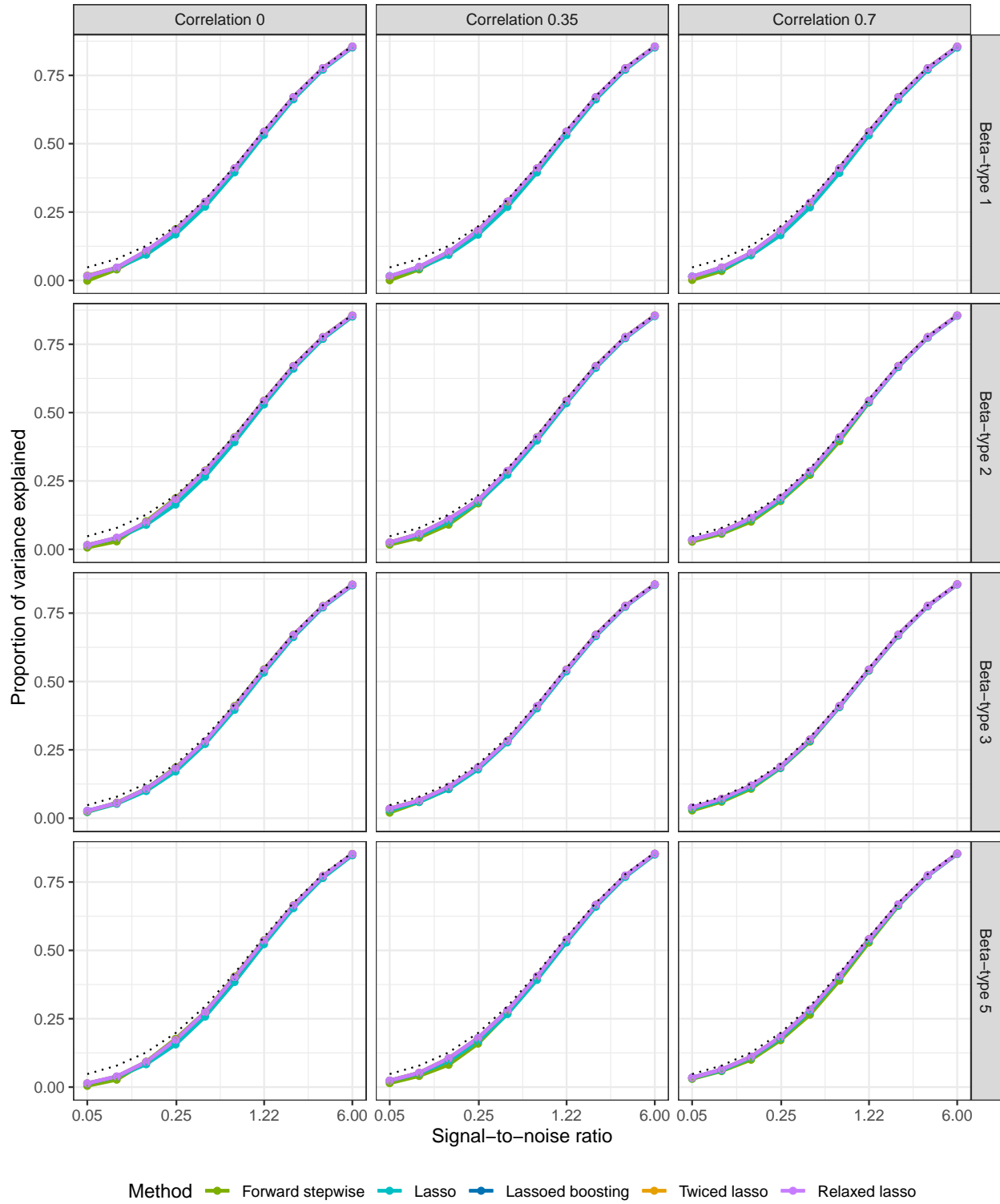
S.3.2.2 Relative test error (to Bayes)

$n=500, p=100, s=5$



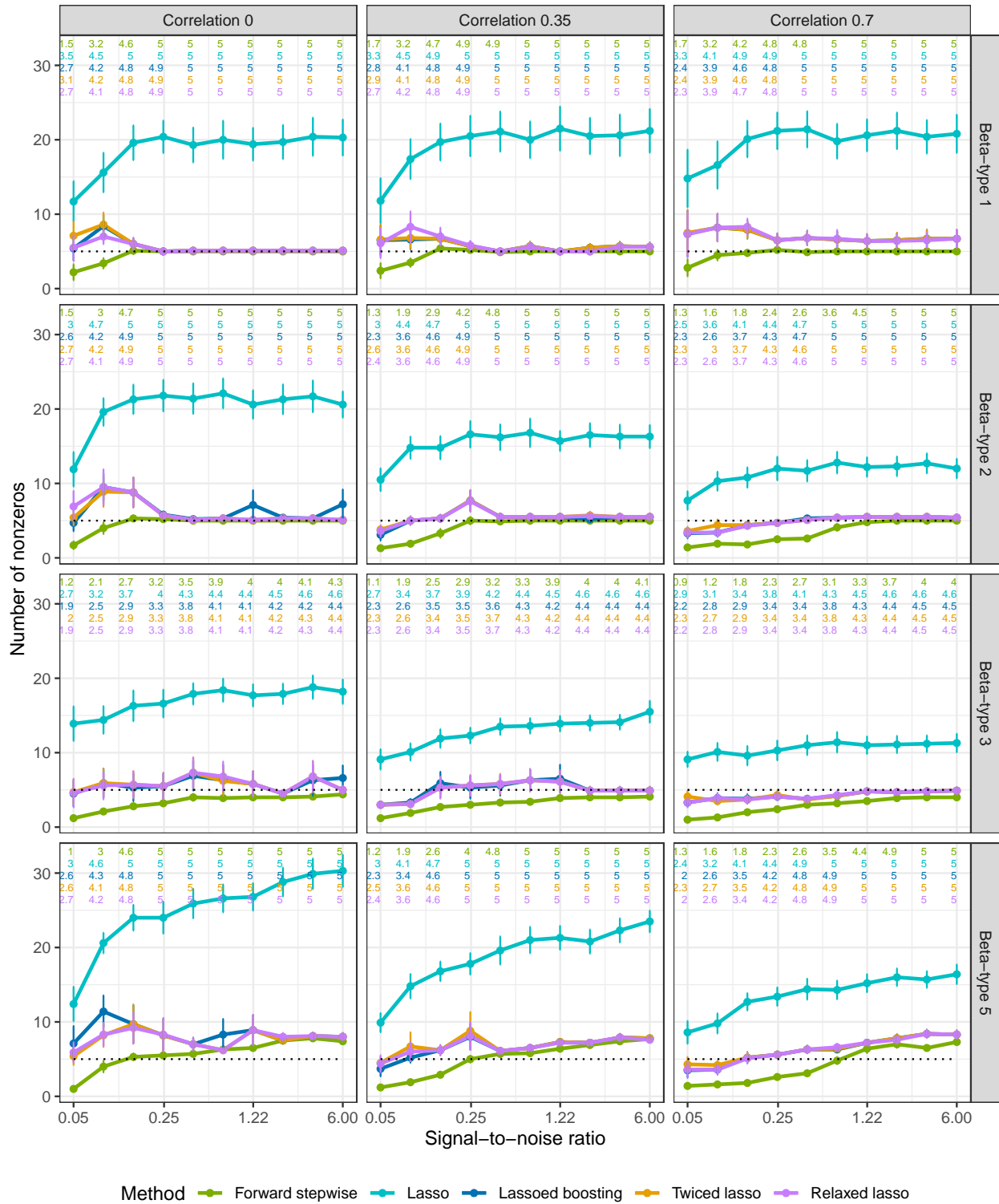
S.3.2.3 Proportion of variance explained

$n=500, p=100, s=5$



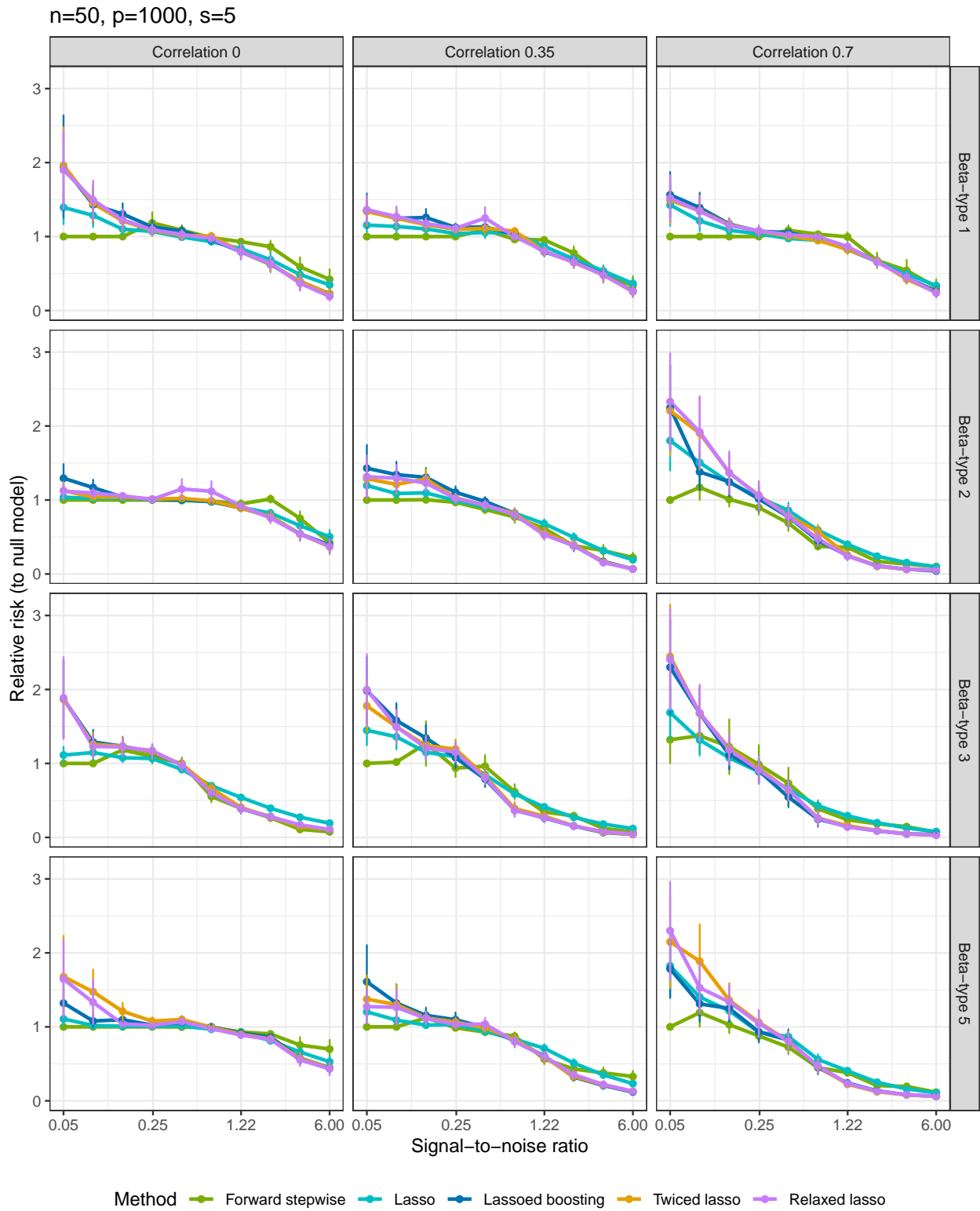
S.3.2.4 Number of nonzero coefficients

$n=500, p=100, s=5$



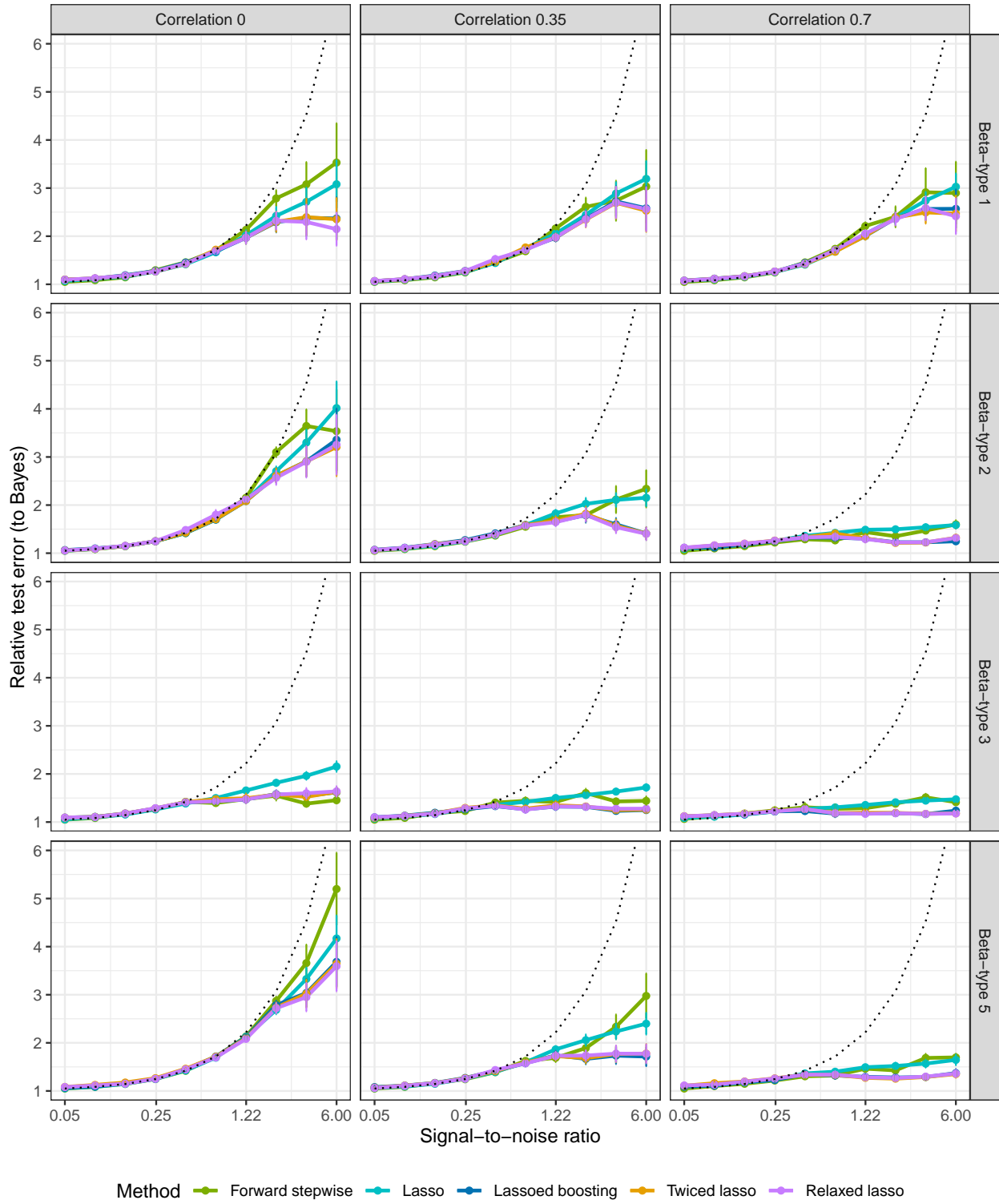
S.3.3 High-5 setting: $n = 50, p = 1000, s = 5$

S.3.3.1 Relative risk (to null model)



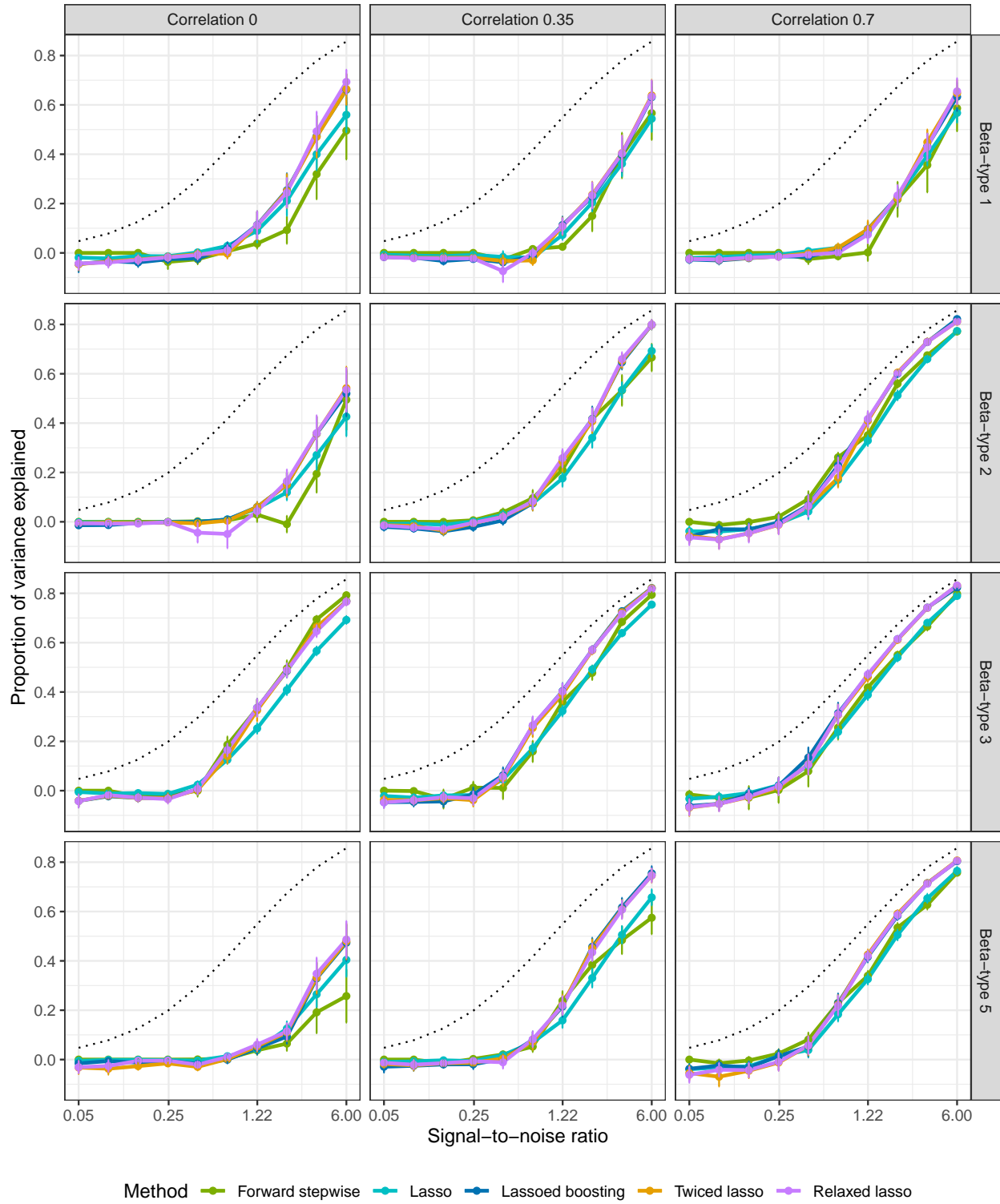
S.3.3.2 Relative test error (to Bayes)

$n=50, p=1000, s=5$



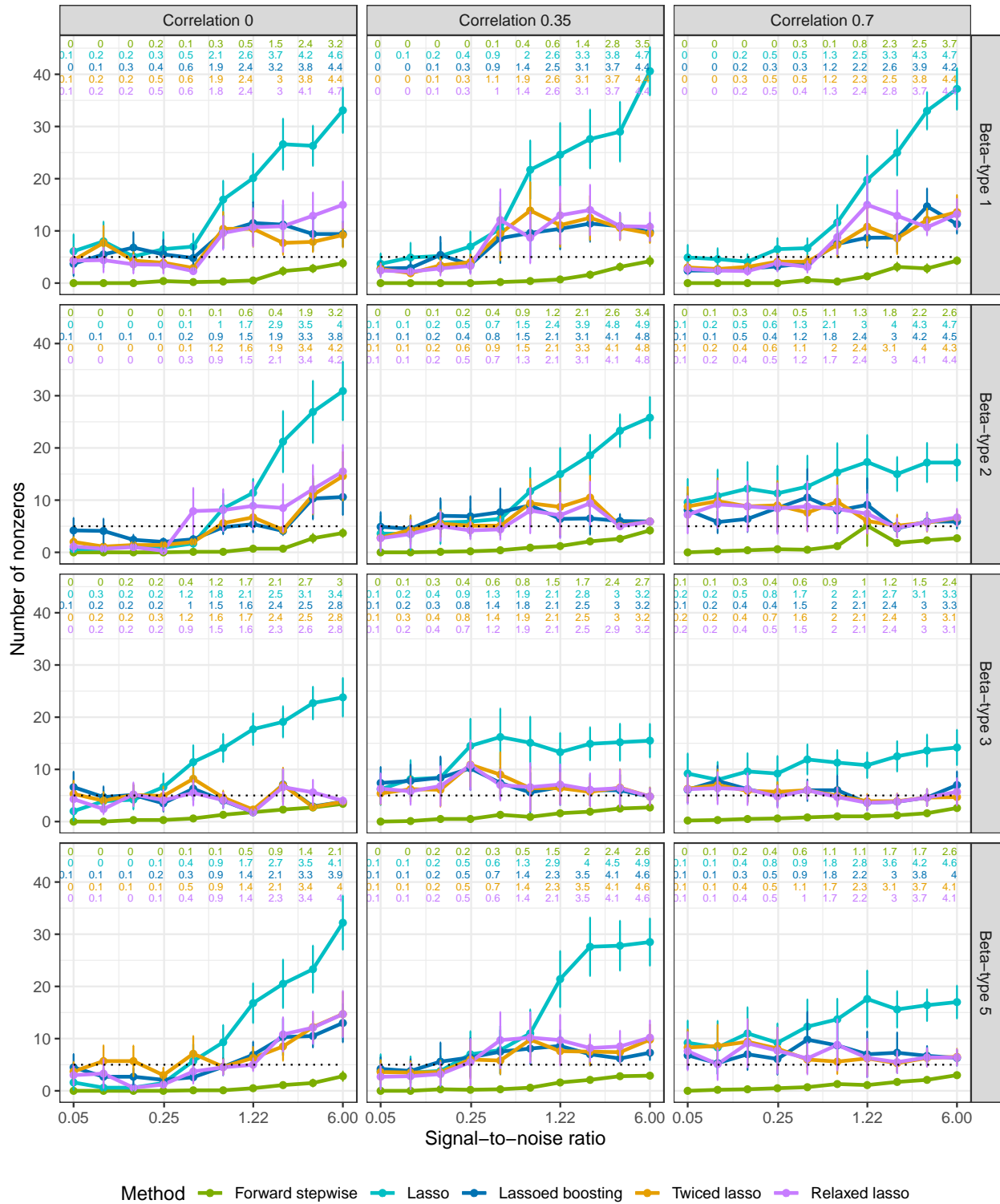
S.3.3.3 Proportion of variance explained

$n=50, p=1000, s=5$



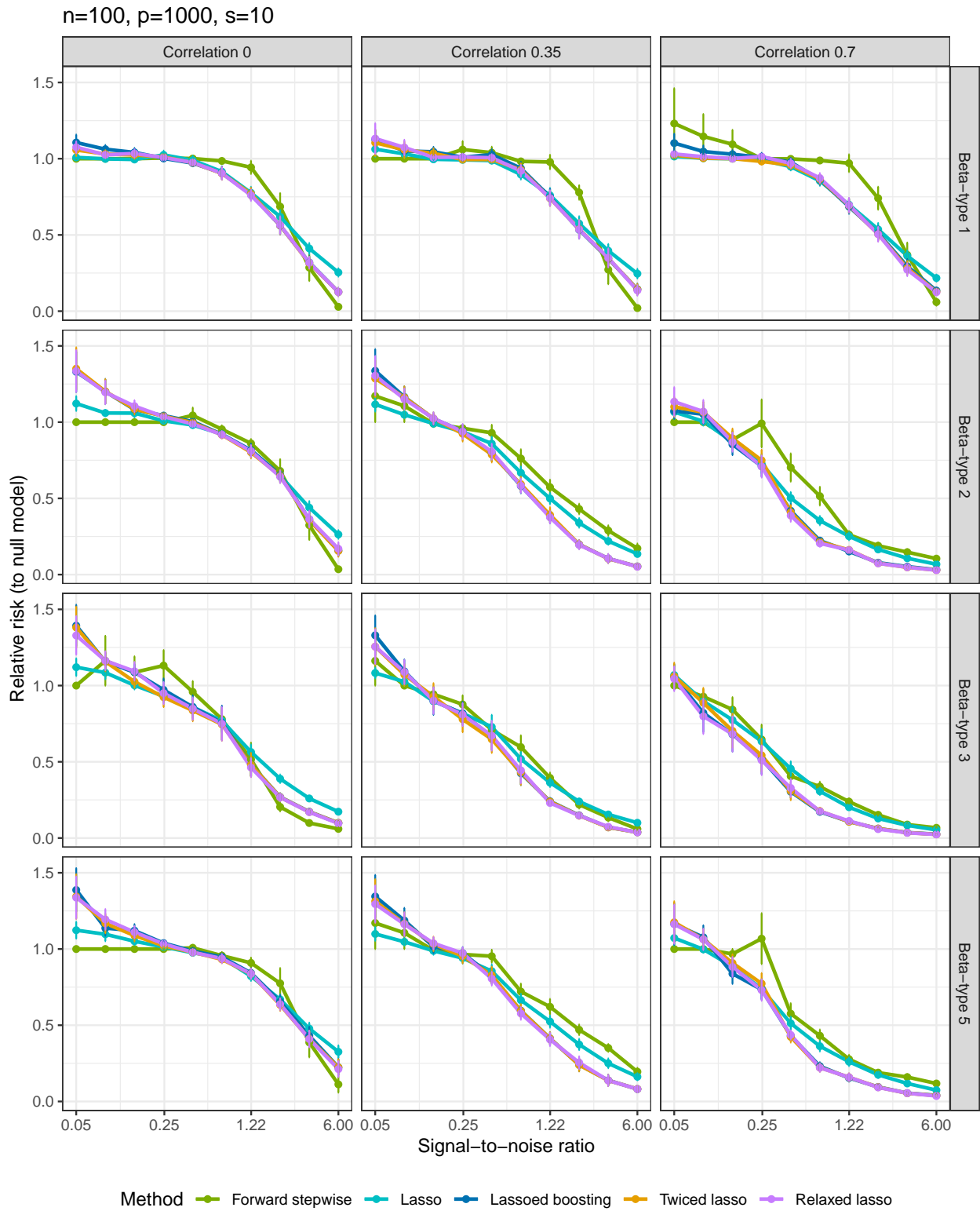
S.3.3.4 Number of nonzero coefficients

$n=50, p=1000, s=5$

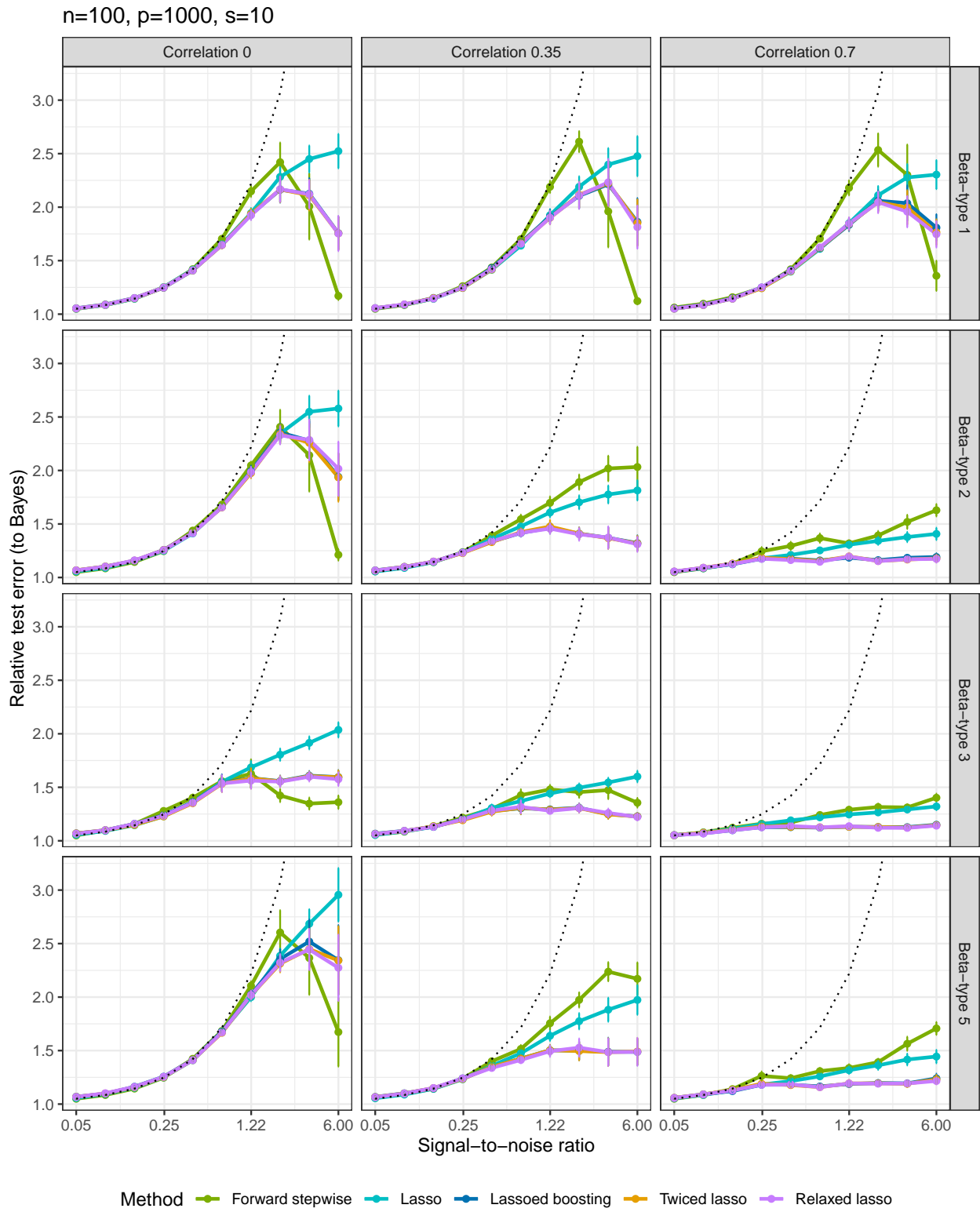


S.3.4 High-10 setting: $n = 100, p = 1000, s = 10$

S.3.4.1 Relative risk (to null model)

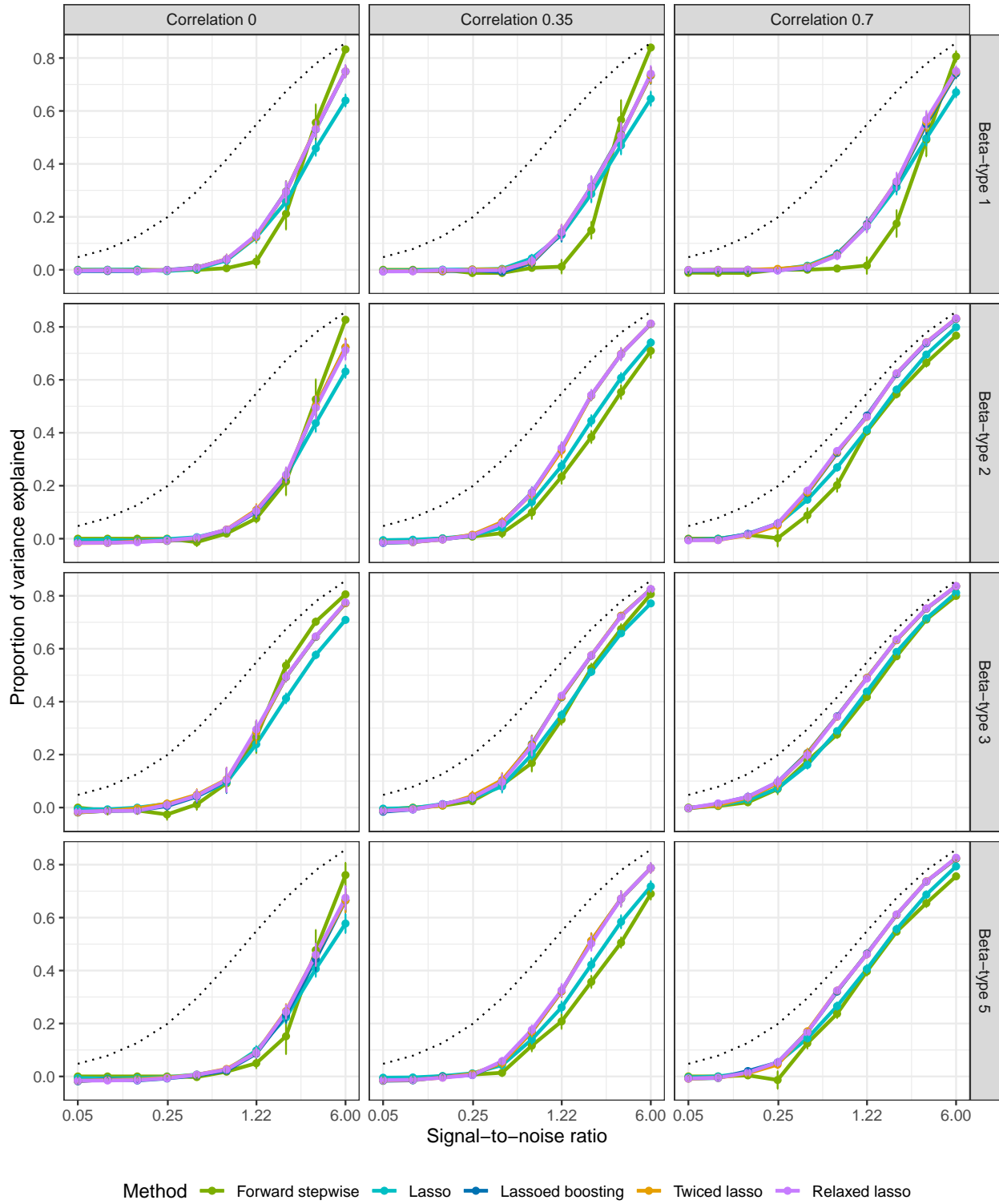


S.3.4.2 Relative test error (to Bayes)



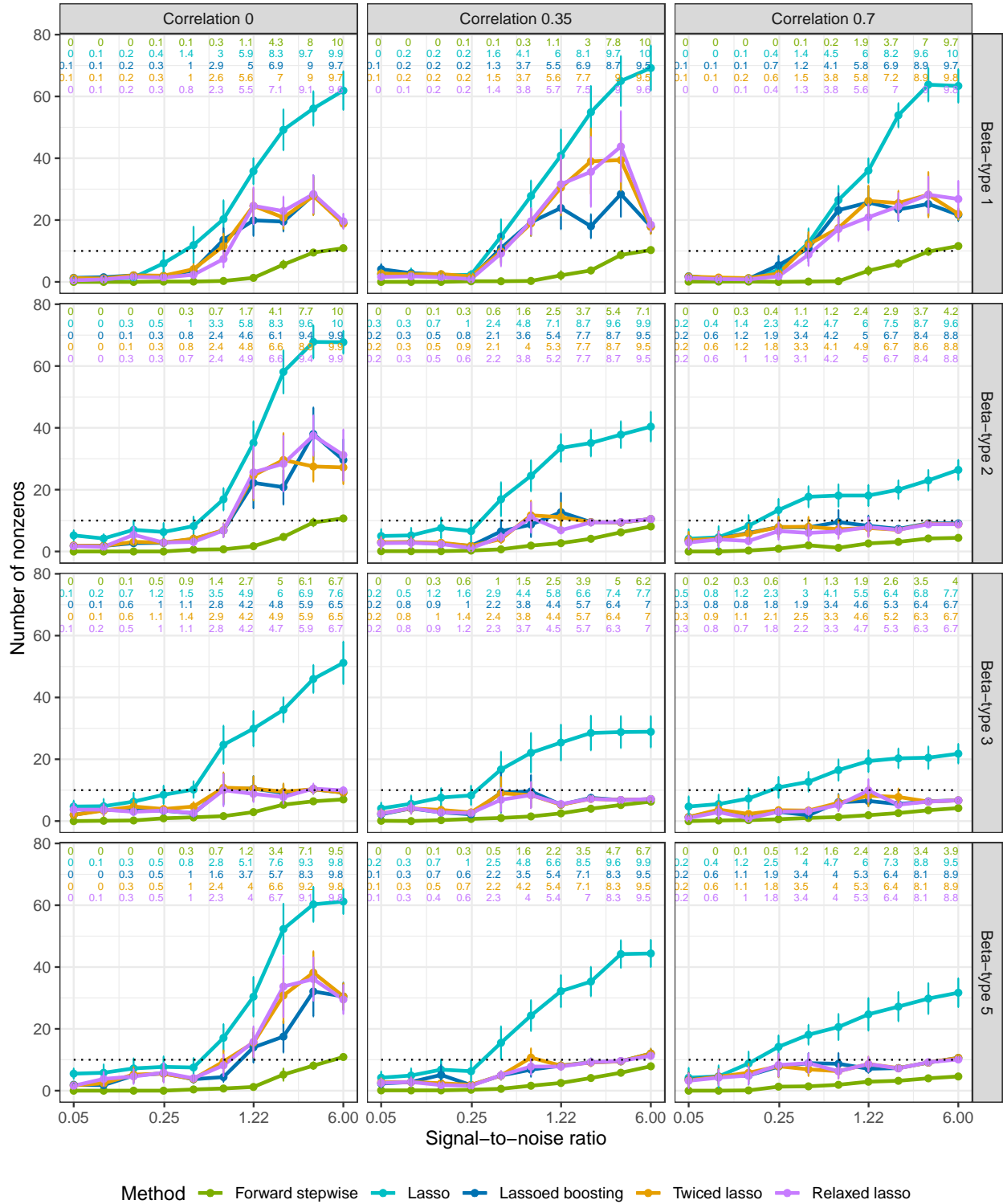
S.3.4.3 Proportion of variance explained

$n=100, p=1000, s=10$



S.3.4.4 Number of nonzero coefficients

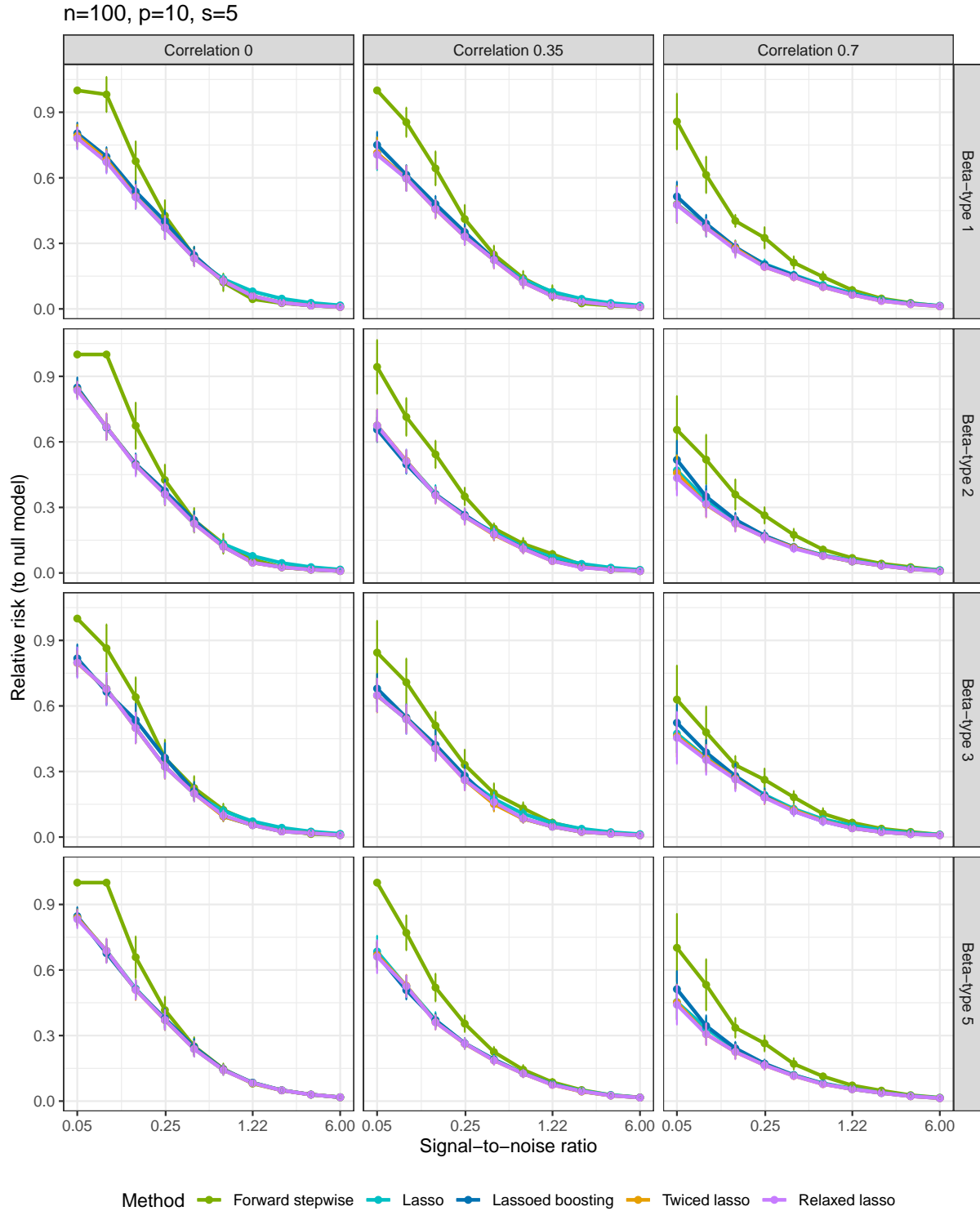
$n=100, p=1000, s=10$



S.4 Oracle tuning figures in simulation

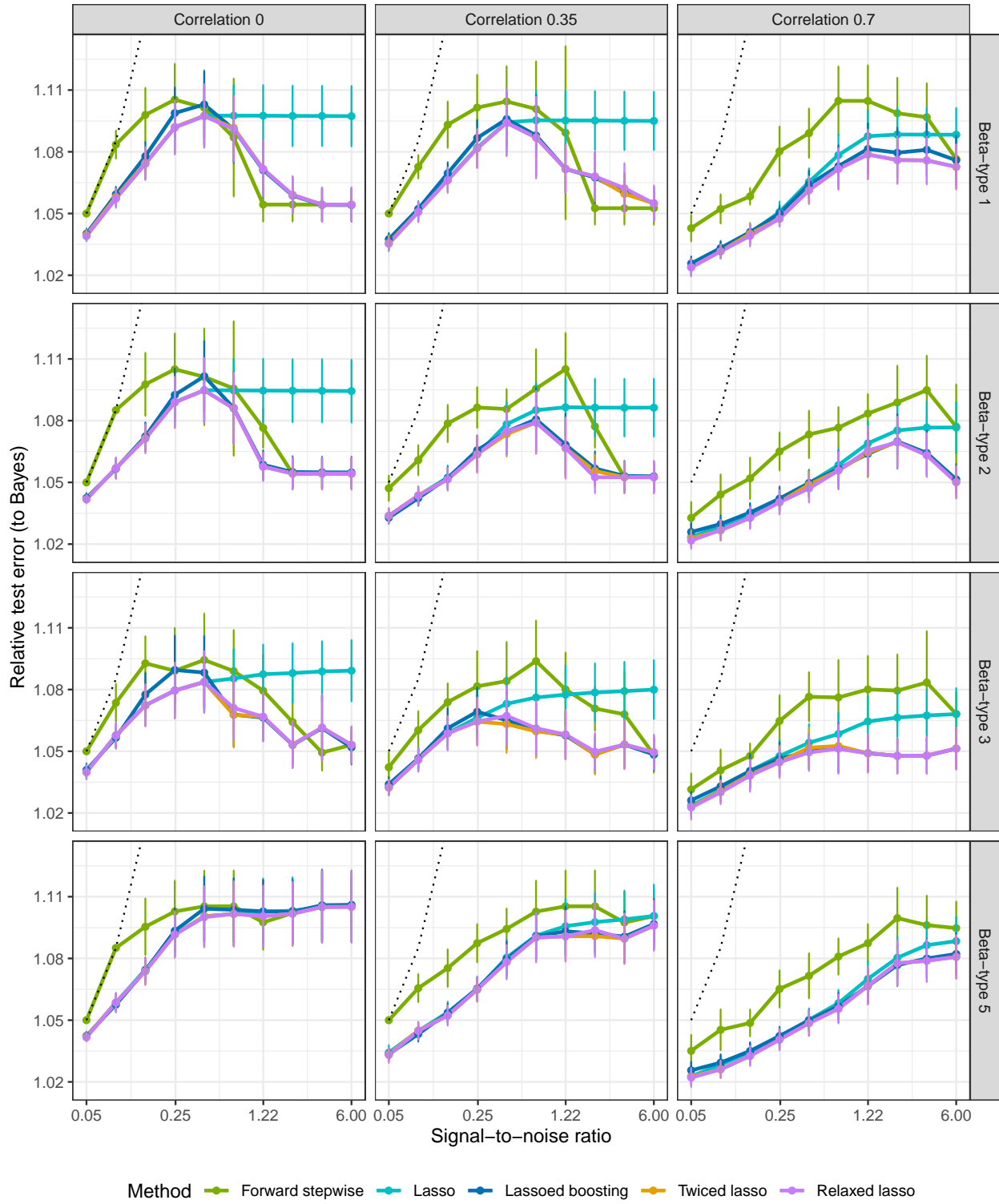
S.4.1 Low setting: $n = 100, p = 10, s = 5$

S.4.1.1 Relative risk (to null model)



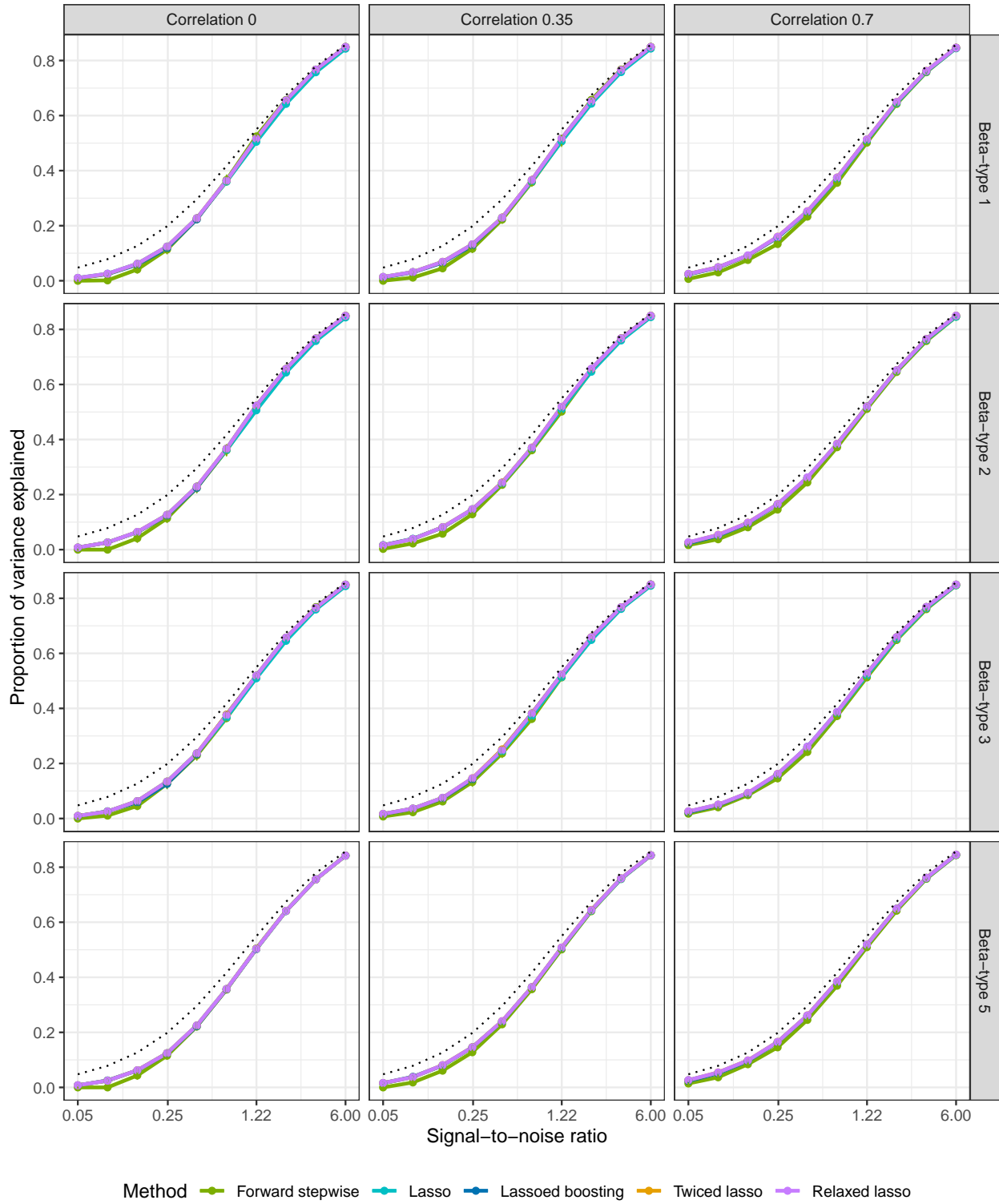
S.4.1.2 Relative test error (to Bayes)

$n=100, p=10, s=5$

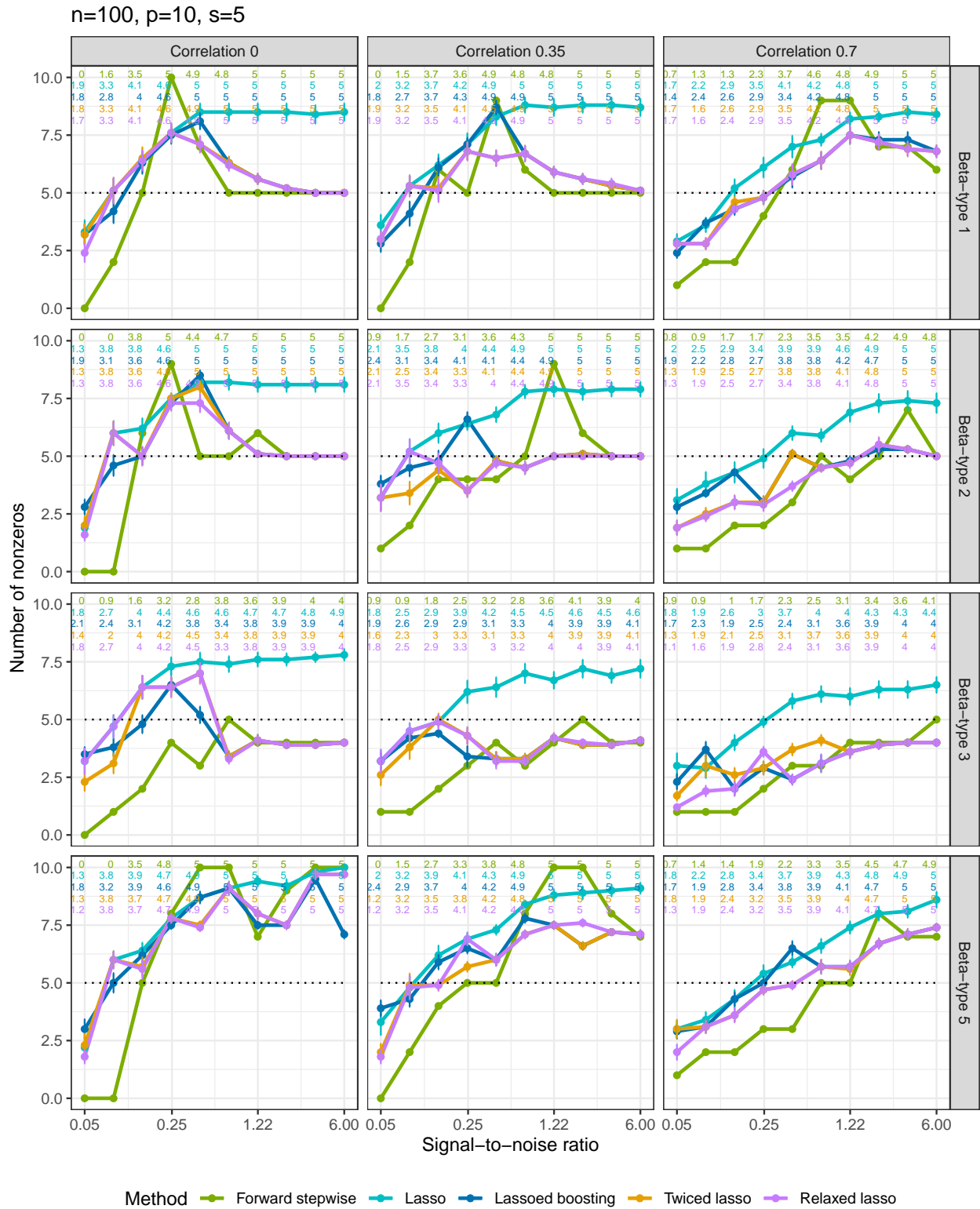


S.4.1.3 Proportion of variance explained

$n=100, p=10, s=5$

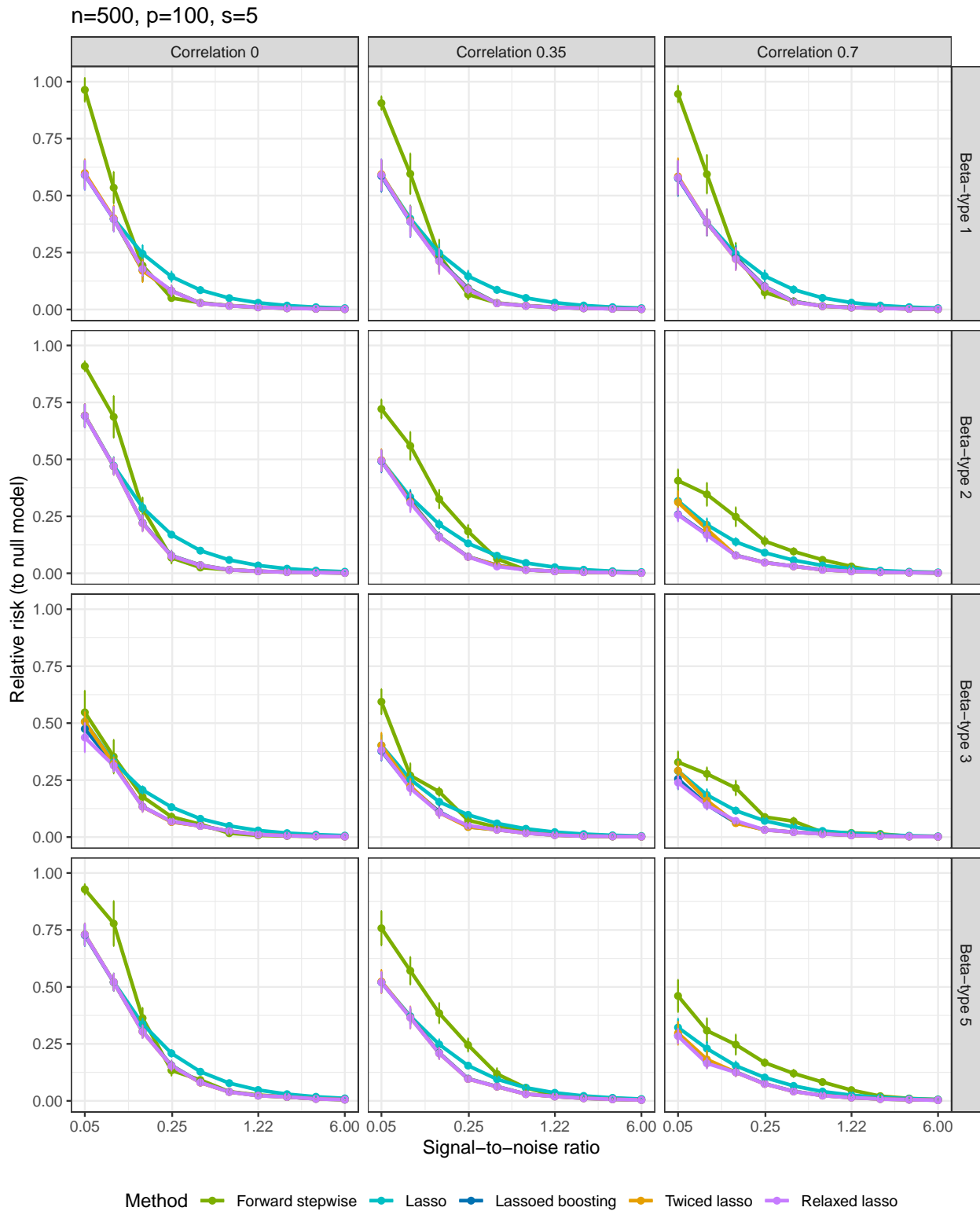


S.4.1.4 Number of nonzero coefficients



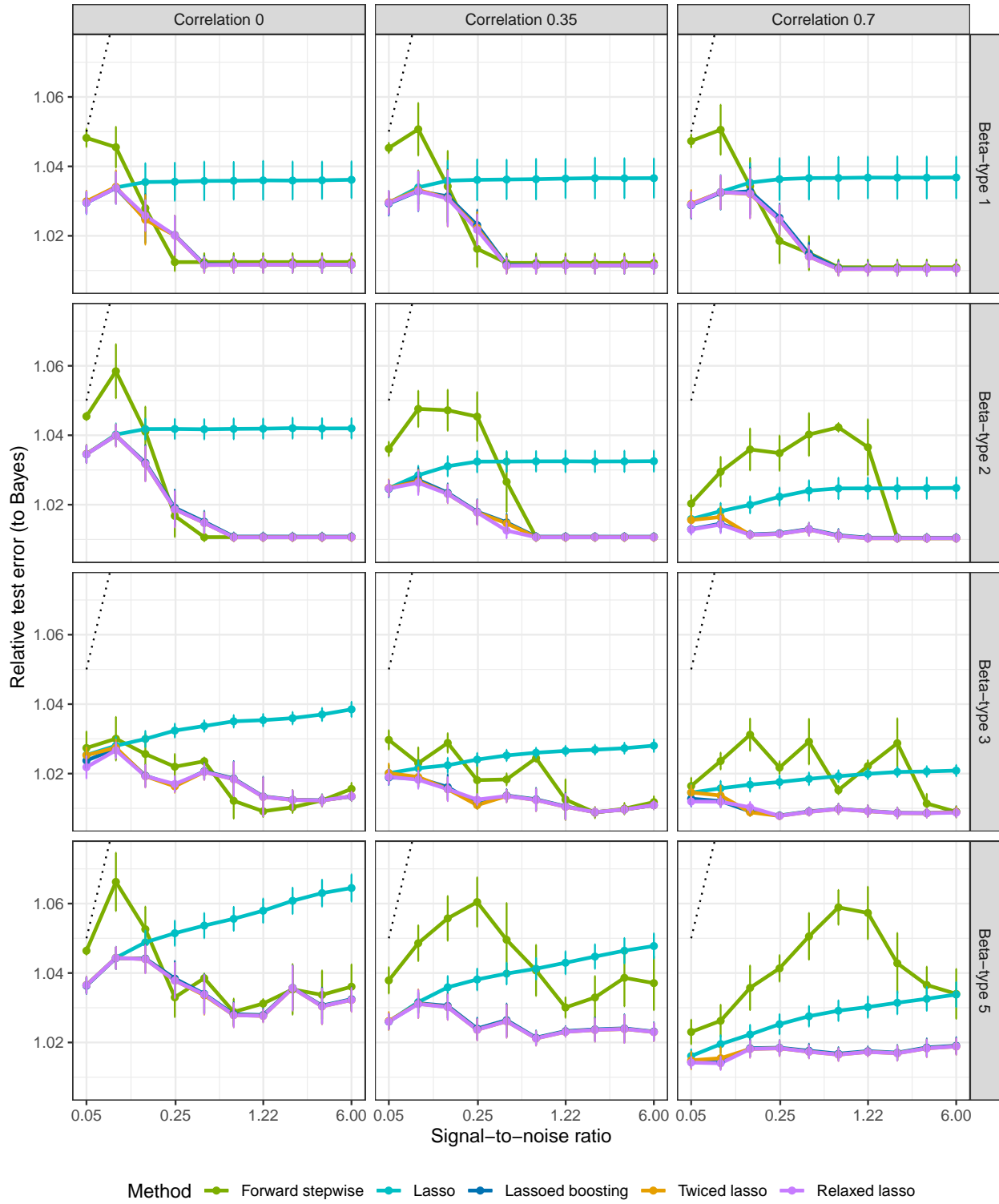
S.4.2 Medium setting: $n = 500, p = 100, s = 5$

S.4.2.1 Relative risk (to null model)



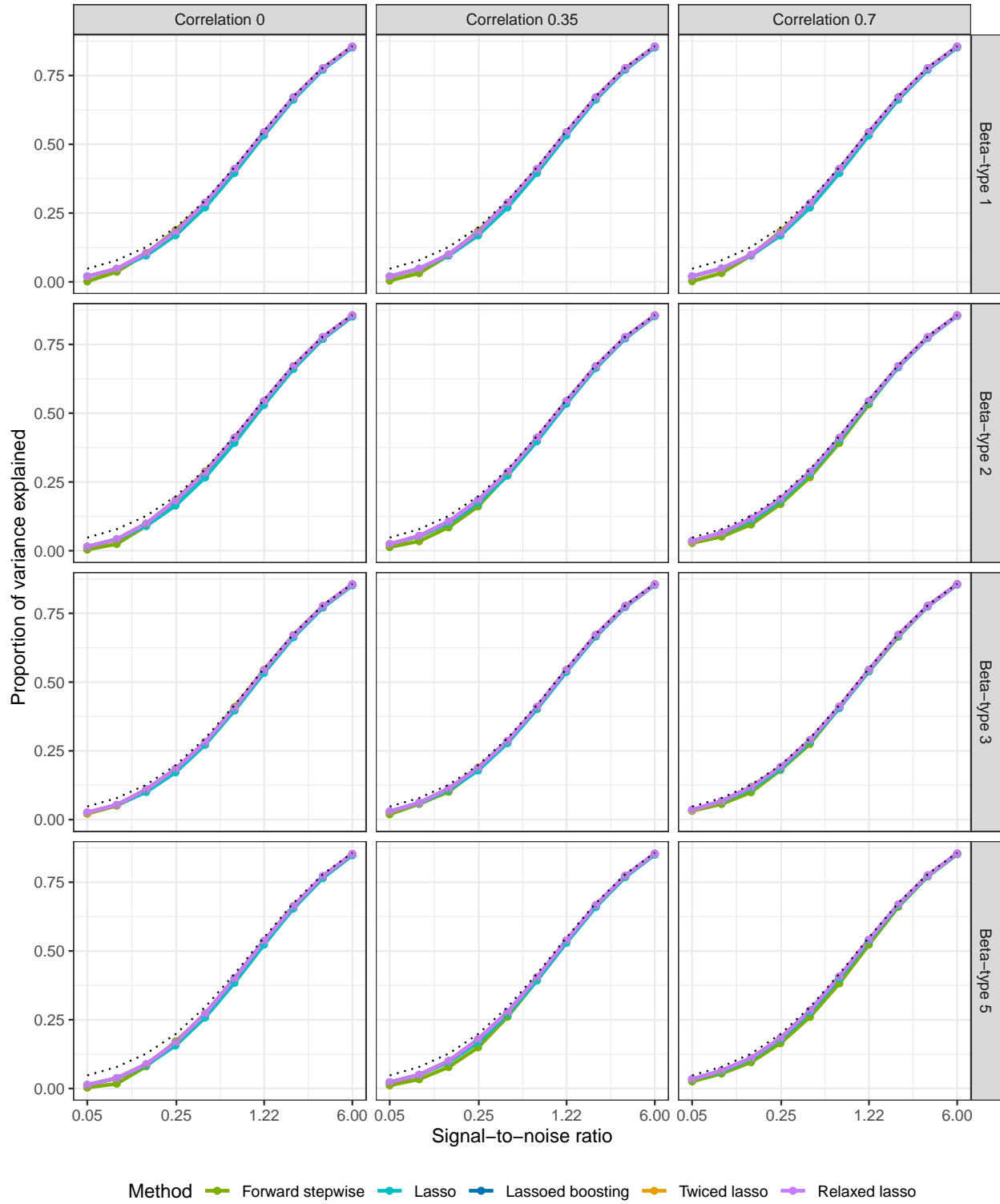
S.4.2.2 Relative test error (to Bayes)

$n=500, p=100, s=5$



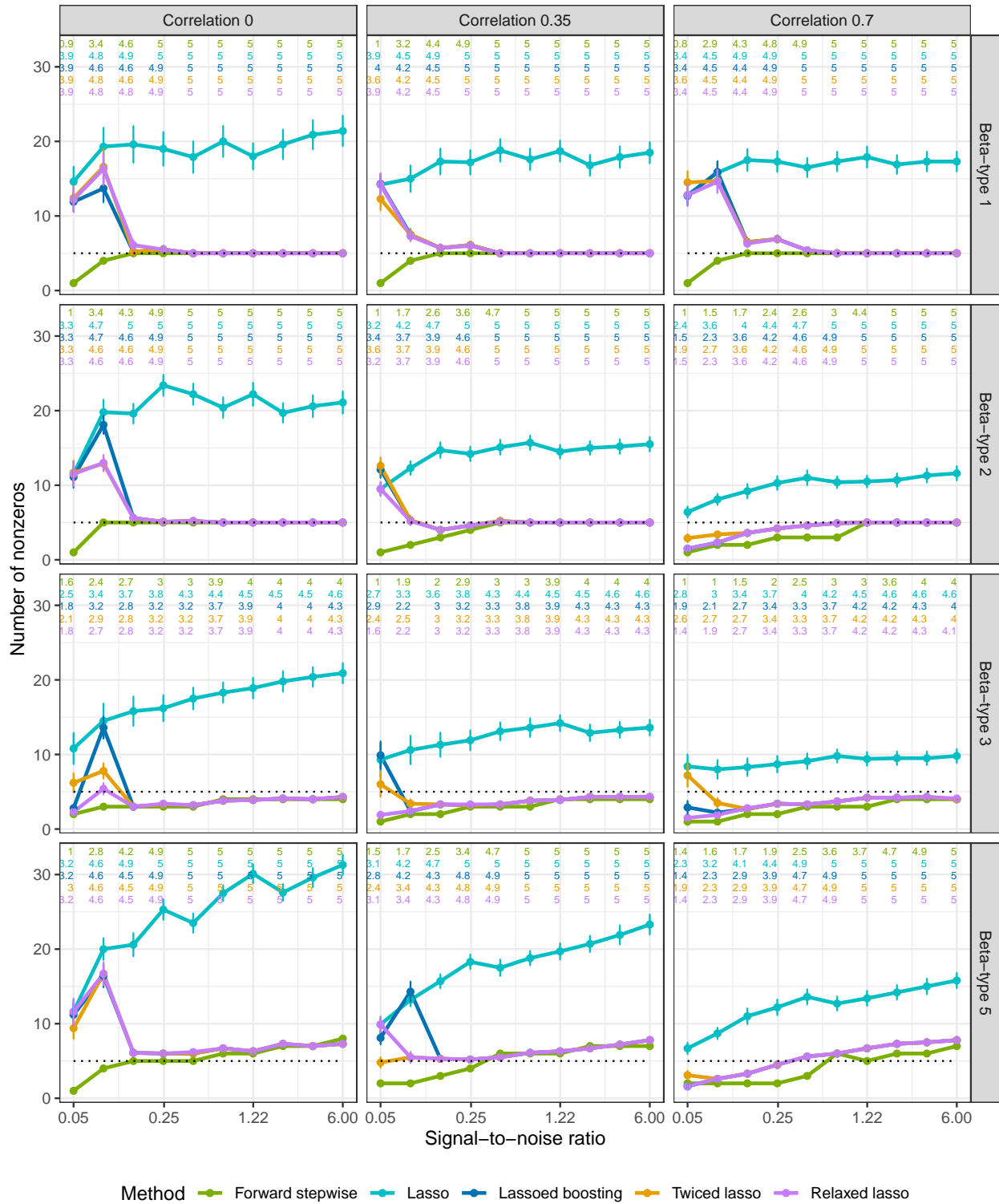
S.4.2.3 Proportion of variance explained

$n=500, p=100, s=5$



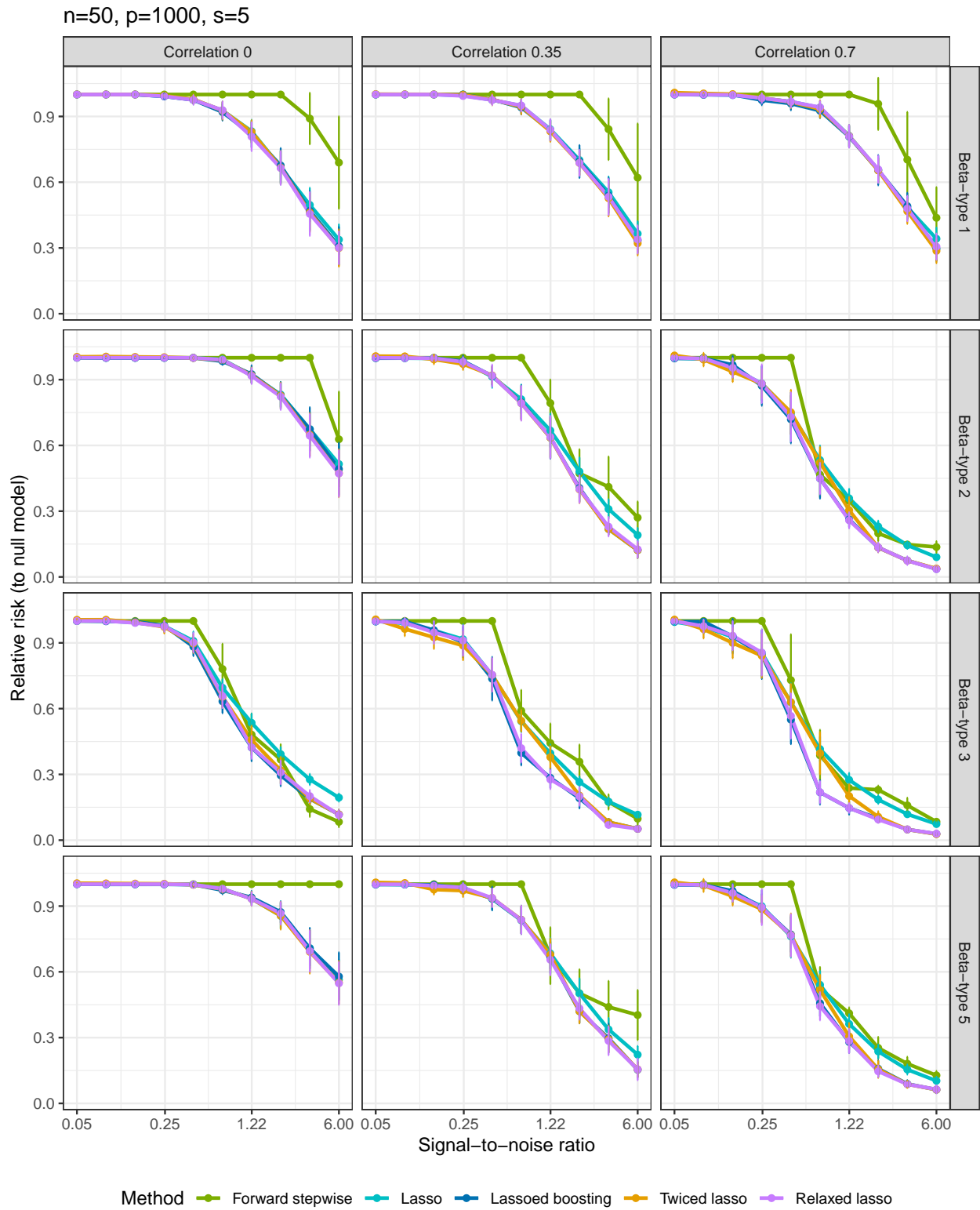
S.4.2.4 Number of nonzero coefficients

$n=500, p=100, s=5$



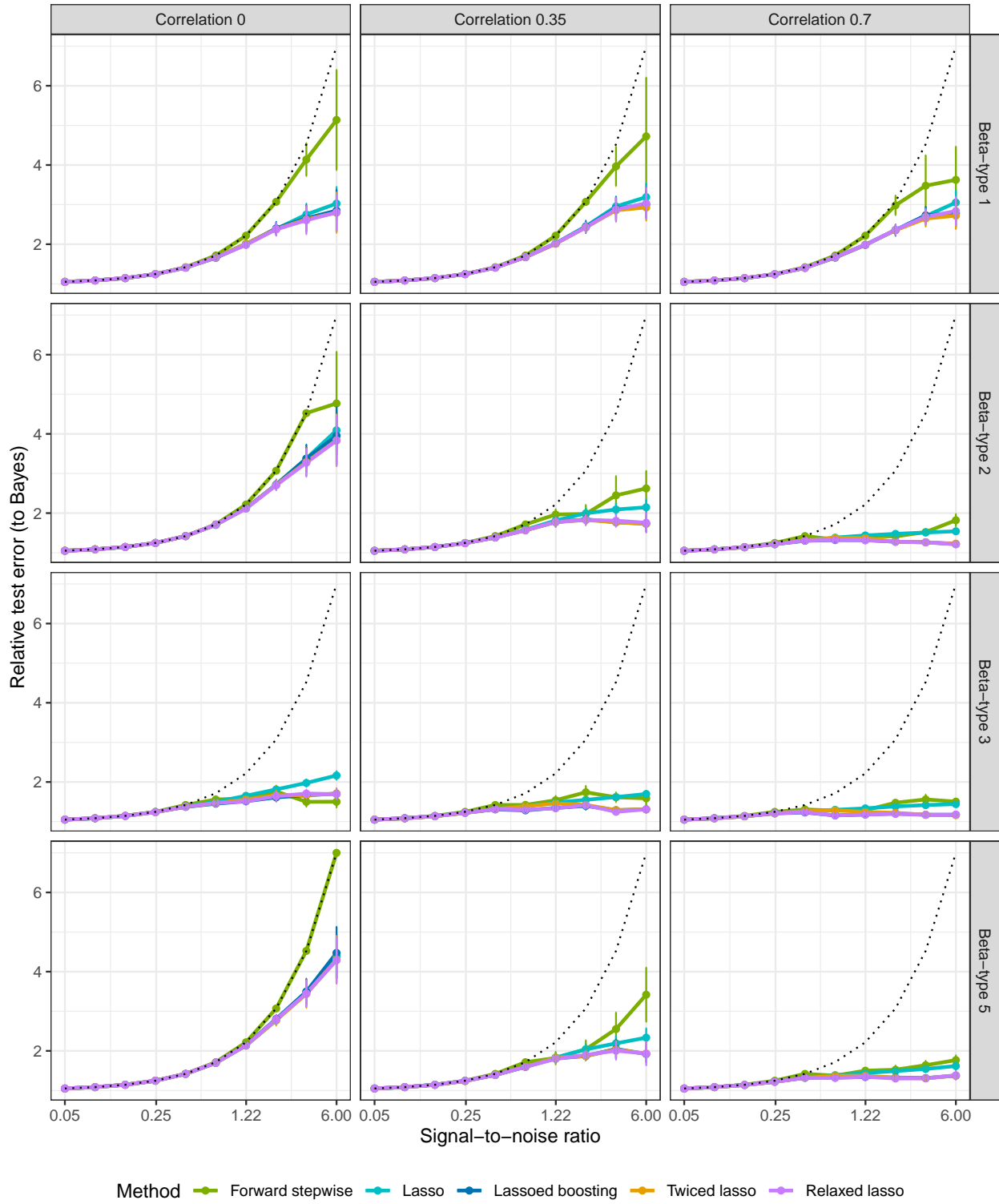
S.4.3 High-5 setting: $n = 50, p = 1000, s = 5$

S.4.3.1 Relative risk (to null model)

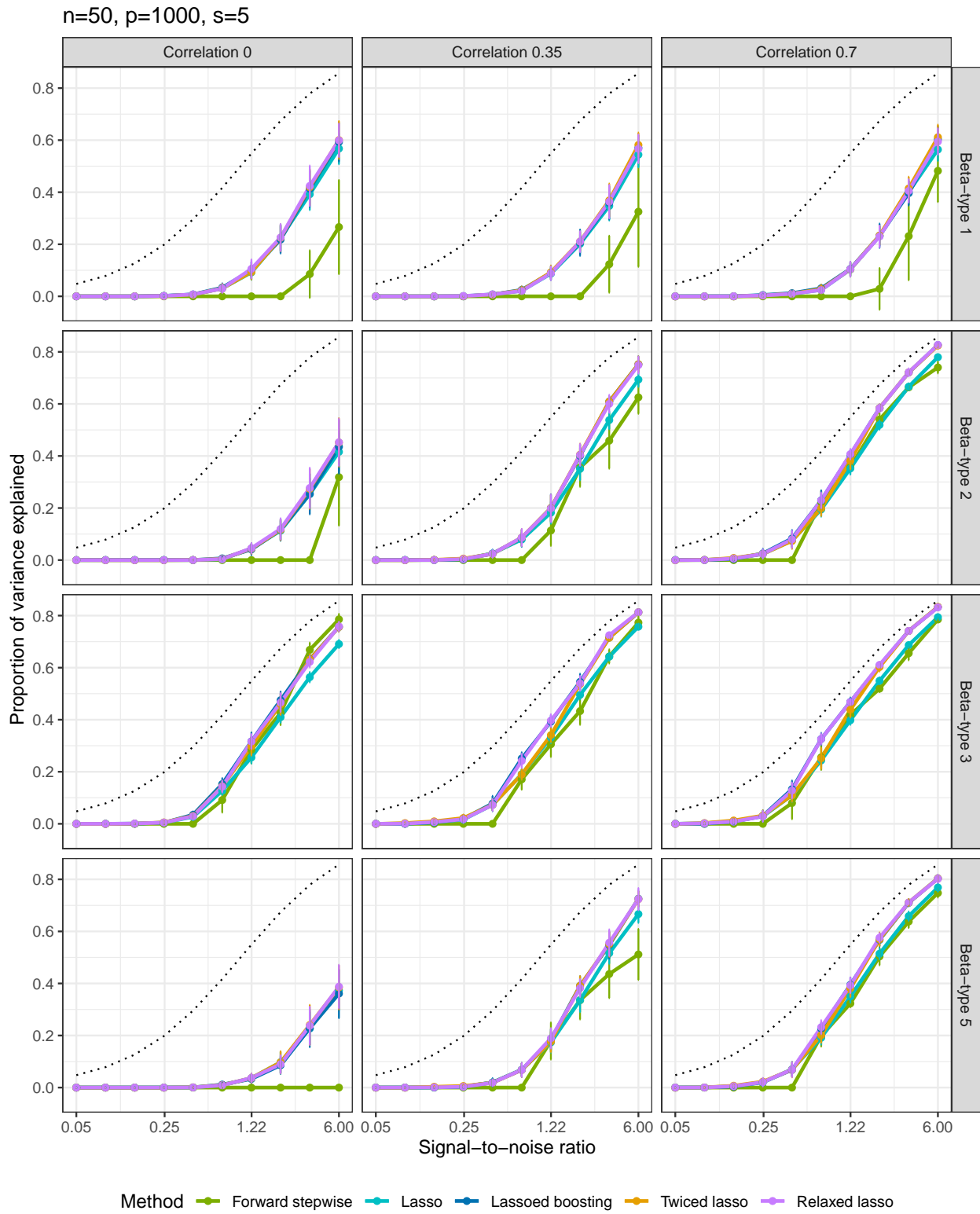


S.4.3.2 Relative test error (to Bayes)

$n=50, p=1000, s=5$

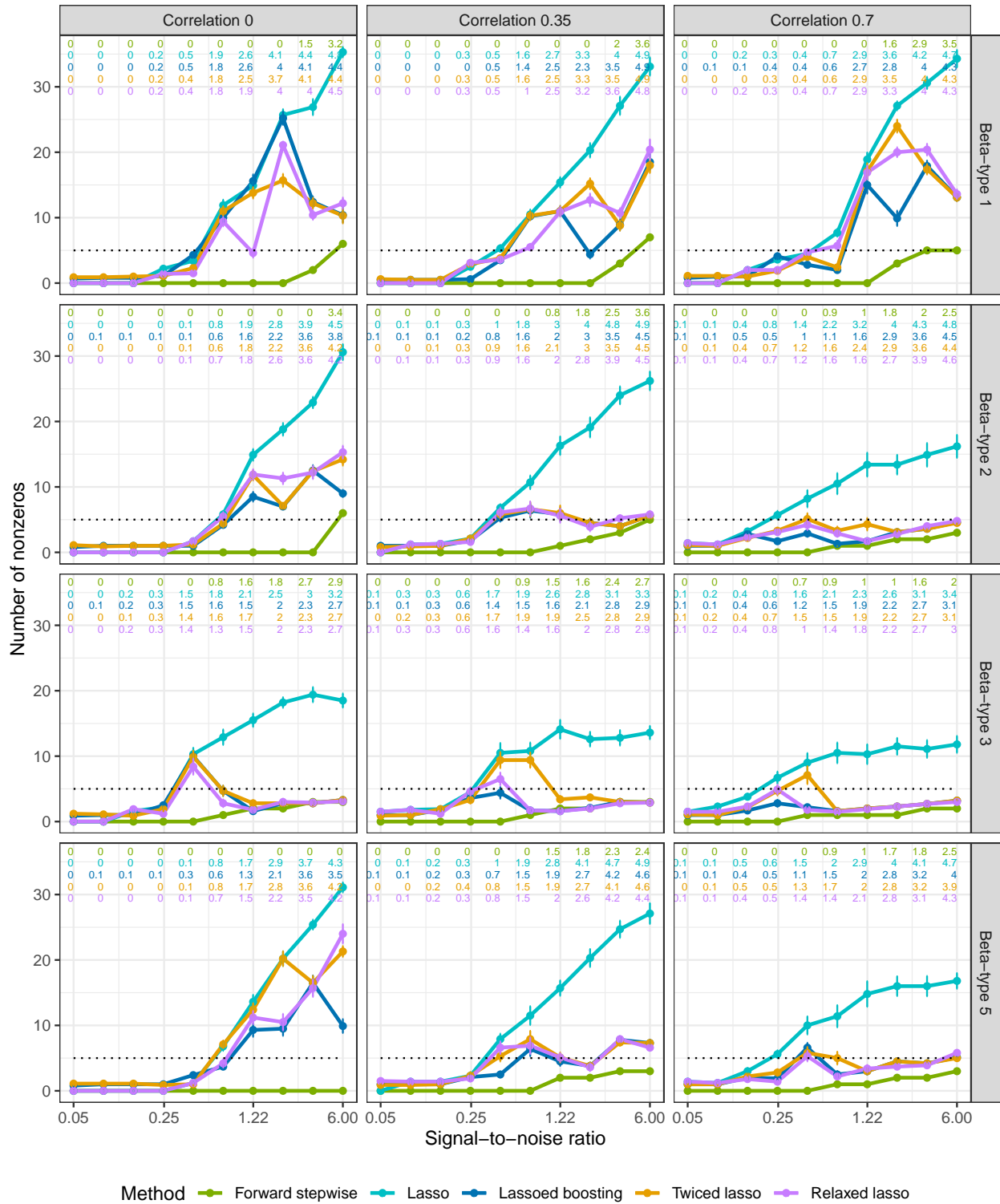


S.4.3.3 Proportion of variance explained



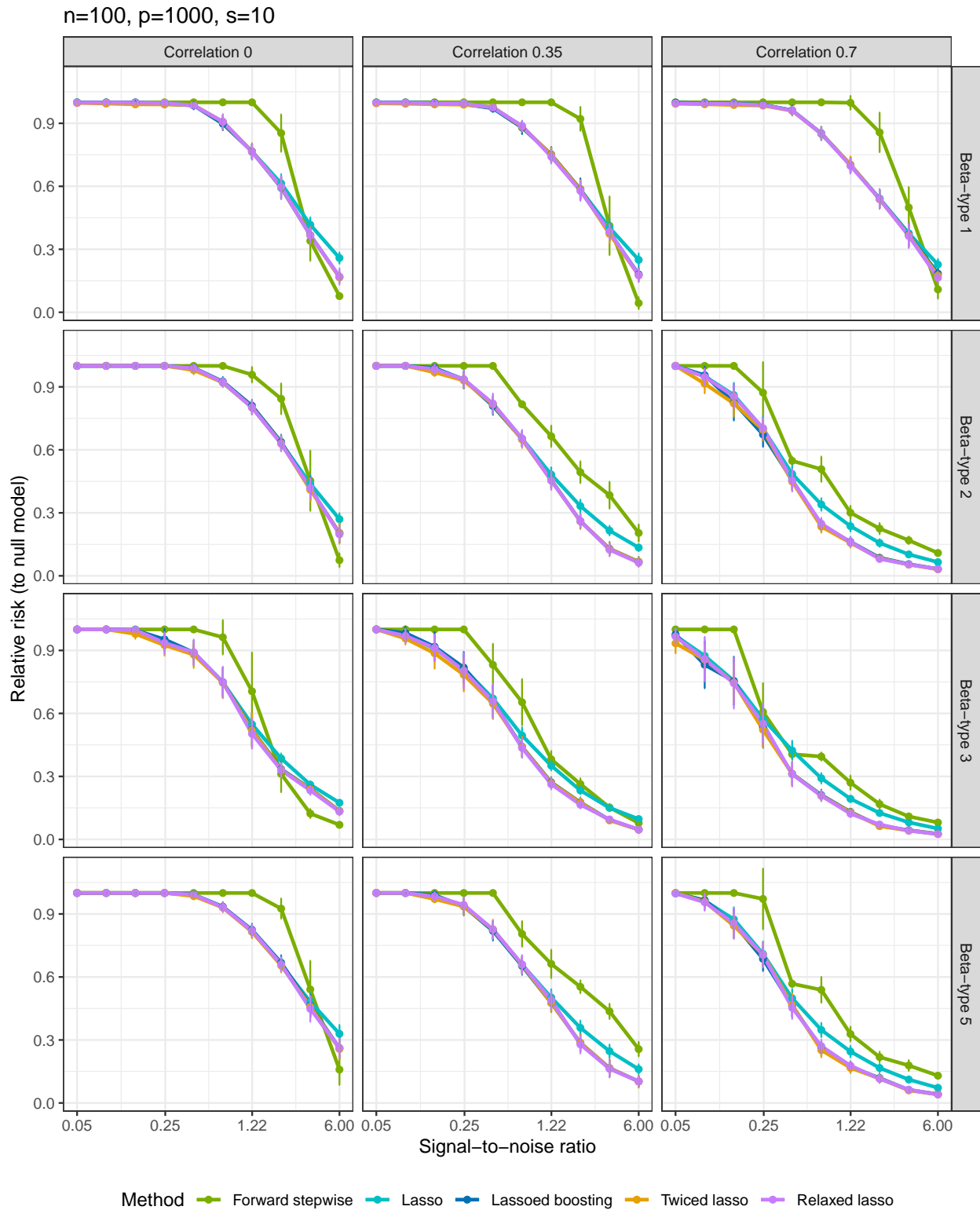
S.4.3.4 Number of nonzero coefficients

$n=50, p=1000, s=5$

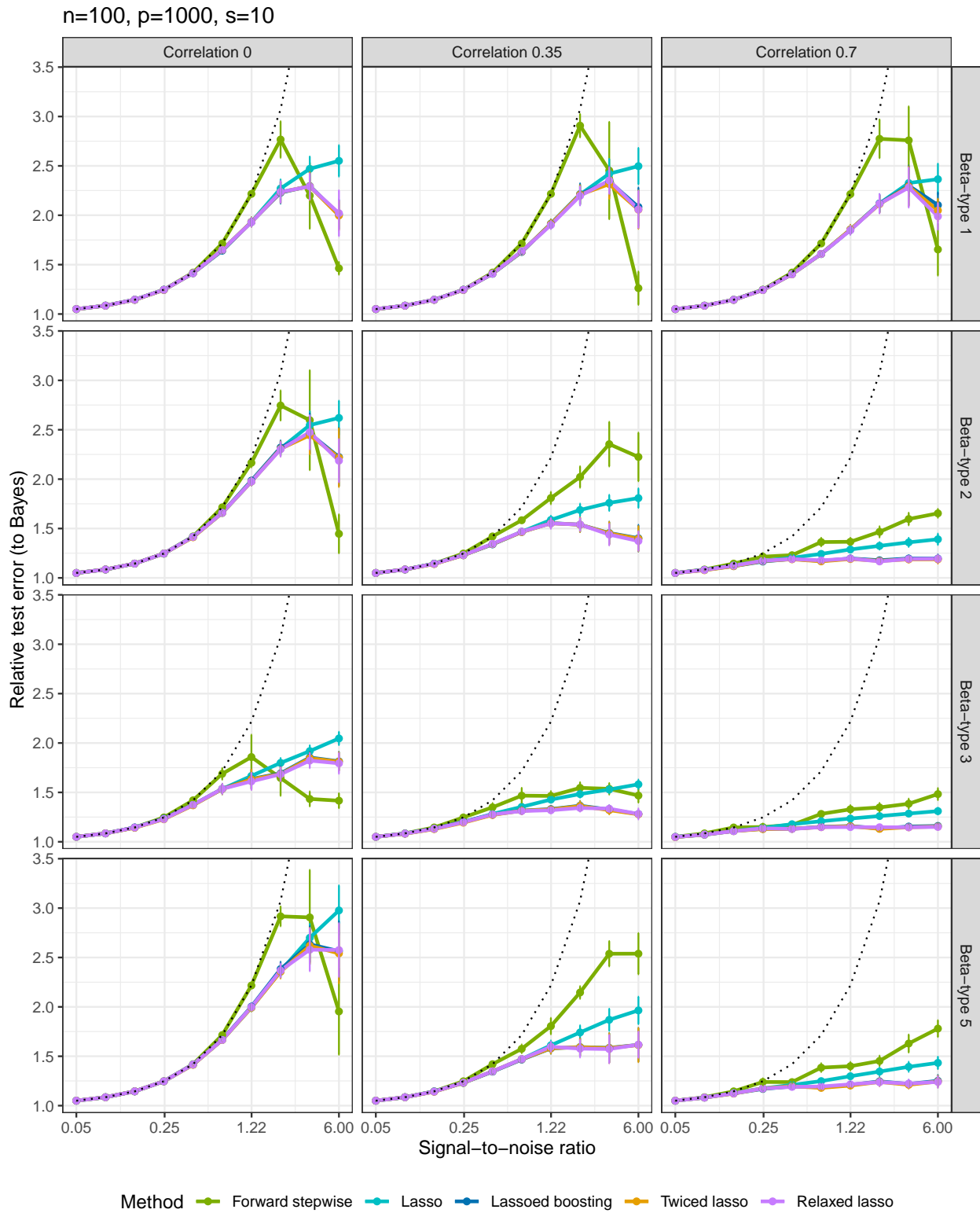


S.4.4 High-10 setting: $n = 100, p = 1000, s = 10$

S.4.4.1 Relative risk (to null model)

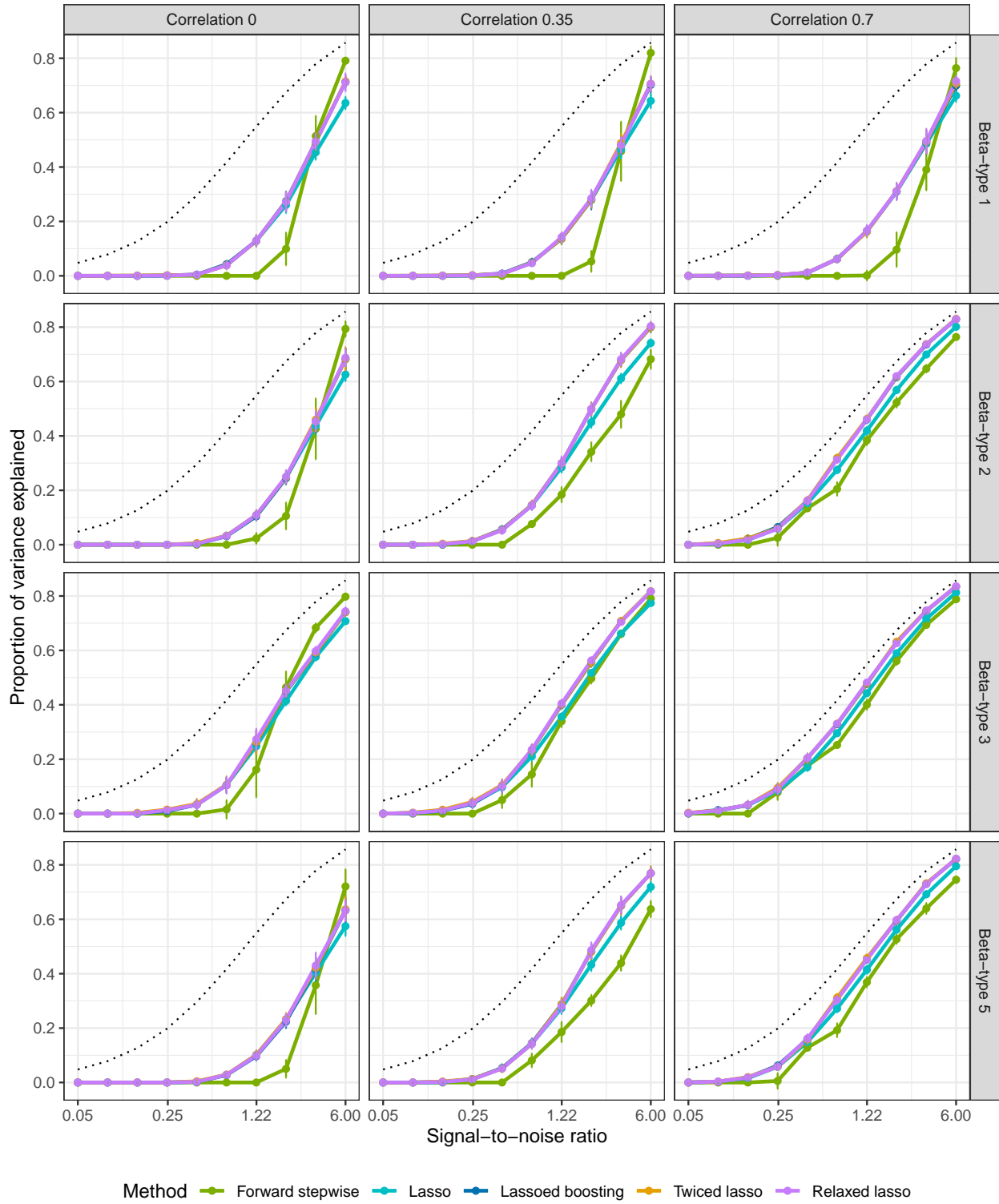


S.4.4.2 Relative test error (to Bayes)



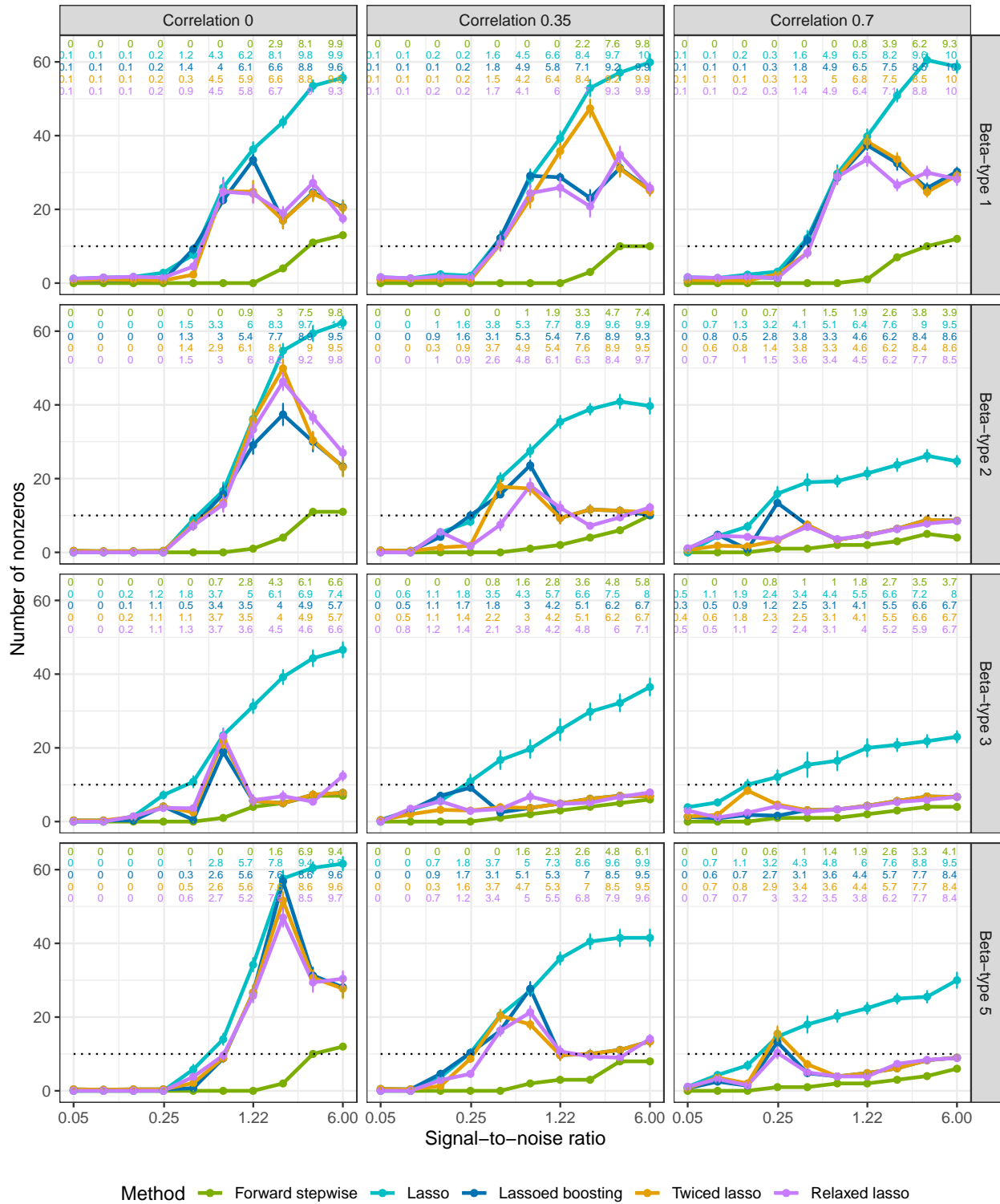
S.4.4.3 Proportion of variance explained

n=100, p=1000, s=10



S.4.4.4 Number of nonzero coefficients

$n=100, p=1000, s=10$



S.5 Variable definitions in the application

Table 2: Variables used in the application (Table 1 in [Green et al. \(2017\)](#))

Acronym	Firm characteristic	Acronym	Firm characteristic
<i>absacc</i>	Absolute accruals	<i>divo</i>	Dividend omission
<i>acc</i>	Working capital accruals	<i>dolvol</i>	Dollar trading volume
<i>aeavol</i>	Abnormal earnings announcement volume	<i>dy</i>	Dividend to price
<i>age</i>	# years since first Compustat coverage	<i>ear</i>	Earnings announcement return
<i>agr</i>	Asset growth	<i>egr</i>	Growth in common shareholder equity
<i>baspread</i>	Bid-ask spread	<i>ep</i>	Earnings to price
<i>beta</i>	Beta	<i>fgr5yr</i>	Forecasted growth in 5-year EPS
<i>betasq</i>	Beta squared	<i>gma</i>	Gross profitability
<i>bm</i>	Book-to-market	<i>grCAPX</i>	Growth in capital expenditures
<i>bm_ia</i>	Industry-adjusted book to market	<i>grltnoa</i>	Growth in long-term net operating assets
<i>cash</i>	Cash holdings	<i>herf</i>	Industry sales concentration
<i>cashdebt</i>	Cash flow to debt	<i>hire</i>	Employee growth rate
<i>cashpr</i>	Cash productivity	<i>idiovoll</i>	Idiosyncratic return volatility
<i>cfp</i>	Cash-flow-to-price ratio	<i>ill</i>	illiquidity
<i>cfp_ia</i>	Industry-adjusted cash-flow-to-price ratio	<i>indmom</i>	Industry momentum
<i>chatoia</i>	Industry-adjusted change in asset turnover	<i>invest</i>	Capital expenditures and inventory
<i>chcsho</i>	Change in shares outstanding	<i>IPO</i>	New equity issue
<i>chempia</i>	Industry-adjusted change in employees	<i>lev</i>	Leverage
<i>chfeps</i>	Change in forecasted EPS	<i>lgr</i>	Growth in long-term debt
<i>chinv</i>	Change in inventory	<i>maxret</i>	Maximum daily return
<i>chmom</i>	Change in 6-month momentum	<i>mom12m</i>	12-month momentum
<i>chnanalyst</i>	Change in number of analysts	<i>mom1m</i>	1-month momentum
<i>chpmia</i>	Industry-adjusted change in profit margin	<i>mom36m</i>	36-month momentum
<i>chtax</i>	Change in tax expense	<i>mom6m</i>	6-month momentum

(continued)

<i>cinvest</i>	Corporate investment	<i>ms</i>	Financial statement score
<i>convind</i>	Convertible debt indicator	<i>mve</i>	Size
<i>currat</i>	Current ratio	<i>mve_ia</i>	Industry-adjusted size
<i>depr</i>	Depreciation / PP&E	<i>nanalyst</i>	Number of analysts covering stock
<i>disp</i>	Dispersion in forecasted EPS	<i>nincr</i>	Number of earnings increases
<i>divi</i>	Dividend initiation	<i>operprof</i>	Operating profitability
<i>orgcap</i>	Organizational capital	<i>roeq</i>	Return on equity
<i>pchcapx_ia</i>	Industry adjusted % change in capital expenditures	<i>roic</i>	Return on invested capital
<i>pchcurrat</i>	% change in current ratio	<i>rsup</i>	Revenue surprise
<i>pchdepr</i>	% change in depreciation	<i>salecash</i>	Sales to cash
<i>pchgm_pchsale</i>	% change in gross margin - % change in sales	<i>saleinv</i>	Sales to inventory
<i>pchquick</i>	% change in quick ratio	<i>salerec</i>	Sales to receivables
<i>pchsale_pchinvt</i>	% change in sales - % change in inventory	<i>secured</i>	Secured debt
<i>pchsale_pchrect</i>	% change in sales - % change in A/R	<i>securedind</i>	Secured debt indicator
<i>pchsale_pchxsga</i>	% change in sales - % change in SG&A	<i>sfe</i>	Scaled earnings forecast
<i>pchsaleinv</i>	% change sales-to-inventory	<i>sgr</i>	Sales growth
<i>pctacc</i>	Percent accruals	<i>sin</i>	Sin stocks
<i>pricedelay</i>	Price delay	<i>SP</i>	Sales to price
<i>ps</i>	Financial statements score	<i>std_dolvol</i>	Volatility of liquidity (dollar trading volume)
<i>quick</i>	Quick ratio	<i>std_turn</i>	Volatility of liquidity (share turnover)
<i>rd</i>	R&D increase	<i>stdacc</i>	Accrual volatility
<i>rd_mve</i>	R&D to market capitalization	<i>stdcf</i>	Cash flow volatility
<i>rd_sale</i>	R&D to sales	<i>sue</i>	Unexpected quarterly earnings
<i>realestate</i>	Real estate holdings	<i>tang</i>	Debt capacity/firm tangibility
<i>retvol</i>	Return volatility	<i>tb</i>	Tax income to book income
<i>roaq</i>	Return on assets	<i>turn</i>	Share turnover
<i>roavol</i>	Earnings volatility	<i>zerotrade</i>	Zero trading days

S.6 Path difference and parameter attribution

Common methods to compare the difference between the lasso and LS-boost include visual inspection of the solution paths, computing MSPEs, *etc.* We show that the integrated gradient along the solution paths of the lasso and LS-boost can also be used to study the difference between these two methods.

In many applications of network modeling, it is useful to attribute the prediction of a network to each input (variables). [Sundararajan et al. \(2017\)](#) propose the idea of integrated gradients for attribution. Consider a function $f : R^p \rightarrow R$. Given a $p \times 1$ input vector z , select a baseline vector z' , the integrated gradient along the j th dimension on the straight line connecting z and z' is defined as:

$$\text{integrated gradient}_j := (z_j - z'_j) \times \int_{\alpha=0}^1 \frac{\partial f(z' + \alpha \times (z - z'))}{\partial z_j} d\alpha, \text{ for } j = 1, \dots, p. \quad (\text{S.8})$$

When the path connecting z' and z is not a straight line, we can use the path integrated gradient for attribution.

$$\text{path integrated gradient}_j := \int_{\alpha=0}^1 \frac{\partial f(\phi(\alpha))}{\partial \phi_j(\alpha)} \frac{\partial \phi_j(\alpha)}{\partial \alpha} d\alpha, \text{ for } j = 1, \dots, p, \quad (\text{S.9})$$

where $\phi = (\phi_1, \dots, \phi_p) : [0, 1] \rightarrow R^p$ is a function specifying a path linking z' and z with $\phi(0) = z'$ and $\phi(1) = z$.

Equations (S.8) and (S.9) describe a method for variable attribution. The same idea can be used for parameter attribution. To see that, consider the objective function in eq. (2) and let $f = L_n(\cdot)$. Since data are given, f becomes a function of β . Let the $\hat{\beta}^{(0)} = \mathbf{0}_{p \times 1}$ be the starting value in an algorithm (the z in eq. (S.8)) and $\hat{\beta}^{(1)}$ be the estimates at the end of the solution path (the z' in eq. (S.8)). Since the solution path for the lasso and LS-boost is not a straight line connecting $\hat{\beta}^{(0)}$ and $\hat{\beta}^{(1)}$, we need to accumulate the gradients along the path on which the coefficients travel and use eq. (S.9). Without specifying a piecewise linear function ϕ for the lasso or LS-boost, we opt for the simple method of numerical integration based on the trapezoid rule. This method seems to work well in our case, probably due to the piecewise linear pattern of the solutions.

Use the data in January, 2010 as an example. Both the relaxed lasso and lassoed boost

select the same 6 variables (*lev*, *mve*, *mom1m*, *baspread*, *mom12m*, *retvol*) while the lasso selects 44 variables. Assume both the lasso and LS-boost start with the same 6 variables. Let the lasso use 1000 equally spaced penalty values on $[0, \lambda_0]$ and LS-boost use the learning rate 0.1 and iteration number 1000 (the iteration number based on the corrected AIC is 127.) Let q denote the step in the lasso or LS-boost. We use the following formula for numerical integration. For $j = 1, \dots, 6$ and $q = 1, \dots, 1000$,

$$G_{jq} = \frac{\partial L_n(\hat{\beta}_{q+1})/\partial\beta_j + \partial L_n(\hat{\beta}_q)/\partial\beta_j}{2} \times (\hat{\beta}_{q+1} - \hat{\beta}_q), \quad (\text{S.10})$$

and we record eq. (S.10) as the jq th element of the matrix G . The approximation to the path integrated gradient in eq. (S.9) becomes the row sums of G

$$G_j = \sum_{q=1}^{1000} G_{jq}, \text{ for } j = 1, \dots, 6. \quad (\text{S.11})$$

To gauge the precision of the numerical integration, we sum the starting value of the loss function $L_n(\hat{\beta}^{(0)})$ and $\sum_{j=1}^6 G_j$, and compare it to the value of the loss function $L_n(\hat{\beta}^{(1)})$. For the lasso, the two quantities are equal up to the 8th digit; for LS-boost, they are equal up to the 15th digit. This simply verifies the fundamental theorem of calculus.

Table 3: Path integrated gradient for each β in the lasso and LS-boost

	β_{lev}	β_{mve}	β_{mom1m}	β_{baspread}	β_{mom12m}	β_{retvol}
lasso	-56.666	-32.765	-26.522	-9.864	-9.653	-3.661
LS-boost	-56.872	-32.803	-26.471	-9.777	-9.646	-3.561

Notes: See Table 2 in the Supplement for the variable definition. The number in each cell is obtained via eq. (S.11). Multiplying the numbers by 10^{-5} gives the actual path integrated gradients. The columns are arranged based on the order in which variables enter the model.

Table 3 reports the path integrated gradient for both the lasso and LS-boost. All numbers are negative because we consider function minimization. The variables are listed in the order in which they enter the lasso and LS-boost models. Because it is not possible for LS-boost to reach a full LS solution even with a large number of iterations, rigorously speaking, the numerical differences in these numbers also reflect a small numerical difference between the

minimized loss of the lasso and LS-boost. In our case, the two minimized loss functions based on demeaned data differ by less than 3×10^{-9} . Hence, numerical difference in Table 3 is largely due to that fact the lasso and LS-boost visit different solution paths. This provides a new perspective on understanding the difference between these two methods.

One should not conclude that the small numerical difference in Table 3 indicates the two methods always have similar parameter attribution. This is a simple regression model with only 6 variables. With many variables, the two methods may select different models, and the attributions in Table 3 will be very different. This is likely to happen more frequently when comparing the lasso to lassoed boosting. Table 3 does not focus on the relaxed lasso. But it is interesting to note that the attribution method for the relaxed lasso is a hybrid procedure of using both eqs. (S.8) and (S.9).

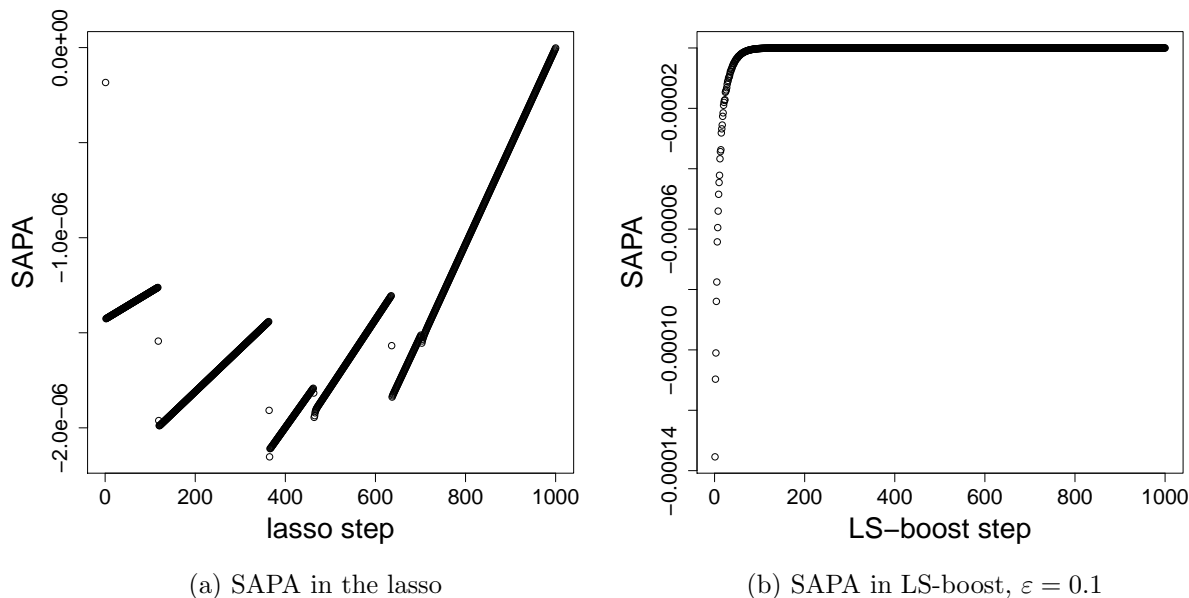


Figure 10: SAPA in the lasso and LS-boost for 6 variables (*lev*, *mve*, *mom1m*, *baspread*, *mom12m*, *retvol*) in January, 2010. In Figure 10(a), there is a small break at the end of the 5th segment, resulting a total of 6 segments.

We can also compute the column sums of G , which measures the stepwise aggregate parameter attribution (SAPA) of a method. SAPA is also the stepwise decrease in the loss function. Figure 10 plots SAPA of both the lasso and LS-boost. We make several observations. The SAPA of the lasso consists of 6 segments, each of which represent a gradual

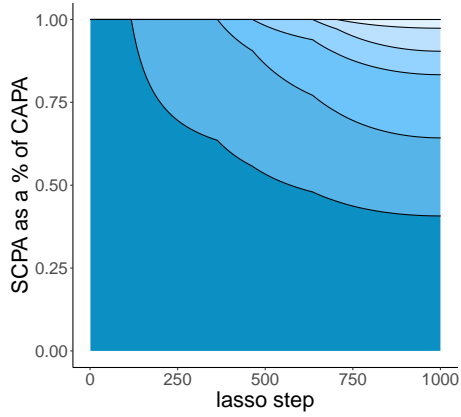
decrease (in absolute value) in SAPA after a new variable enters the model. Interestingly, for LS-boost, its SAPA exhibits a smoother, continuous pattern. This indicates that the lasso and LS-boost may give completely different descending pattern of the loss function during optimization. For the lasso, SAPA at the beginning of each segment always shows up as a jump. This is due to the fact that when a new variable is just selected, its path integrated gradient at the current step is computed w.r.t. a zero value in its coefficient. After that, its path integrated gradient is computed w.r.t. a nonzero coefficient, which helps smooth the values, and they mostly line up along a straight path until the next variable enters the model. We also observe that these segments of the lasso SAPAs have different length and slope. A long and relatively flat segment indicates lasso is traveling on a solution path that might drive down the loss function considerably. The pattern of the SAPA in Figure 10(a) is also implicitly connected to the well-known fact that the lasso solution path is piecewise linear. Our analysis shows that path integrated gradient can be a useful tool to study the differences between the lasso and LS-boost. The above analysis also applies to lassoed boosting.

S.7 Additional figures for parameter attribution in the lasso and LS-boost

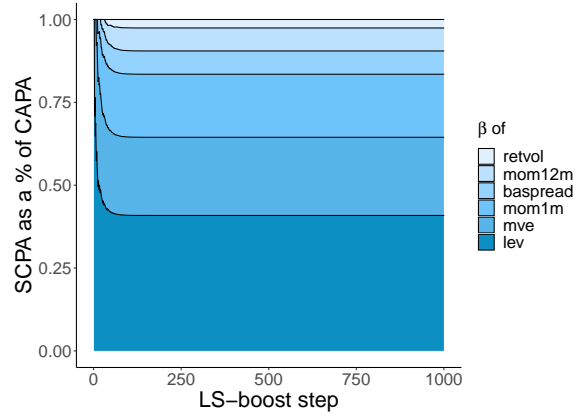
Figures 11(a), 11(b) and 11(d) plot, at each step, a parameter estimate $\hat{\beta}_j$'s stepwise cumulative parameter attribution (SCPA) as a percentage of the cumulative aggregate parameter attribution (CAPA) up to each step. These three figures provide an additional way to visualize the difference between the lasso and LS-boost. Compared with Figure 10(b), Figure 11(c) illustrates how a different learning rate can alter the pattern of SAPA in LS-boost.

References

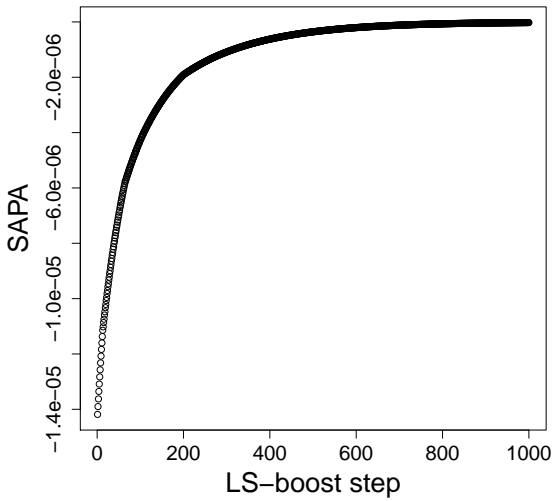
- Rigollet, P. and Hütter, J. (2019). High Dimensional Statistics, lecture notes for the MIT course 18.S997.
- Sundararajan, M., Taly, A. and Yan, Q. (2019). Axiomatic Attribution for Deep Networks, Proceedings of the 34th ICML Vol. 70, p. 3319–3328.



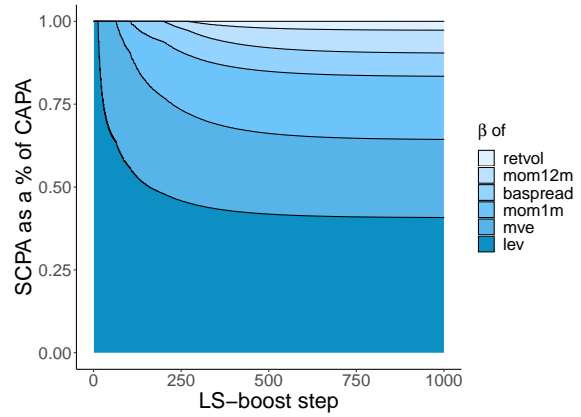
(a) SCPA plot for the lasso



(b) SCPA plot for LS-boost, $\varepsilon = 0.1$



(c) SAPA in LS-boost, $\varepsilon = 0.01$



(d) SCPA plot for LS-boost, $\varepsilon = 0.01$

Figure 11: Figures 11(a), 11(b) and 11(d) are SCPA plots for lasso and LS-boost. Figure 11(c) is the SAPA plot for LS-boost with $\varepsilon = 0.01$.